INTEGRATED APPROACH TO THE EXPLORATION OF THE OLIGOCENE VICKSBURG RESERVOIRS, TCB FIELD KLEBERG COUNTY, TEXAS

By

AMY REBECCA CLOSE

Bachelor of Science

Oklahoma State University

Stillwater, Oklahoma

1999

Submitted to the Faculty of the
Graduate College of the
Oklahoma State University
in partial fulfillment of
the requirements for
the Degree of
MASTER OF SCIENCE
May, 2002

INTEGRATED APPROACH TO THE EXPLORATION

OF THE OLIGOCENE VICKSBURG

RESERVOIRS, TCB FIELD

KLEBERG COUNTY,

TEXAS

Thesis Approved:

Zuhair al-Shaieb

Thesis Adviser

Jim Puckette

Gary J. Stewart

Timothy J. Petterson

Dean of the Graduate College

ACKNOWLEDGEMENTS

I would like to give Thanks to Jesus Christ through which all things are done. I giv joyful gratitude to God for his grace and everlasting love.

I wish to express my sincere appreciation to my mentor and friend Dr. Zuhair Al-Shaieb for his constructive guidance and inspiration. Doc Al, you have contributed a great deal to my life. Also, deep appreciation to Dr. Jim Puckette whose helpful suggestions and guidance were crucial in this endeavor. To Dr. Stewart whose editing and insightful comments were priceless.

More over, I would like to honorably mention the Gas Research Institute for funding this research. Mr. Paul Chandler and Kerr-McGee Oil and Gas Onshore for the donation of the data used in this study. I would like to thank my friend and fellow graduate students for their helpful comments and advice especially, Phebe Deyhim, Melanie McPhail and Ken Rechlin.

I would also like to give my special appreciation to my husband, David, my parents, George and Gena Cox, and my sisters Polly Owen and Debbie Sturgill for their suggestions, strong encouragement, love and understanding throughou my entire college career.

TABLE OF CONTENTS

LIST OF FIGURES

CHAPTER I

INTRODUCTION

General Statement

The Vicksburg Formation has been a lucrative exploration target in the Gulf Coast region. Evaluation of these reservoirs is very complex as a result of variability in their facies, texture, and composition. A significant segment of the Vicksburg sandstone section consists of low resistivity /low contrast (LR/LC) reservoirs. Al-Shaieb et al. (2001); and Deyhim (2001) described the architecture of these reservoirs and utilized high- resolution and microimaging logs to differentiate reservoirs and seals.

Al-Shaieb et al. (2001) and Han (2001) developed petrophysical techniques to correct water-saturation (Sw) values of the LR/LC reservoirs. They evaluated and modified specific petrophysical parameters used in the Archie, Waxman-Smits, and Dual-Water models. Consequently, they were able to derive water-saturation (Sw) values that match closely those determined by core-plug analysis. LR/LC reservoirs were often ignored because they are thin-bedded; this prevented their detection and evaluation by wire-line logging tools. LR/LC log signatures were suppressed, resulting in incorrect calculations of Sw and estimations of reserves.

The sequence-stratigraphic framework of the Vicksburg was established by Al – Shaieb et al. (2000), Birkenfeld, (2000), and Coleman, (1986.) Specific reservoir types were identified as Lowstand Systems Tract (LST), Transgressive Systems Tract (TST), and Highstand Systems Tract (HST).

Complexity of Vicksburg reservoirs and resulting difficulties in wire-line log evaluation are related directly to the sequence-stratigraphic framework. The TST reservoirs typically are composed of thinly bedded shale and sandstone. Sandstones generally contain abundant authigenic clay minerals. Conventional wire-line log analyses of these zones yield high Sw values. On the other hand, LST and HST reservoirs are thicker and contain less authigenic clay. Thus, evaluation of LST and HST reservoirs is less complex.

A major emphasis of this study is to show that new technological developments can be used to evaluate reservoirs and seals more efficiently. These techniques improve exploration and production strategies by accurately identifying the presence of oil and gas within non-typical reservoirs such as the low contrast/low resistivity zones within the Vicksburg trend.

Objectives

The primary objective of this study is to provide an in-depth view of techniques utilized to evaluate the productive potential of reservoirs within the Vicksburg Sandstone interval in the TCB field area. These techniques should be applicable to similar

reservoirs in other oil and gas provinces. To accomplish this goal supporting data must be analyzed and evaluated. This phase included the following components:

1) Examine responses of conventional wireline logs and specialized tools such as microimagers.
2) Use capillary pressure, fluid-inclusion stratigraphy, and high-resolution log data to determine seal and reservoir intervals.
3) Determine the effects of petrology and diagenesis on reservoirs within the study area.
4) Analyze depositional facies and how they affect reservoir quality.
5) Establish sequence stratigraphy.
6) Develop implications for exploration within the Vicksburg trend.

Study Area

The Tijerina-Canales-Blucher (TCB) field is the focus of this study. TCB field is located within Jim Wells and Kleberg counties in South Texas portion of the Gulf Coast region (Fig. 1). This field is a prolific gas producer from the Oligocene Vicksburg Sandstone at depths from 8,000 to 11,500 feet.

Within the TCB field the Vicksburg formation has produced more than 105 billion cubic feet (BCF) gas and 2 million barrels of liquids (MBL) since 1942 (Petroleum Information/Dwights, 1999; Taylor and Al-Shaieb, 1986). The Vicksburg Trend (Fig. 2)

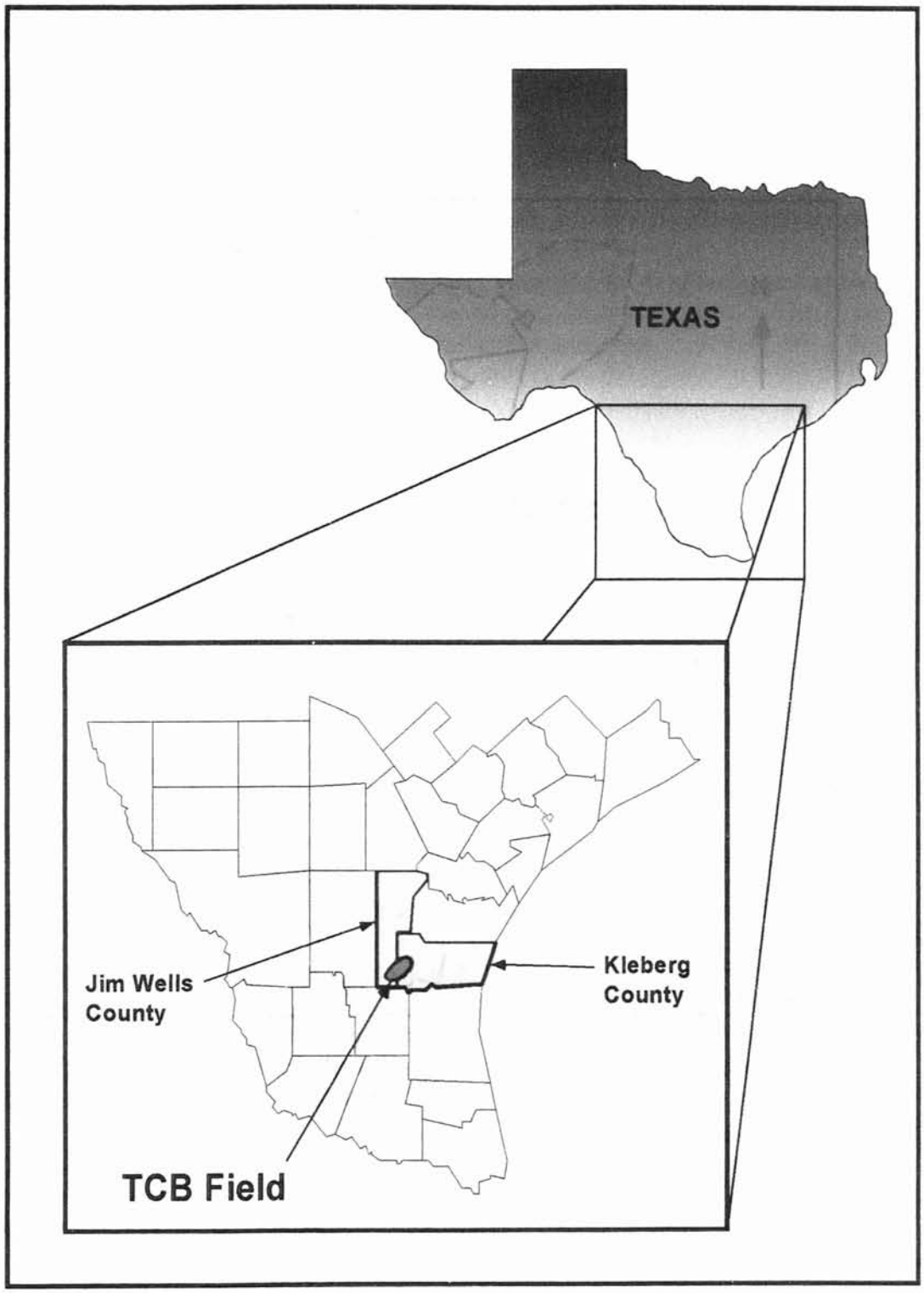

Figure 1. Location of TCB Field in Kleberg and Jim Wells Counties, Texas.

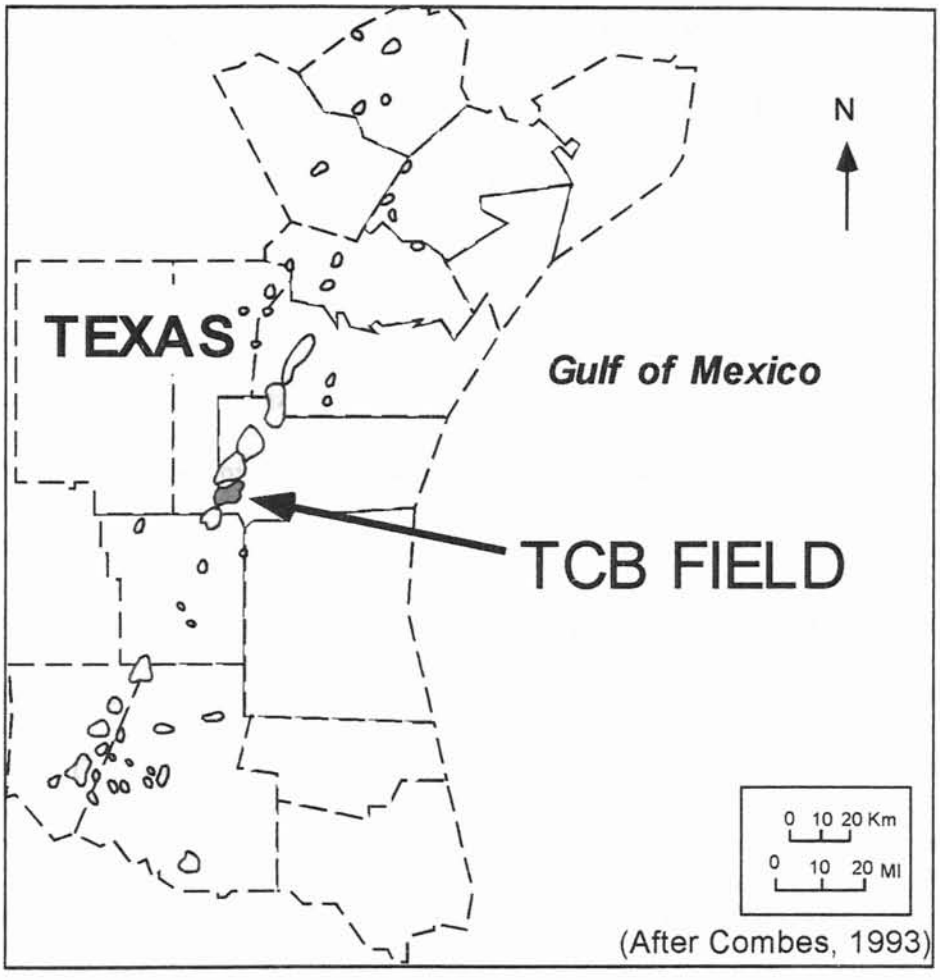

Figure 2. Location of the TCB field and Vicksburg production trend, Texas Gulf Coast.

has cumulative production of greater than 5 trillion cubic feet (TCF) gas and 320 million barrels of liquids (Combes, 1993). Within TCB field, LR/LC reservoirs have produced approximately 20.4 BCF and 451,000 barrels of liquids as of 1993 (P.I./Dwight's and Int. Oil Scouts Assoc.). Production in this area is considerable despite the difficulty that arises from the shaly sandstone problem. This study will discuss characteristics of reservoirs and seals within the Vicksburg sandstones. Methods of analysis may be applicable to oil and gas reservoirs with similar characteristics.

Procedure

Data was collected, utilizing wire-line logs, production records, and core evaluation. Kerr-McGee provided nine full-size cores representing both conventional and low contrast/low resistivity zones. Conventional zones are defined as intervals that lack abundant clay content, thus yielding correct log responses. On the other hand, low contrast/low resistivity zones contain abundant clay minerals, which mask the log responses. These cores became the foundation of the study and provided porosity, permeability, and fluid saturation data that were used to evaluate the effectiveness of petrophysical analyses in estimating rock and fluid properties. The LR/LC zones were identified in two cores; locally referred to as the 9900-ft sandstone. The cores above and below this stratigraphic interval contain conventional sandstone reservoirs. All cores were calibrated to wireline logs and studied using x-ray diffraction, petrographic methods, core-plug analysis, capillary pressure, and fluid-inclusion stratigraphy. In addition, the LR/LC (9900-ft) interval data set included high-resolution logs and micro-imaging logs that were calibrated to core. Data accumulated by these techniques were

integrated in order to identify reservoir and seal zones and evaluate reservoir fluid content.

The 9900-ft sandstone is a thick interval of thinly interbedded sandstone and shale. Conventional wire-line logs, such as dual-induction, do not resolve beds that are thinner than their vertical resolution. High-resolution logs and formation microimaging resolve beds as thin as one to six inches thick. These tools enhance wire-line log evaluation of LR/LC interbedded sandstone by identifying reservoirs and seals and improving Sw calculations.

Conventional zones above and below the 9900-ft sandstone interval were described and studied using similar rock and petrophysical techniques. Rock and fluid properties for these thicker conventional reservoirs normally can be determined using conventional wire-line log suites.

Petrographic methods

Detailed petrography included core description, thin-section analysis and scanning-electron microscopy. In all cores, sedimentary structures, textures, lithofacies, and fossil content were recorded.

Thin-section analysis focused on characterizing these rocks by identifying the detrital/authigenic constituents, porosity, and diagenetic alterations, such as cementing and dissolution. Thin-sections were selected according to different permeability and porosity zones.

The samples were analyzed using x-ray diffraction and scanning electron microscopy (SEM). X-ray diffraction was used to determine clay type. Authigenic clays, which are abundant in the 9900-ft sandstone, are considerably less apparent within the conventional sandstones above and below this interval. Clays identified in the 9900-ft sandstone are illite-smectite mixed layer, chlorite, and kaolinite. Clay is evident on x-ray diffractograms shown in Appendix C and in scanning electron microscope photomicrographs. X-ray diffractometry and scanning electron microscopy were used to determine the structure and amount of clay.

Formation Microimaging

Formation microimaging is a resistivity-measuring technology that measures micro-conductivity with closely spaced button electrodes found on pads (Halliburton, 1997 and Schlumberger, 1992). Typically the tools have six to eight pads and each pad has 24 electrodes (fig3). The numbering and spacing of the electrodes allow this tool to have a resolution of 0.2 to 0.3 inches. Microimaging tools originally were used as dip-meters and to identify fractures, faults and sedimentary structures. Microimaging tools are designed for fresh-water-based mud. Although the depth of investigation can be as much as 30 inches, this tool is most effective in measuring resistivity within the flushed zone (Rxo). Resistivity is affected by rock composition, fluid properties, and/or grain texture. Formation Microimager measurements are taken in the flushed zone, which result in the pore fluid remains relatively constant. Flushed zone resistivity is affected minimally by formation fluids, but is affected by mud resistivity and gas content. The microimager records differences in composition and the digital resistivity measurements are then

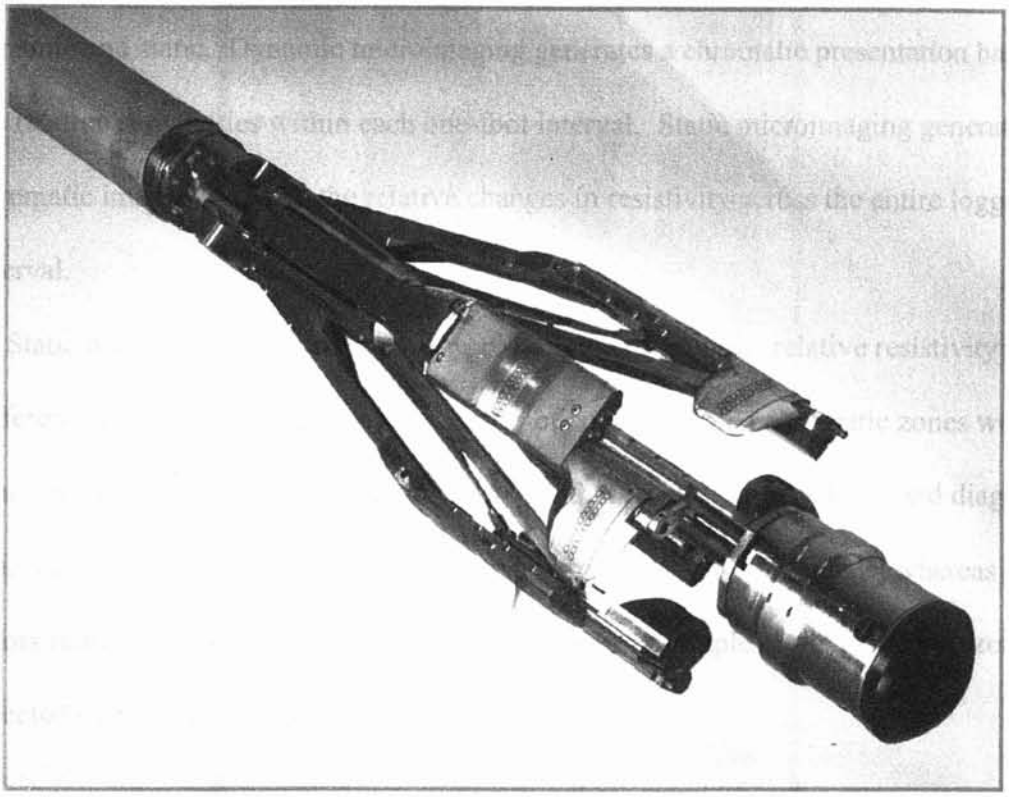

Figure 3: Photograph of Formation MicroImager (© Schlumberger).

converted to a color scale (Fig. 4). This scale identifies various chromatic zones that reflect differences in rock resistivity. Microimaging resolves lithology on the inch scale and thereby identifies sandstone packages and seal zones within the thinly bedded LR/LC interval.

Two methods of recording and presenting microimaging data are commonly used: dynamic and static. Dynamic microimaging generates a chromatic presentation based on the relative resistivities within each one-foot interval. Static microimaging generates chromatic images based on the relative changes in resistivity across the entire logged interval.

Static microimaging presentations were used to compare the relative resistivity with differences in lithology. As a result, a series of core-calibrated chromatic zones were established that reflect differences in resistivity that result from lithologic and diagenetic properties. In general, dark colors indicate low resisitivity, such as shale, whereas light colors represent higher resistivity. Figure 4 shows an example of the chromatic zones detected by microimaging.

Fluid-Inclusion Stratigraphy

Standard petrographic analysis was augmented by fluid-inclusion stratigraphy (FIS). Fluid inclusions were identified in thin section (Fig. 5) and analyzed using FIS. FIS analyzes volatiles trapped within fluid inclusions, using a quadrapole mass spectrometer (Fig. 6). Drill cuttings and core pieces were sampled for this test. Samples were loaded into trays covered with metal impact slug and placed into a vacuum oven. This process eliminated remaining adsorbed organic and inorganic volatile material up to Carbon 13.

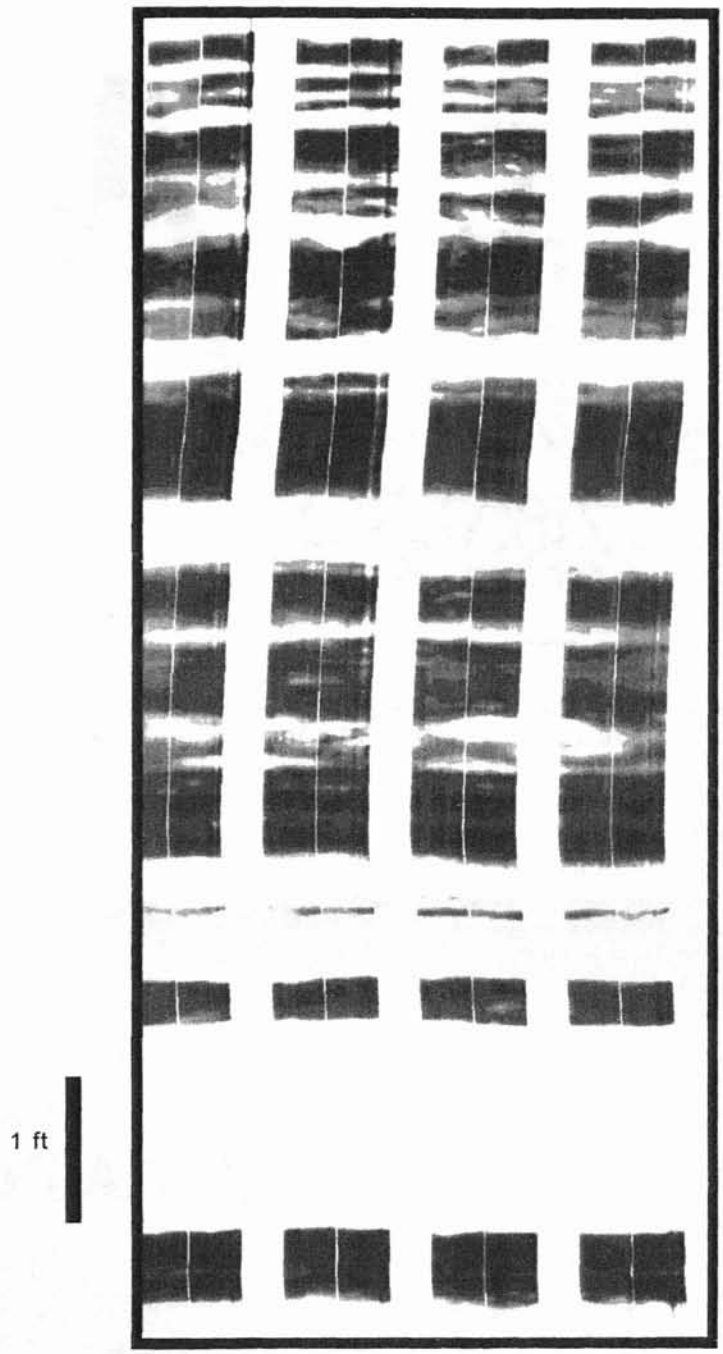

Figure 4. Formation Micro-Imaging Log depicting the various chromatic zones. Dark colors indicate low resistivity, while lighter colors reflect higher resistivity.

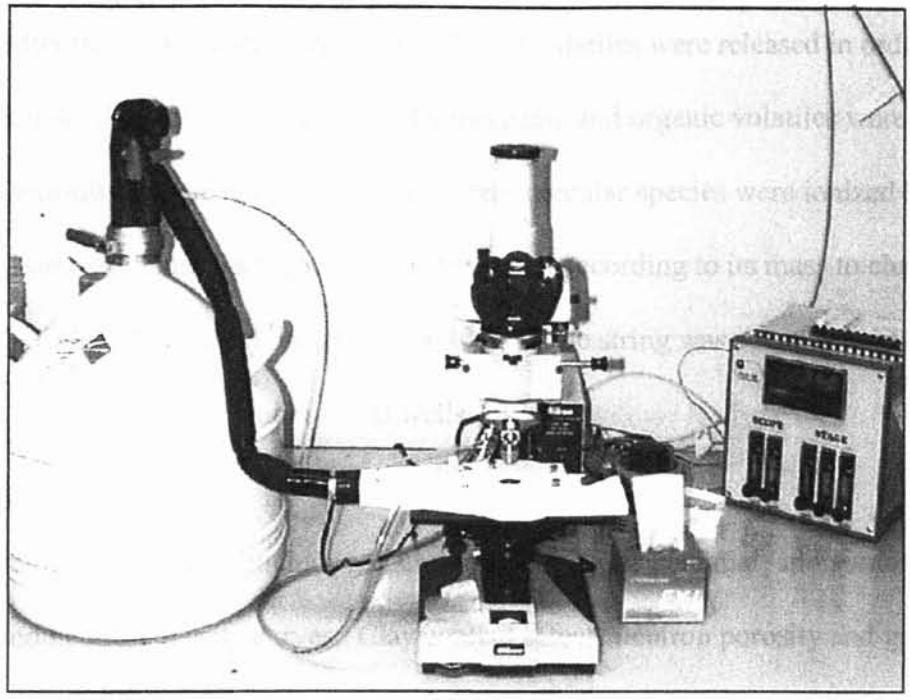

Figure 5: Petrographic microscope with USGS-type Gas-Flow heating/freezing stage allows highly accurate measurement of various phase transitions observable within fluid inclusions that are used to constrain pressure-temperature-timing relationships and the API gravities of oils .
(Fluid Inclusion Technology, Inc.)

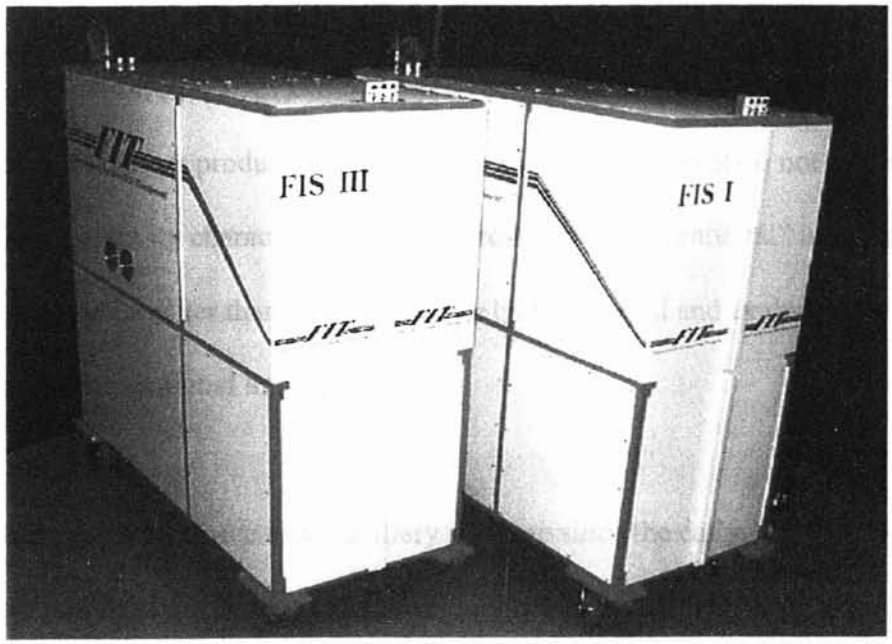

Figure 6: Automated Fluid Inclusion Analyzers
(Fluid Inclusion Technology, Inc)

Next the trays were placed into an ultra-high vacuum chamber and evacuated for eight hours. After the vacuum, the bulk fluid inclusion volatiles were released in order by an automated mechanical crusher. The inorganic and organic volatiles were sent through four-quadropole mass analyzers where molecular species were ionized by electron bombardment. Each species was separated according to its mass to charge ratio (m/z). (Hall, 1999; and Deyhim, 2000.) A 403-sample string was constructed from cuttings and core samples from several wells.

Wireline Logs

Conventional log suites include resistivity, spontaneous potential, and gamma ray, caliper and neutron/density curves. Clay content affects neutron porosity and generally results in high porosity.

High-resolution logs, such as array induction logs, record resistivity at five different investigation depths: 10, 20, 30, 60, and 90 inches. High-resolution tools that investigate at depths of 10 and 20 inches have vertical resolution of 1 foot and significantly improve formation evaluation (Li, 2001).

The upper and lower productive zones of the Vicksburg interval do not exhibit low contrast/ low resistivity characteristics. These zones are "conventional" in that the sandstone beds are thicker than 1.5 feet and can be recognized and evaluated by high resolution and conventional log suites.

Capillary Pressure

Petroleum engineers have used capillary pressure since the early 1940's to predict multiphase fluid behavior in reservoirs. Capillary pressure is defined as the difference in pressure between hydrocarbons and water. This pressure is the result of the interaction

between and within the fluid and the rock. It increases with increasing surface tension and decreasing pore-throat aperture.

Capillary Pressure can be utilized for many purposes, such as: determine sealing capacity, pressuring, pore throat aperture, evaluating fluid saturation and oil recovery, measuring irreducible water saturation, determination of displacement mechanisms, pay verses non-pay zones, thickness of the transition zone, and depth of reservoir fluid contacts. In this study, capillary pressure was used to evaluate the height of the hydrocarbon column, a measurement that reflects the ability of fluid to move through the rock. Capillary pressure data also indicate pore types within a reservoir and are especially useful in identifying bimodal porosity distribution between larger moldic or intergranular pores and micropores (Vavra, et. al 1992).

Capillary pressure can be measured by using the porous plate method, or mercury injection (porosimetry). The porous plate method is more expensive and uses actual or simulated hydrocarbon/brine systems to approximate wetting properties. Mercury injection is the least expensive method to obtain capillary pressure data. The mercury injection method uses a mercury/air system, which is converted mathematically into reservoir (gas/brine) conditions. Mercury injection was the method utilized in this study. Figure 7 shows the AutoPore IV mercury porosimeter used in this evaluation. Capillary Pressure data were obtained by the mercury injection of rock chips.

Two types of forces act upon capillaries. Cohesive forces are forces that act between surface tension and interfacial tension. Adhesive forces are the forces between the liquid and solid phases. When adhesive forces are greater than cohesive forces, the wetting fluid

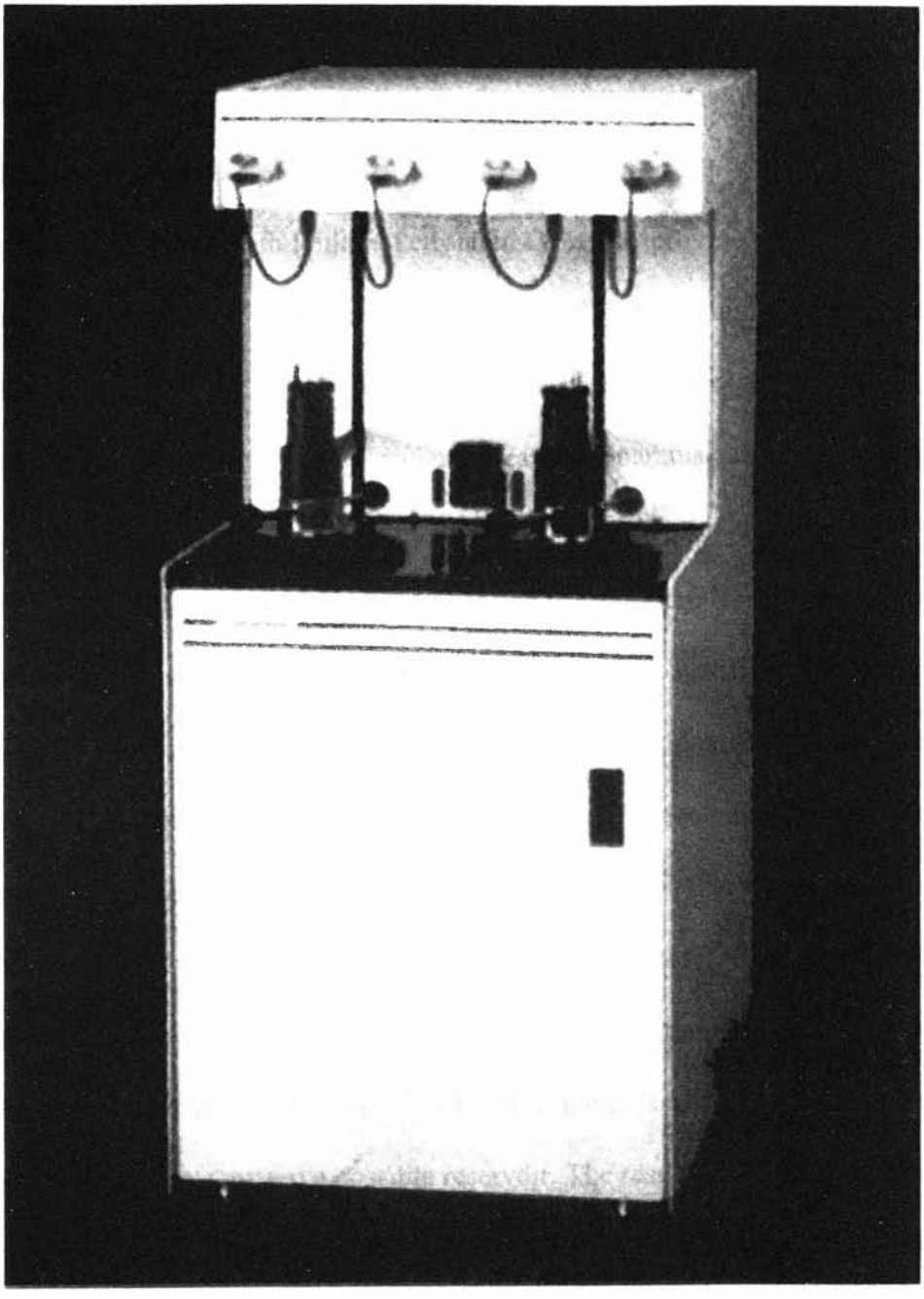

Figure 7: AutoPore IV Mercury Porosimeter. This apparatus can accurately gather data for calculation pore sizes, total pore volume, and many other parameters. Phillips Petroleum Company.

is the formation water. Capillary pressure occurs due to forces between fluids and the rock that bounds them (fig. 8).

Capillary pressure is greater when pore throats are smaller. This means that under these conditions more force is required for the nonwetting phase (hydrocarbons) to displace the wetting phase (water).

James Howard with Phillips Petroleum Company provided capillary-pressure measurements. Samples were taken from the 9900-ft, 9000-ft, and 10,250-ft sandstones. Rock chip samples were cleaned and porosity measured. Then samples were placed within the sample chamber of the capillary pressure apparatus used for measuring mercury injection pressure data (fig.9). Pressure began at 1 atm and was increased systematically. The amount of mercury injected was measured with each increase of pressure. With each pressure increment, the mercury-rock system was allowed to reach equilibrium while imbibition occured. It is possible to calculate injection pressure vs. mercury saturation by dividing the amount imbibed in the rock chip and the total pore volume of the rock chip. Mercury porosimetry measures capillary pressure and quantitatively describes seal capacity and pore-throat aperture. Pore-throat aperture dictates whether a rock is a seal or reservoir. Small pore-throat apertures have high capillary pressures and create seals. On the other hand, large pore-throat aperture results in low capillary pressure and a possible reservoir. The results show injected mercury as a function of pressure. These data are vital in understanding how capillarity works with reservoirs. Understanding how capillary pressure affects migration aids in the prediction of reservoir and seal zones, thus improving exploration stratagies.

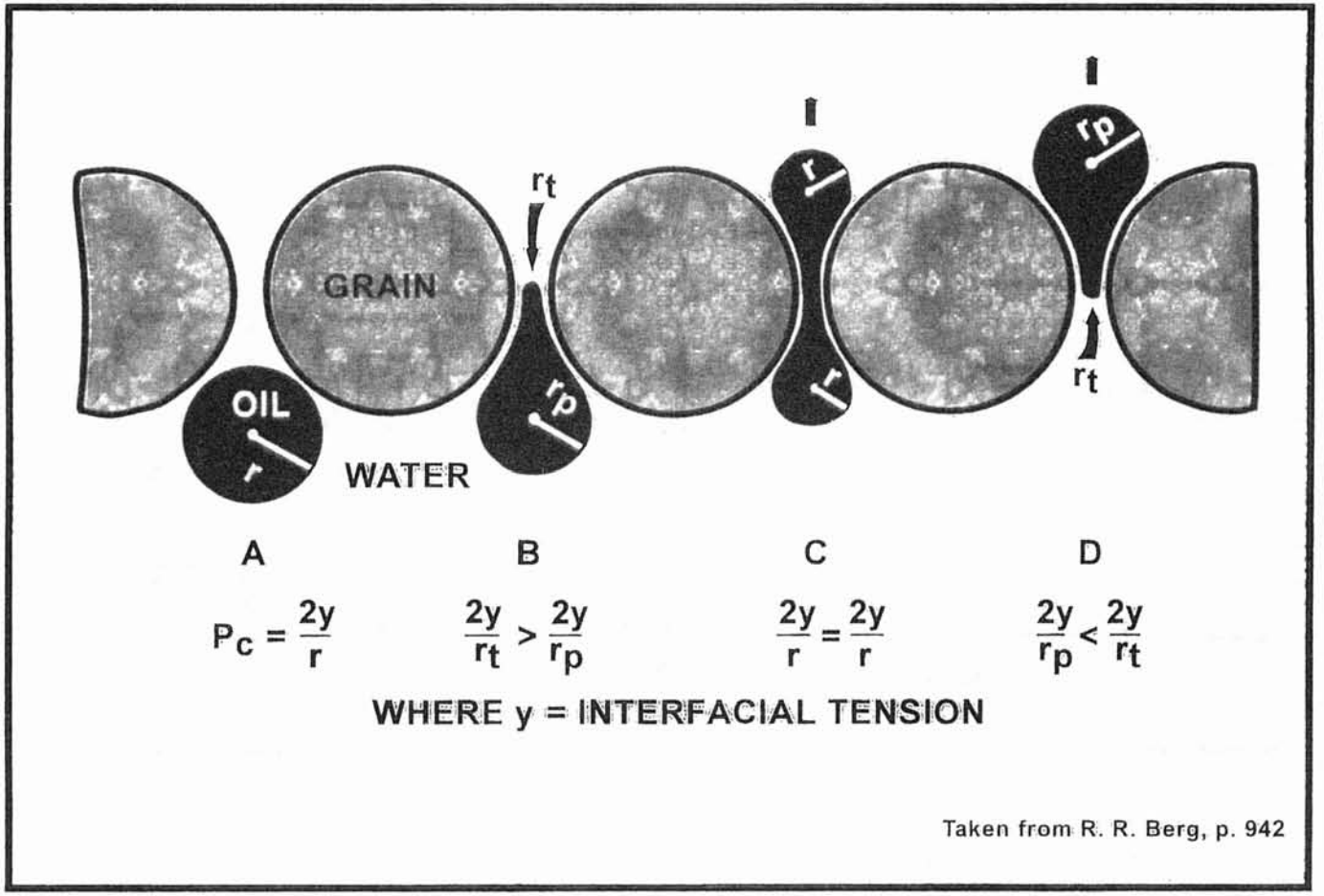

Figure 8: Capillary pressure occurs due to forces between fluids and the rock tht bounds them.

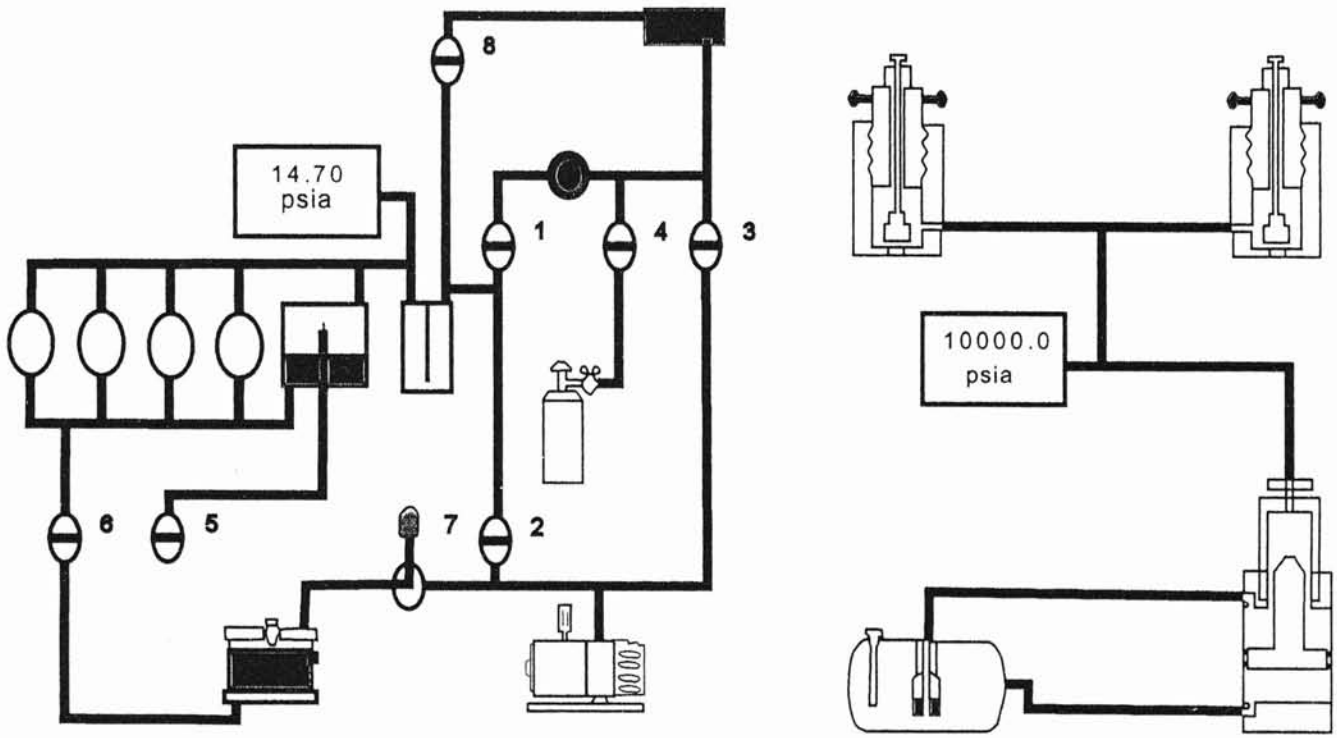

Figure 9. Schematic of the mercury injection porosimeter

CHAPTER II

GEOLOGIC SETTING

Stratigraphy

The Vicksburg Formation is Oligocene, and overlies the Eocene Jackson Shale and underlies the Oligocene Frio Formation (Fig. 8). The Vicksburg Formation is only present in the subsurface in Texas; however it crops out in Louisiana, Mississippi, Alabama, and Florida (Fig. 9). Locally, the Vicksburg is divided into upper, middle and lower intervals. Sandstone intervals are named according to depth encountered in early wells in Tijerian-Canales-Blucher (TCB) field (Fig.8) (Combes, 1993, and Al-Shaieb, 2000). Structural Setting

The Vicksburg is a series deltaic to shallow marine sandstones and shales, whose depositional setting of which was influenced by structural features. Three distinct structural features are the Houston embayment, San Marco arch and the Rio Grande embayment (Fig. 10). The Houston embayment is a sub-basin located in the east central part of the coastal plain. The San Marco Arch is located farther south along the coast. This arch provided a stable platform during deposition in the Oligocene age. The Rio

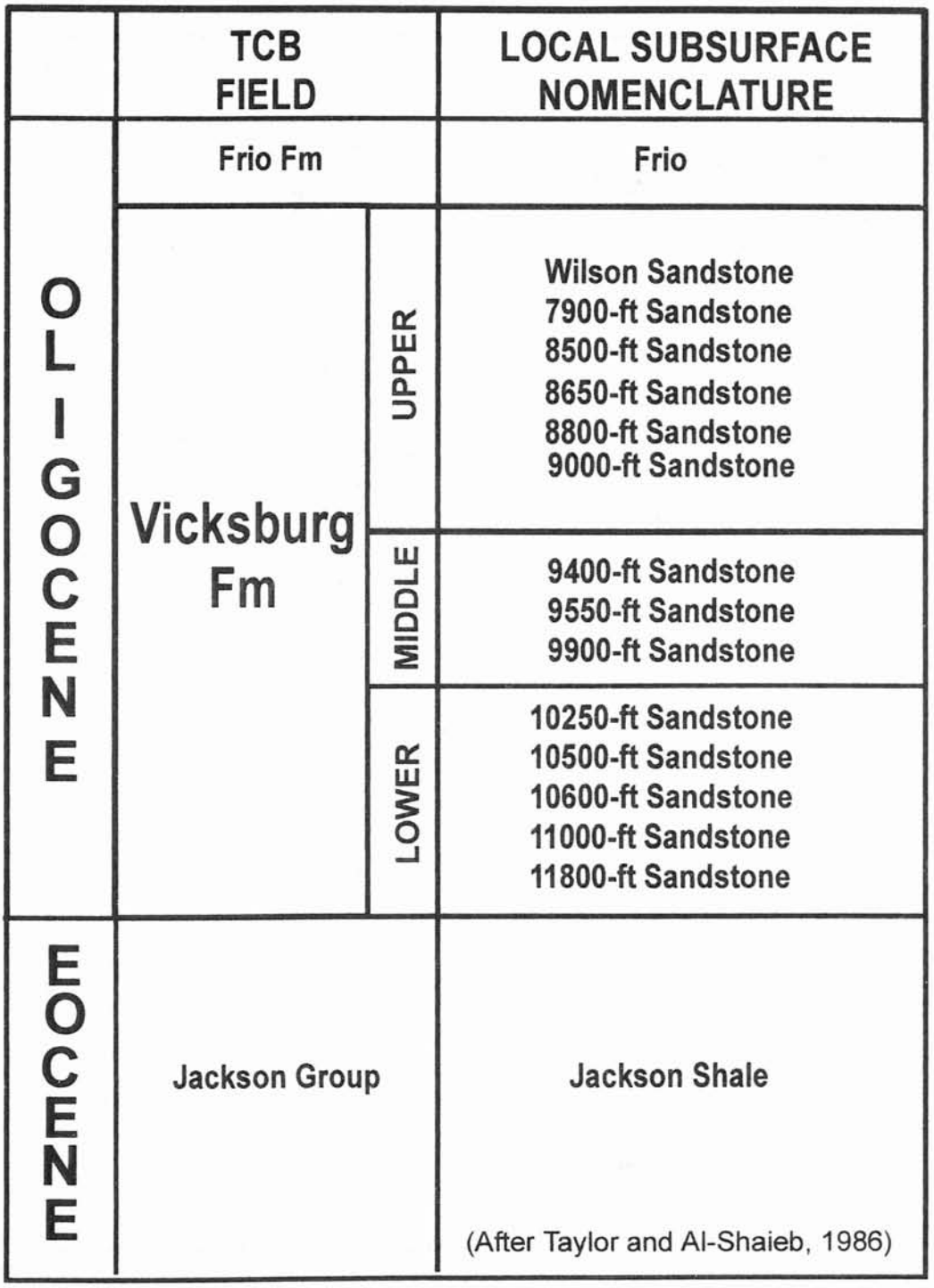

Figure 8. Stratigraphic nomenclature of the TCB field area.

VICKSBURG ISOPACH

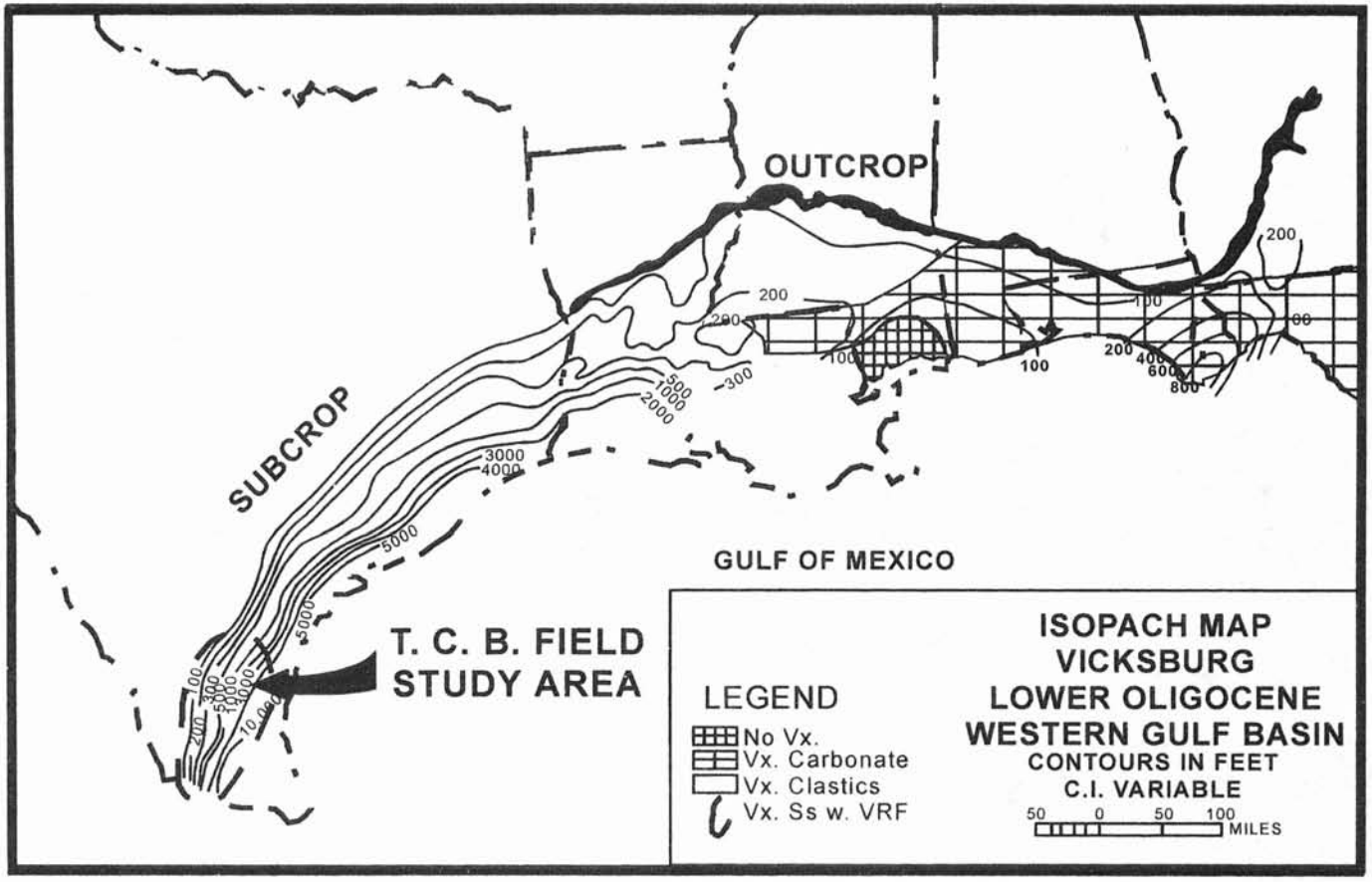

Figure 9. Vicksburg isopach map showing outcrop, subcrop, lithologic variation and location of TCB study area within volcanoclastic anomoly. Modified from Tipsword (1969), Hunter (1979), and Han (1981).

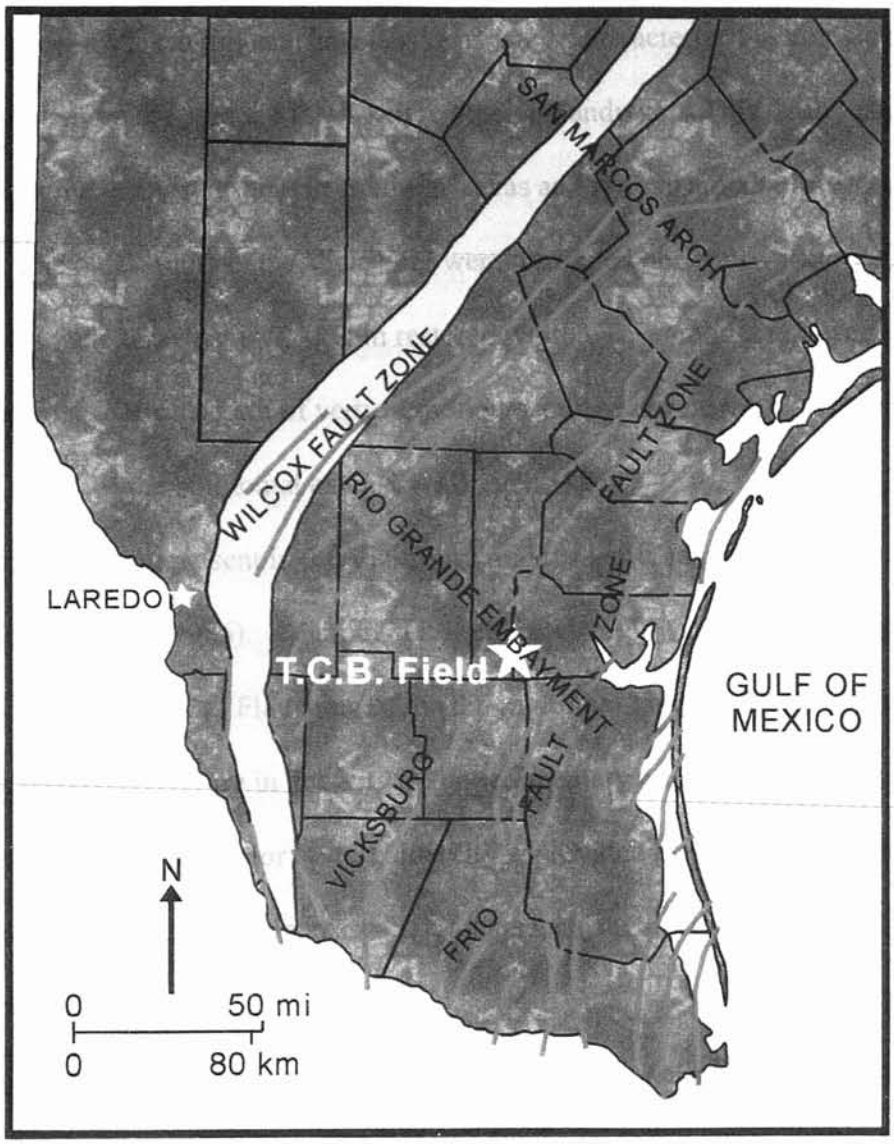

Figure 10. Map of south Texas showing location of TCB field in relation to major fault zones. (Modified from Berg,Marshall, and Shoemaker).

Grande Embayment is found farther south along the coastal plain. TCB field is located within this sub-basin (Coleman, 1982).

The Oligocene Vicksburg detachment system can be characterized as containing expanded sequences of sediment that become younger landward. This large shale-based detachment is recognized onshore in southern Texas and is an example of extreme extension. The oldest units in the Vicksburg were translated horizontally more than 16km along a fault zone that is 2.4 km in restored width. This amount represents over 600% extension. About 1.2 km of vertical motion occurred during the Vicksburg extension, or 7% of the horizontal extension (Diegel, 1995).

The type of faulting present in the Vicksburg trend is listric normal growth faults (Taylor and Al-Shaieb, 1986). A listric fault is characterized by a decreasing angle of dip with depth (Shelton, 1986). Flattening of the dip of normal faults in the Rio Grande embayment is due to increase in ductility in the sedimentary prism.
According to Coleman and Prior (1982), ductility is provided by the Eocene Jackson shale and resulted in extension-increased fault displacement and a more pronounced rollover structure.

Faults along the Vicksburg trend were active syndepositionally as a result of rapid sedimentation at the shelf margin on ductile Eocene strata (Winker, 1982). Fault systems consist of interconnected faults that generally parallel the present coastline and track the shelf margin position at the time of deposition (Winker, 1982). Faulting occurred at the time of basinward shifting of the continental shelf margin, in response to deposition associated with prograding lower Vicksburg deltas. Sedimentary sections tend to thicken

across the fault zones, due to syndepositional movement along growth faults (Combes, 1993).

Rollover anticlines formed due to the syndepositional faulting and were identified seismically (Fig 11). These rollovers provide a structural closure to trap hydrocarbons and are located on the downthrown side of the fault (Coleman and Prior, 1982). Rollover anticlines form when materials containing high amounts of water and gas flow from higher levels on the delta front, and sediments accumulate on the downthrown side of the fault resulting in dewatering and degassing of the sediments. The volume of sediment decreased, allowing change in density to occur at approximately the same time as the fault movement. The increased amount of sediment added to the overburden pressure and increased displacement along the fault, thus creating a rollover structure that can be recognized in seismic data (Coleman and Prior, 1982). These penecontemporanous growth-faults strongly influenced deposition, generating the Vicksburg structural style.

Sequence Stratigraphy

Tectonics and eustasy control the amount of space available for sediment to accumulate, and tectonics, eustasy and climate interact to control the sediment supply and how much of the accommodation space is filled (Emery and Myers, 1996).

Systems tracts are composed of three-dimensional assemblages of lithofacies that are defined by their position within the depositional sequence and by their parasequence-stacking pattern (Fig 12). Each sequence consists of three systems tracts arranged in this vertical succession, the lowstand, transgressive and highstand systems tracts.

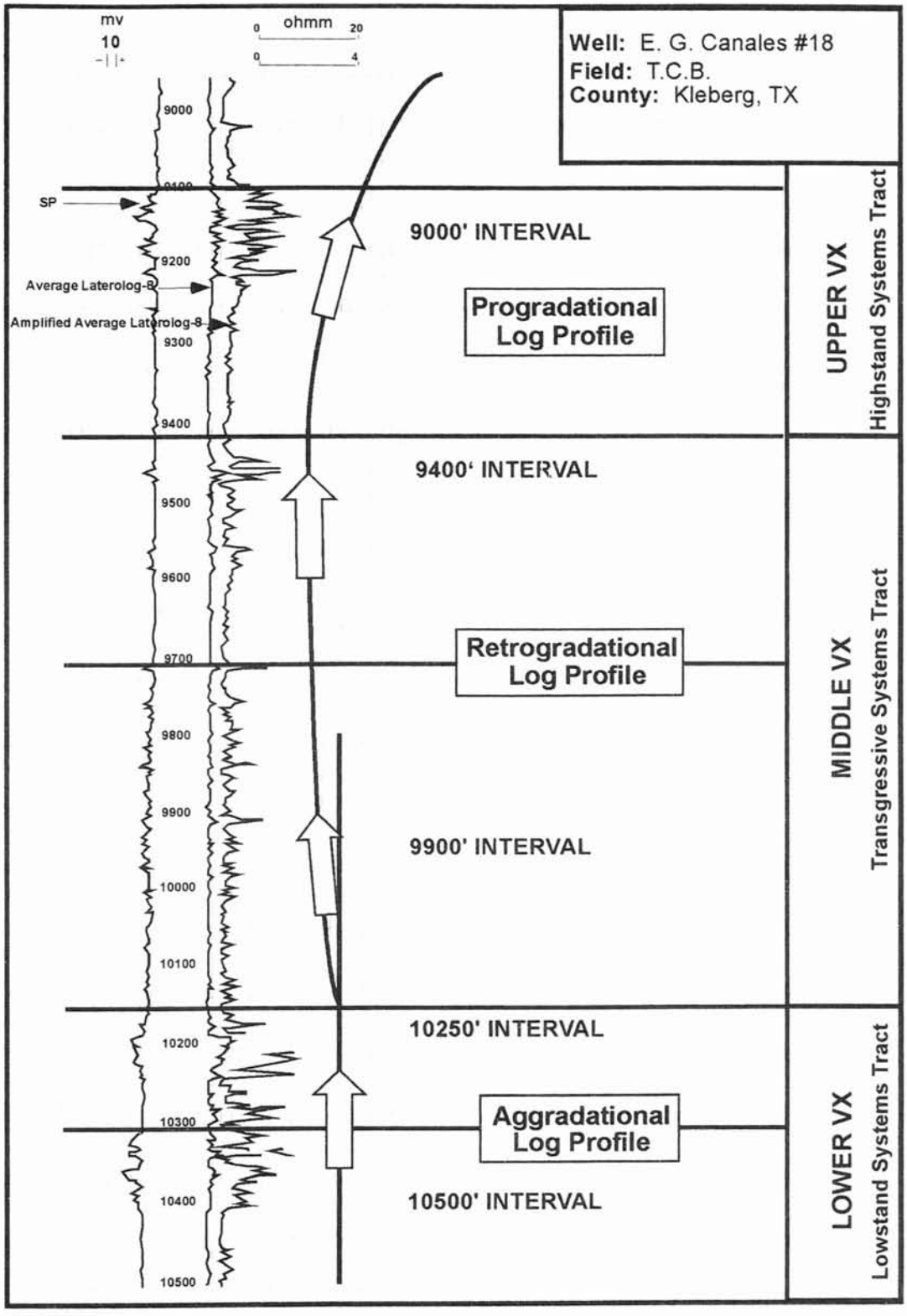

Figure 12. Well log lithofacies interpreted for sequence stratigraphic parasequence stacking patterns and systems tracts.

The lowstand systems tract overlies a type 1 sequence boundary and is capped by a transgressive surface. It is composed of progradational and/ or aggradational parasequence sets.

The transgressive systems tract is characterized by an overlying transgressive surface and capped by a maximum flooding surface. It is composed of retrogradational parasequence sets.

The highstand systems tract succeeds the maximum flooding surface, and is capped by a sequence boundary. It is composed of aggradation and/or progradational parasequence sets. The sequence stratigraphy of the TCB field was studied by Al-Shaieb and Birkenfeld (2000). Their methodology included 3-D seismic analysis, core calibration to logs, and facies characterization from core analysis. The lower Vicksburg (10,250-11,800 ft) is described as a progradational wedge that is deposited within an aggradational lowstand systems tract (Al-Shaieb et al., 2000; Combes, 1990). The depositional trend of this interval was determined using well logs. The logs suggest a repetitive nature of progradational patterns. The data were utilized to created isopach maps of the 10,250-ft. sandstone (Fig. 13). The map depicts a prograding delta lobe.

The upper Vicksburg (9,000ft- Wilson) represents sheet sands that were deposited within the highstand systems tract. These sheet sands can be identified as continuous high-amplitude beds on the seismic cross section (Fig. 14). An isopach map was constructed using well-log data to delineate the general trend of the 9,000-ft. sandstone (Fig. 15). The thickness distribution suggests that the upper Vicksburg is a prograded fluvial/deltaic system.

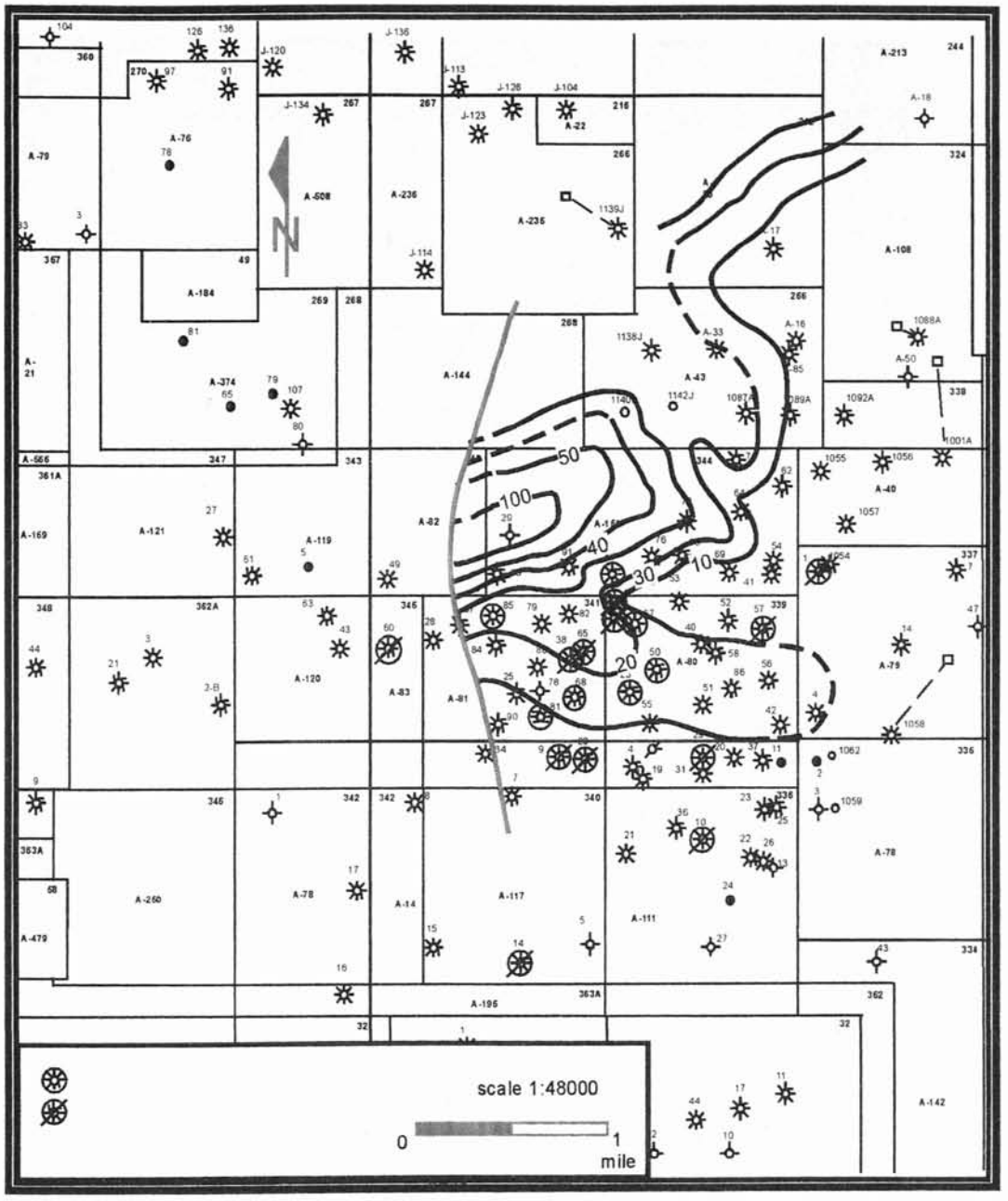

Figure 13. Isopach map showing the prograding deltaic nature of the 10250 ft. Lower Vicksburg interval.

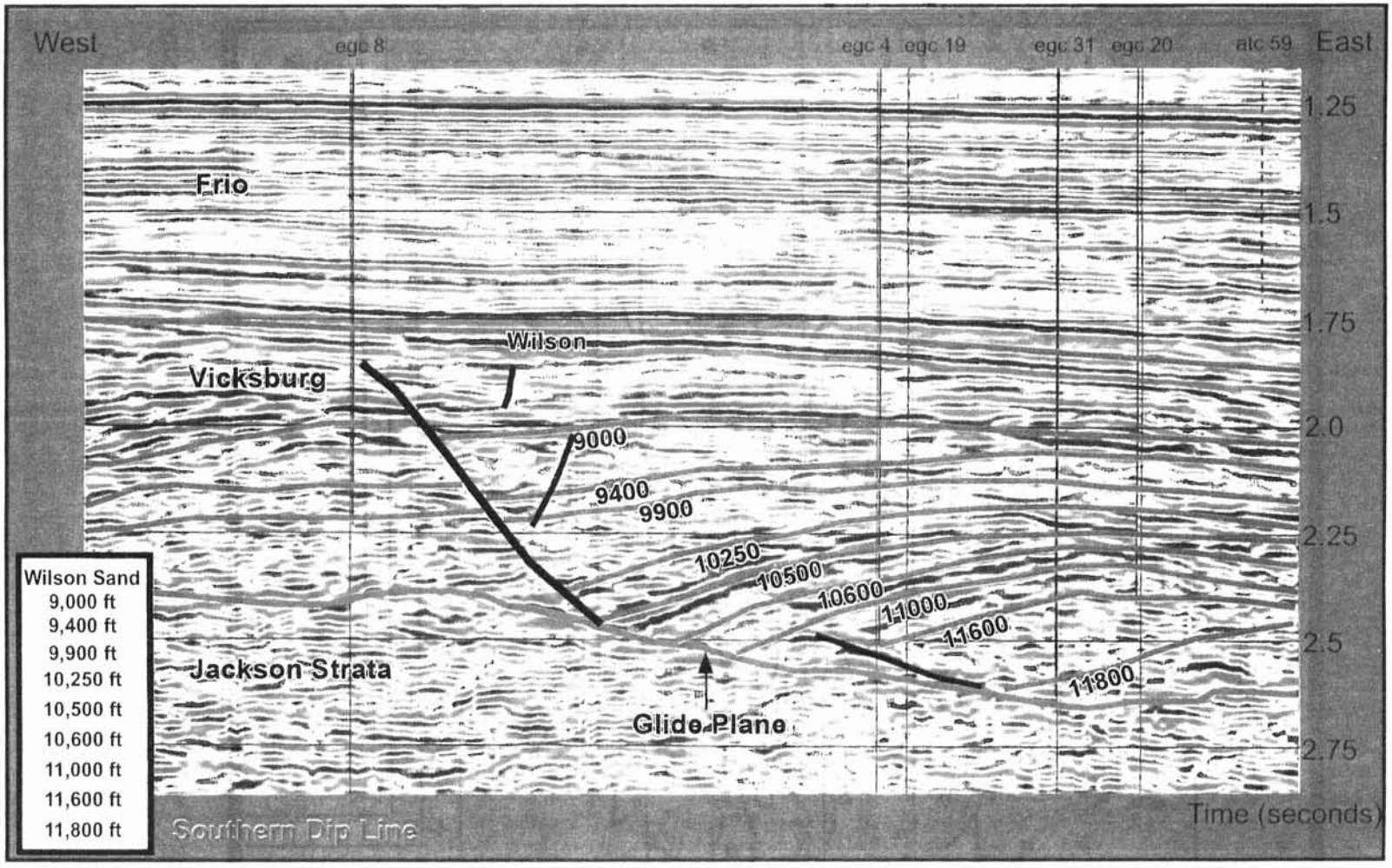

Figure 14. Dip oriented color amplitude seismic section interpreted with TCB field stratigraphy. The 9,000-ft sandstone depicts continous sheet sands which display high amplitudes.

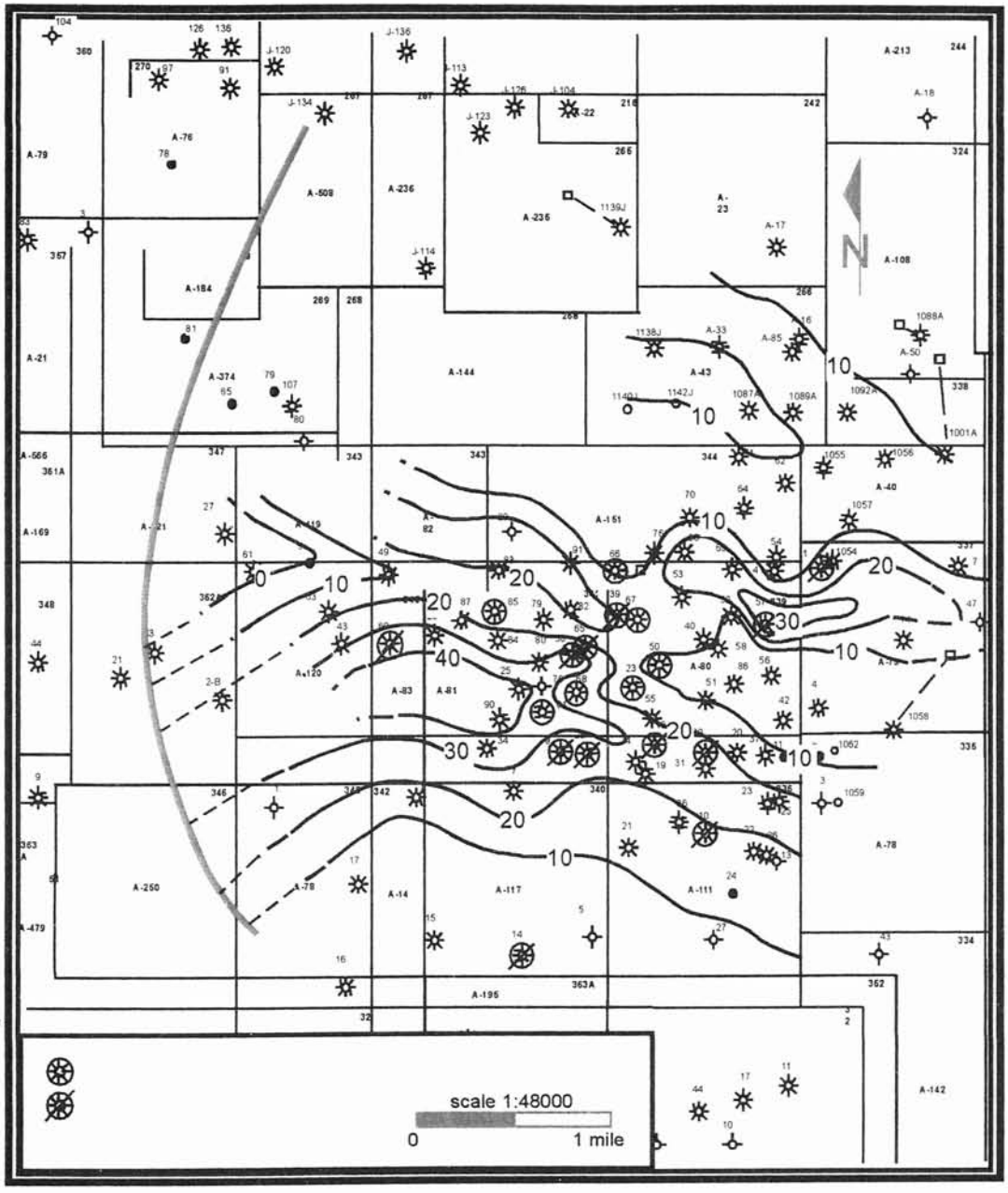

Figure 15. Isopach map of the 9000 ft. interval representing the Upper Vicksburg style of deposition. The overall prograding deltaic trend is illustrated.

The middle Vicksburg interval contains indicators of a marine influence including increased fossils, and glauconite. Thickening of sandstone and shale interbeds is evident within this interval. This suggests that movement along the fault was the greatest during this time. Movement along the growth fault can be determined from seismic data. Deposition during the middle Vicksburg tends to be repetitive due to sea level fluctuation. The resulting isopach map of the 9,900-ft sandstone indicates retrogradational depositional style within the transgressive system tract (Fig. 16).

The sequence-stratigraphic interpretation of the Vicksburg Formation in the TCB field is based on the integration of chronostratigraphic charts, patterns of core based well log lithologies, well log facies stacking patterns and seismic sequence stratigraphy. These separate sources of data were assembled and used to develop the Vicksburg depositional model in the TCB field area.

Depositional Environment

The Oligocene Vicksburg Formation is interpreted as a series of prograding deltas that are separated by marine transgressions (Combes, 1993; Combes-Coleman 1990; and Taylor and Al-Shaieb, 1986). The depositional style is influenced by structure as thicker sand sequences accumulated on the downthrown sides of faults. These sand sequences thinned over the crest of the anticlines and distally into the basin. The depositional environment for the Vicksburg sandstone ranged from shallow marine to fluvial-deltaic. Cores from six wells were examined by Birkenfeld (2000), in order to establish three informal subdivisions of the Vicksburg, the Lower, Middle and Upper. Cores were calibrated to wireline logs, and environments and lithofacies were interpreted. The

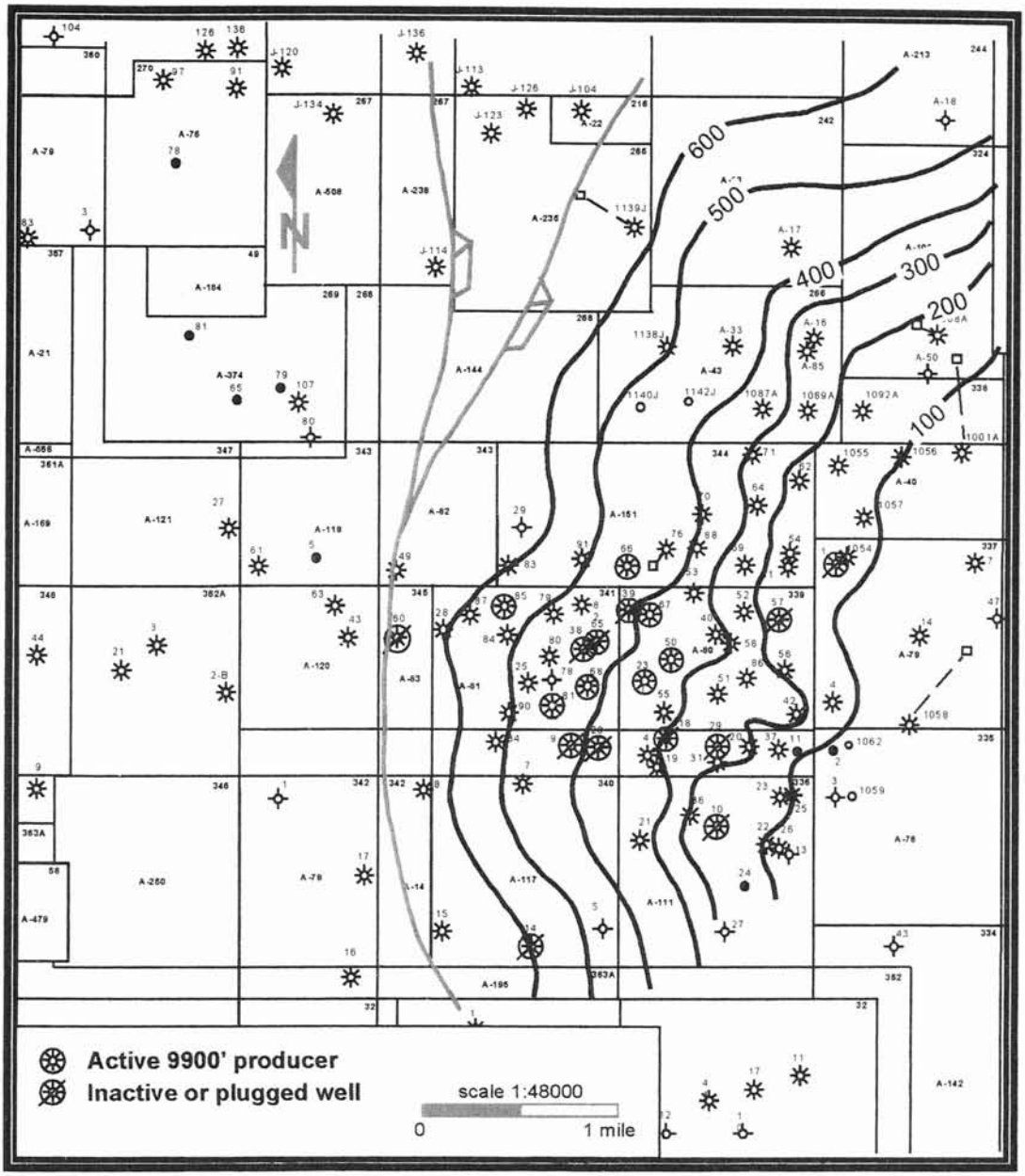

Figure 16. Thickness of the 9900-ft sandstone interval showing thickening of the sandstone toward the fault and thinning basinward across the crest of the rollover anticline in the TCB field.

environments ranged from deltaic to marine shoreface. Lithofacies observed in the cores/logs were grouped into three basic depositional environments based on Coleman's and Prior's (1982) work. These lithofacies are the upper delta plain, the lower delta plain and the subaqueous delta plain.

Lower Vicksburg Facies

Two wells contained cores within the lower Vicksburg: the E.G Canales #18 and A.T. Canales #55. The cored intervals included 10,600-ft, 10,500-ft and 10,250-ft sandstones. Through core description, petrolog and thin-section analysis the depositional environment was determined.

This portion of the Vicksburg strata was interpreted as a subaqueous prograding to upper delta plain system. The base of each interval started as a prodelta mud that shallowed upward into a bar facies that is capped by channel-fill sands. This interval is then capped by another prodelta complex of the next prograding interval.

The Lower Vicksburg facies was correlated to wire-line logs of well #18 and #55 in order to determine a characteristic lithofacies log response for each interval. A repetitive progradational pattern characteristic of the sandstone intervals was interpreted from these well log responses (Fig. 17).

Middle Vicksburg

The wells examined within this zone are the A.T Canales #85 and #81. This interval contains the 9,900-ft sand. This portion of the Vicksburg section is interpreted as representing a subaqueous delta plain environment of deposition. The interval is divided

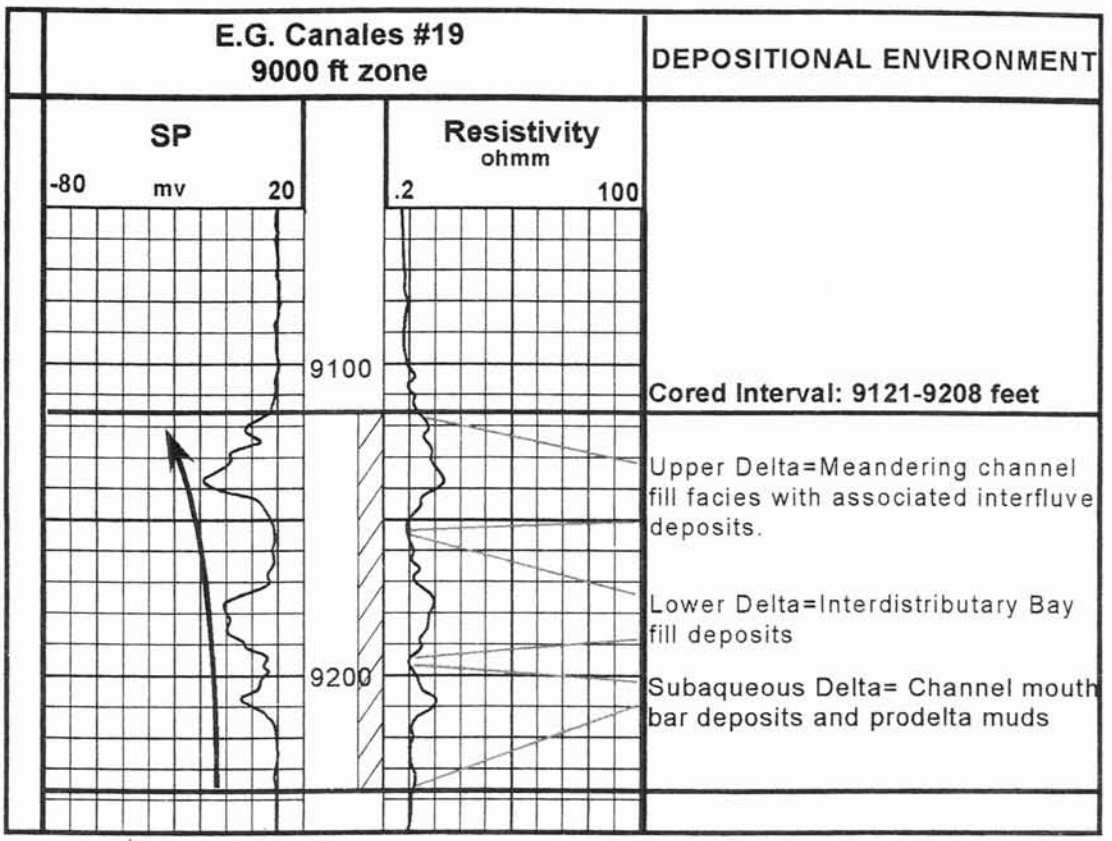

Figure 17. Well log response depicts the progradational nature of the Upper Vicksburg interval. (After Birkenfeld, 2001)

into a basal shale-dominated open marine environment that grades into shallower marine and then reverts to deeper marine as sea level fluctuated. This depositional pattern is repetitive and the sand/mud ratio generally increases with depth suggesting an overall shallowing or upward cleaning. The characteristic well-log response for this interval tends to reflect an overall retrogradational trend of deposition (Fig. 18).

Upper Vicksburg

The cores examined within this interval are the E.G. Canales #19, and #26. Both sandstone intervals examined in the upper Vicksburg strata are interpreted as representing deposition in a subaqueous delta plain environment that prograded into an upper delta plain environment (Fig. 19). The base of each interval began with channel mouth bar deposits that graded upward into a channel fill or point bar deposits. The 8800-ft interval contains facies similar to the underlying 9,000-ft interval. This stratigraphic relationship suggests that each interval represented a separate stage of progradation as the fluvial/deltaic system in the Upper Vicksburg built upon itself.

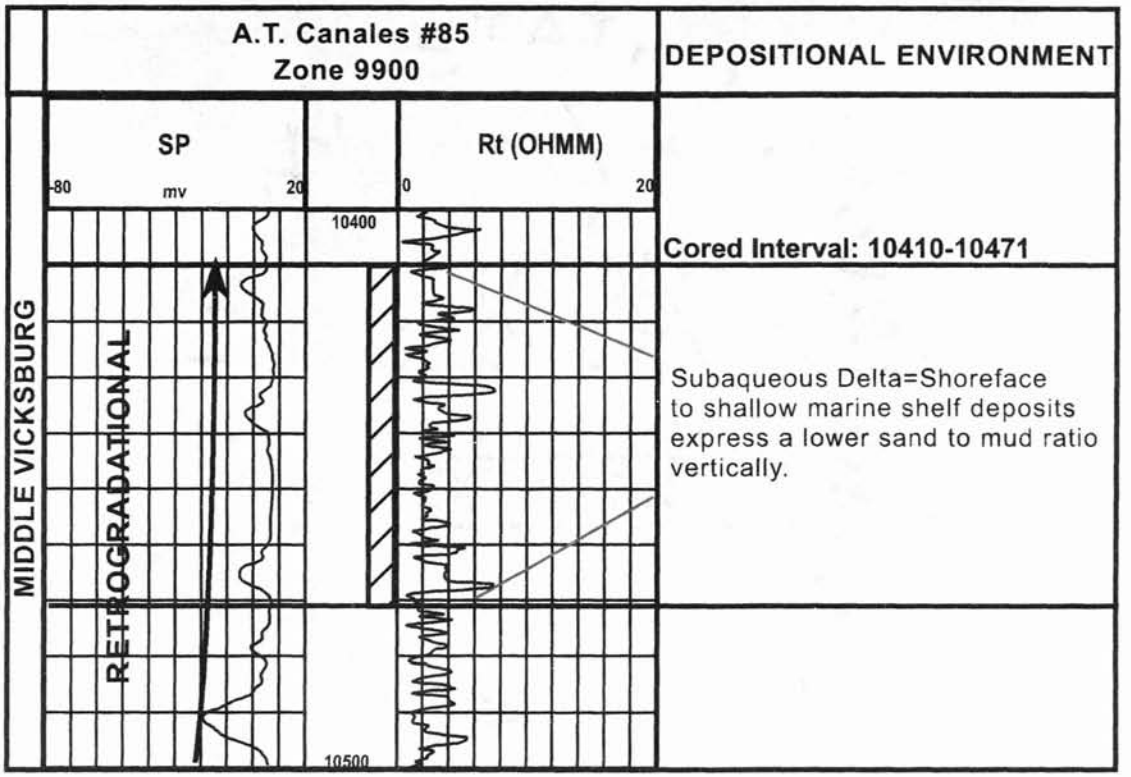

Figure 18.. Well log to lithofacies response calibrated to core taken from the 9900 ft. interval . The retrogradational characteristic of the Middle Vicksburg is illustrated. After Birkenfeld, 2001

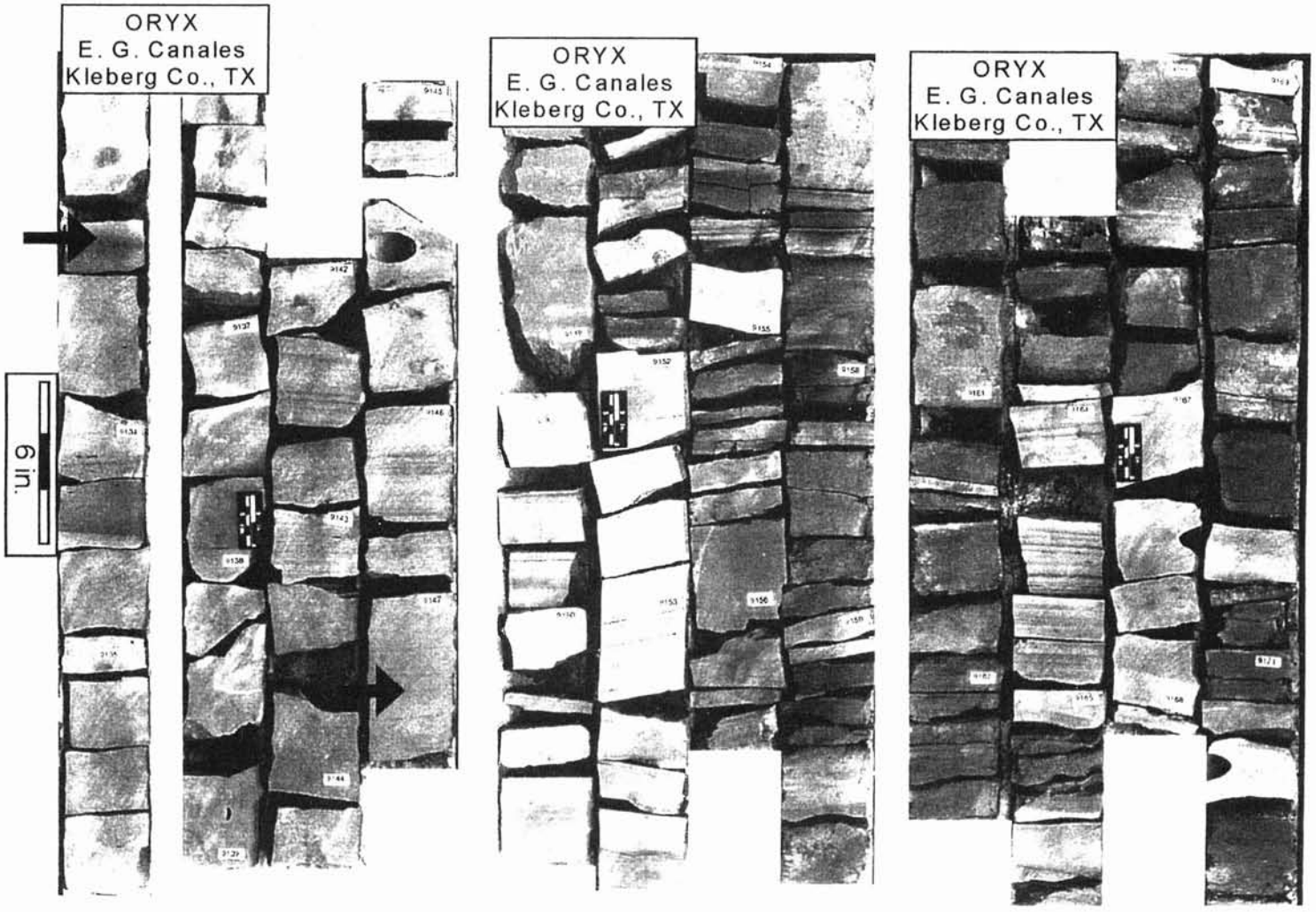

Figure 19: E.G. Canales #19 interpreted deposition is subaqueous delta plain environment.

Chapter III

Reservoir Controls

General Statement

Vicksburg sandstones were analyzed comparatively to determine if indivdual systems tracts exhibit differences in composition (detrital and authigenic constituents) and porosity. This analysis was conducted primarily using forty-eight thin sections from five Vicksburg cores. The fabric of the sandstones was described and constituent percentages determined by the point count method. Ten point counts were acquired from each thin section. Thin section data was supplemented with capillary pressure measurements, formation microimaging and fluid inclusion stratigraphy analyses. These data aided in determining factors that control reservoir quality within the Vicksburg Sandstone.

Reservoir controls of the Highstand systems tract

Introduction

Vicksburg Highstand system tract (HST) rocks were studied in two wells: the E.G. Canales #19, which contains the 9,000-ft sandstone and the A.T. Canales #26 that contains the 8,800-ft sandstone (Fig. 20). Petrologic and petrophysical parameters were established to evaluate the reservoir quality. The upper Vicksburg interval is composed

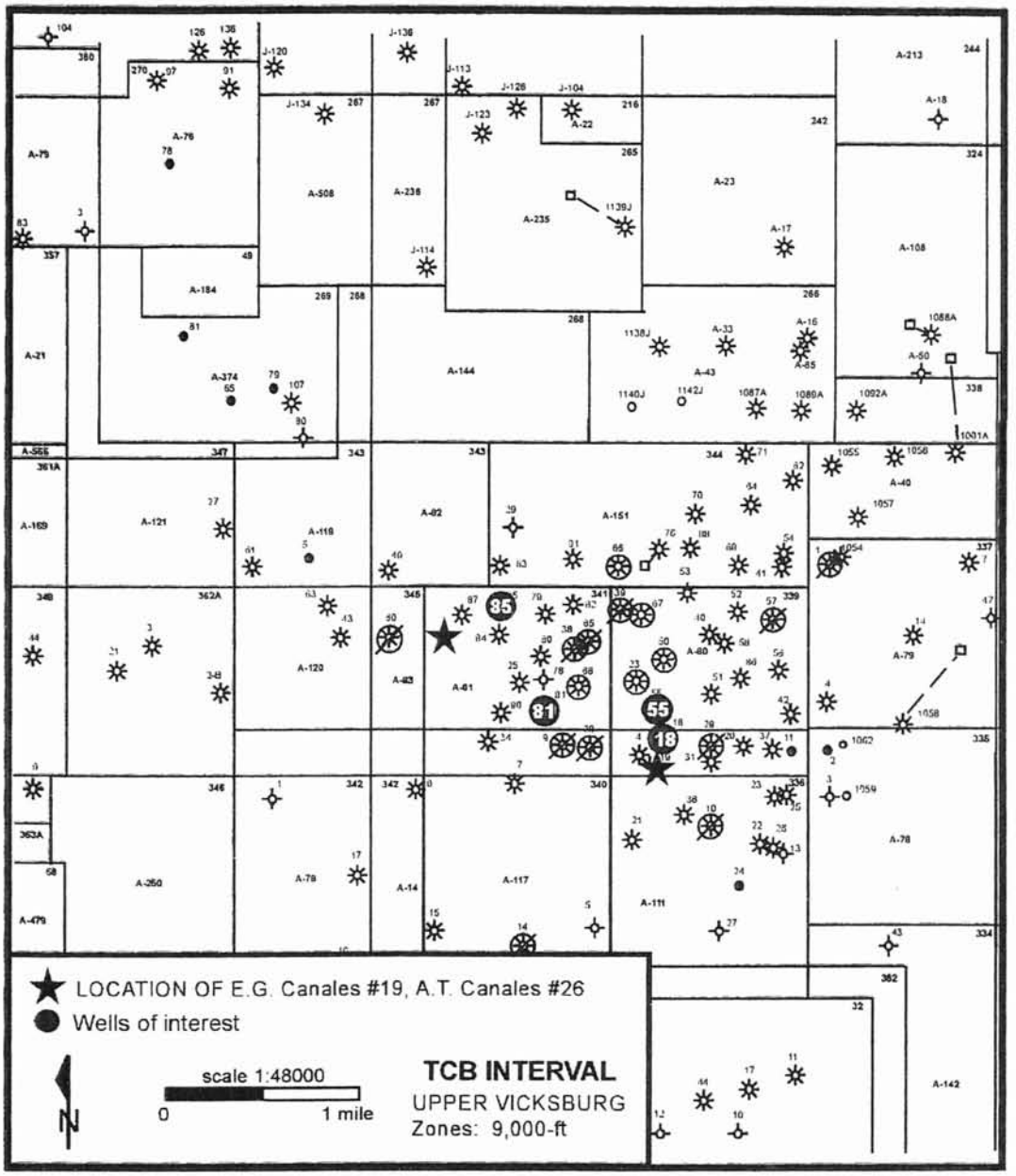

Figure 20. Location of the E.G. Canales #19 and the A.T. Canales #26 in the Upper Vicksburg interval.

of thicker sandstone units and micro-imaging techniques and high-resolution logs were not necessary to acquire wireline log derived properties within this zone.

Petrology

Classification

The Vicksburg sandstone within all systems tracts studied consists of similar detrital and diagenetic products. According to the Folk (1974) QRF ternary diagram, HST sandstones classified on average as a feldspathic litharenite (Fig. 21). The average grain size of the samples varied according to the zone. Within reservoir zones, grain size is relatively larger than in seal zones. Grain sizes in the HST range from very fine sand to coarse silt.

Detrital Constituents

Major detrital consitituents of the 8800-ft and 9000-ft sandstones are quartz, feldspar, chert, volcanic rock fragments (VRF), and carbonate rock fragments (CRF) Quartz is the most abundant detrital constituent, representing on average 26.5% of the rock studied (Fig. 22). Although most quartz grains displayed typical straight extinctions, some quartz grains developed undulose extinction due to stress. Fluid inclusions are common within quartz. Feldspar, which averages 9.3% in the samples studied, is mainly plagioclase that exhibits albite twinning. The plagioclase has undergone high levels of diagenesis and is often partially dissolved (Fig. 23). The

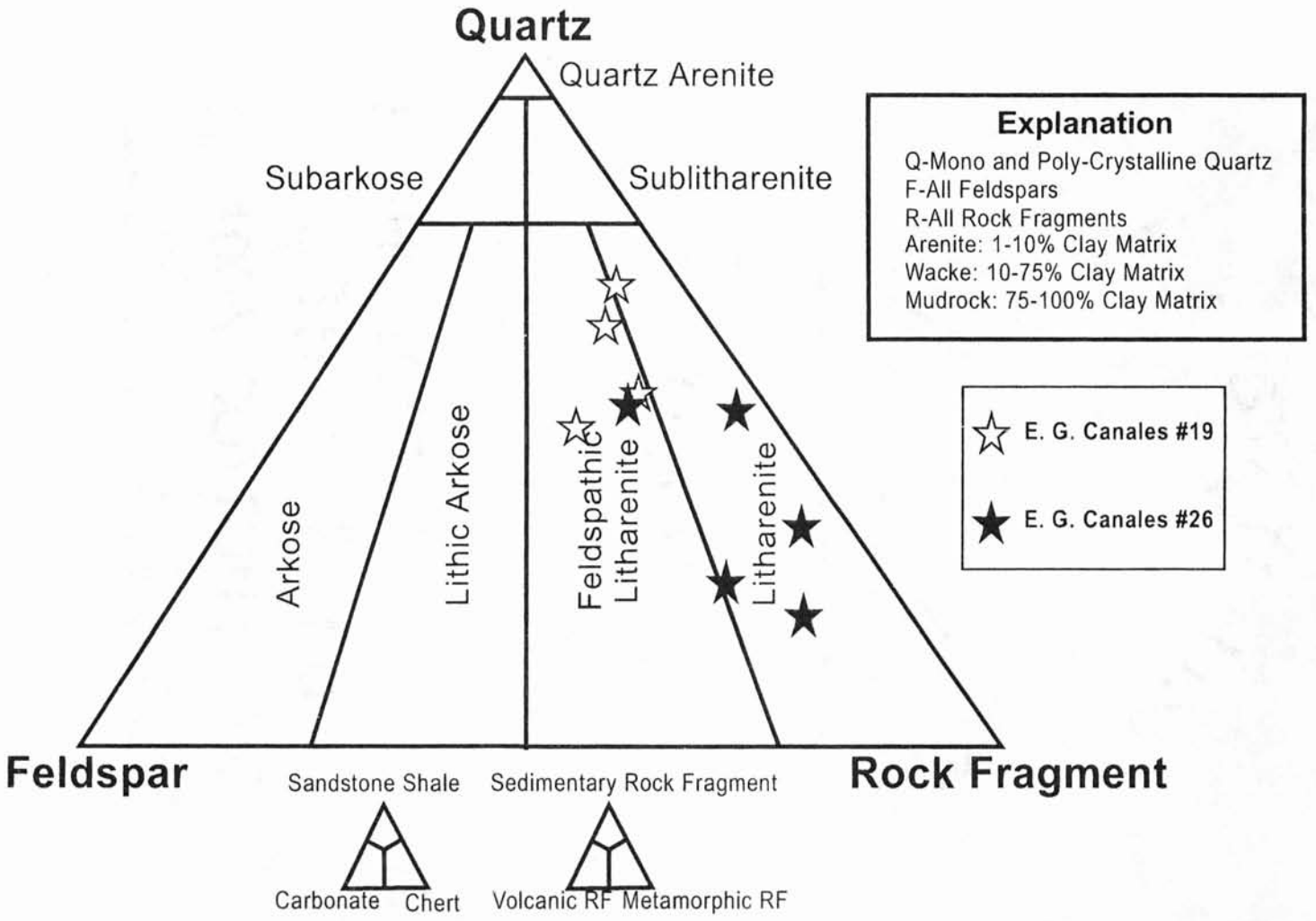

Figure 21. Compositions of the HST, wells #19 and #26 plotted on QRF diagrams (Folk, 1974).

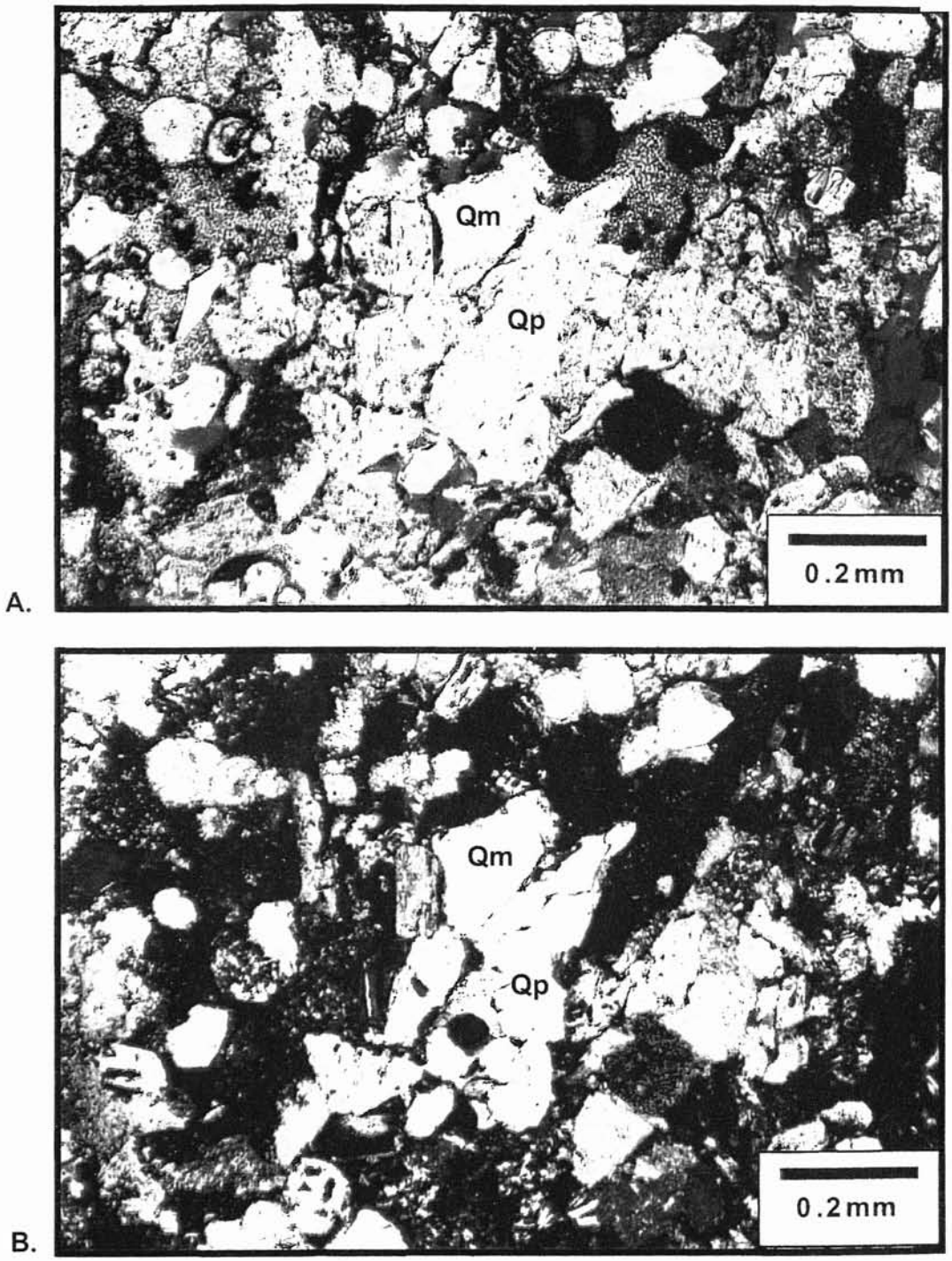

Figure 22. Photomicrograph of monocrystalline(Qm) and polycrystalline (Qp) quartz grains.
A. Plane polarized (PPL).
B. Cross-nichols (XN).

A.

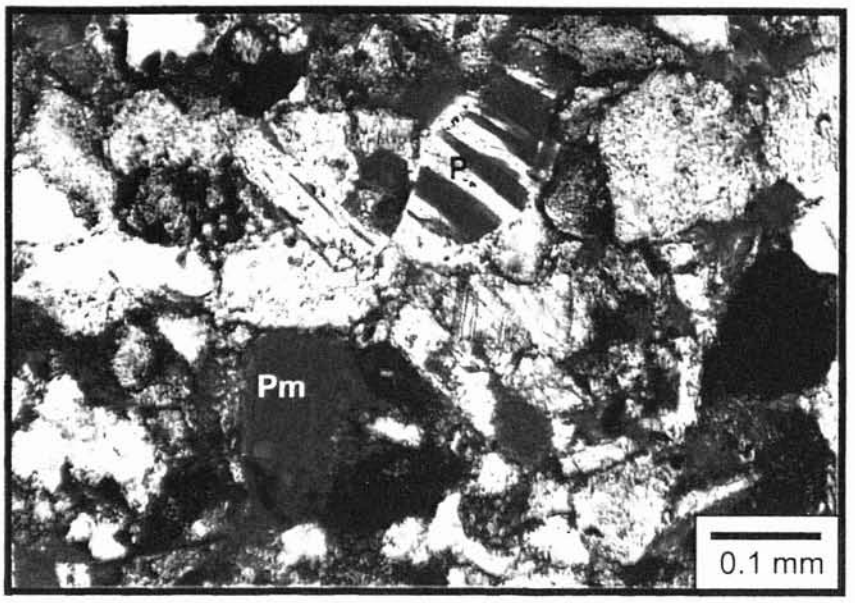

B.

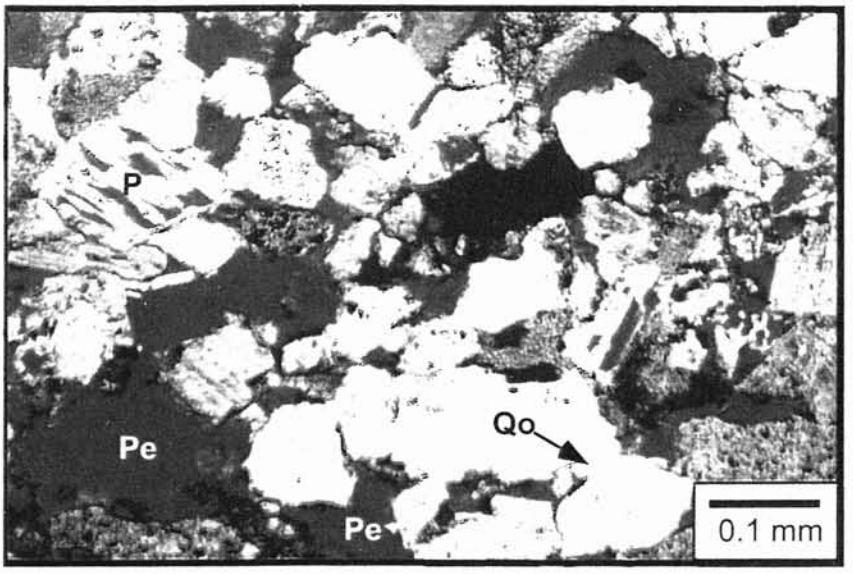

Figure 23. Photomicrograph displays partially dissolved plagioclase (P), enlarged porosity (Pe), moldic porosity (Pm), and quartz overgrowth (Qo)
A. Plane Plorized (PPL).
B. Plane Plorized (PPL).

dissolution of plagioclase occurs in acidic (<7pH) environments which in turn increases the amount of secondary porosity. Volcanic rock fragments (VRFs) are abundant and contribute to 8.5 to 12.9% of the rock. Volcanic textures of randomly oriented plagioclase laths are evident (Fig. 24). VRFs are often dissolved adding to secondary porosity. Minor detrital constituents include chert, foraminifera, glauconite, tourmaline, and pyrite (Fig 25).

Diagenetic Constituents

Cements. Calcite is the major cement with an average content of 4.5% in reservoir intervals. On the other hand, seal zones contain approximately 45% calcite cement. Cement within these zones occluded porosity, resulting in a higher capacity to block fluid migration (Fig. 26). Therefore zones with increased calcite cement are likely to resist fluid flow, thus creating a seal or barrier to trap potential hydrocarbons.

Authigenic Clay. Clays identified in the cores studied are illite/smetite mixed layer, kaolinite, and chlorite. These clay minerals are affected by diagenetic changes in many ways. Alteration of precursor grains, such as feldspars and volcanic glass result in the formation of clays. Illite/smectite mixed layer clay in the samples likely originated from the alteration of precursor grains such as plagioclase and volcanic rock fragments. Illite/smectite mixed layer clay coats grains (Fig. 27). In addition, clay minerals can be altered to produce other types of clay minerals. Clays often precipatate within pore spaces where no obvious precursor minerals are present. Kaolinite and chlorite formed within pore spaces without precursor minerals (Fig. 27).

A.

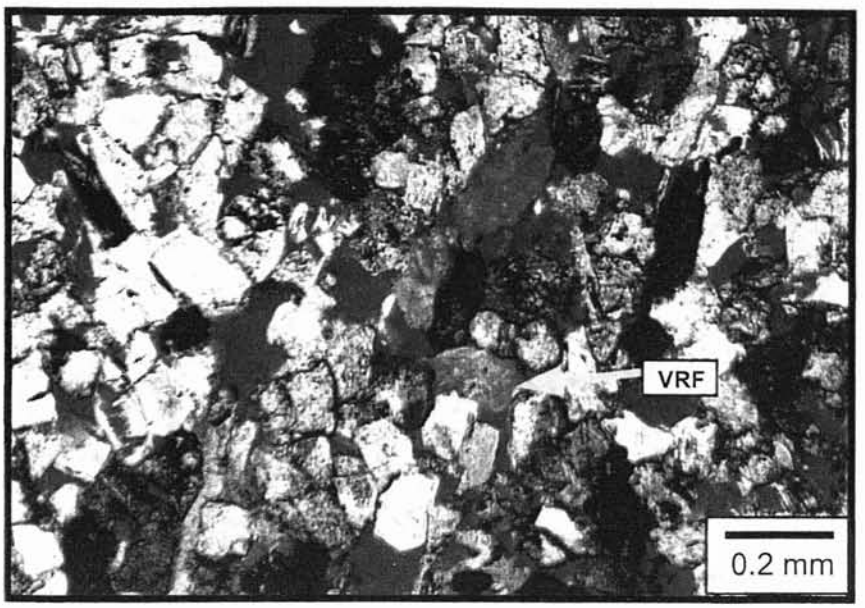

B.

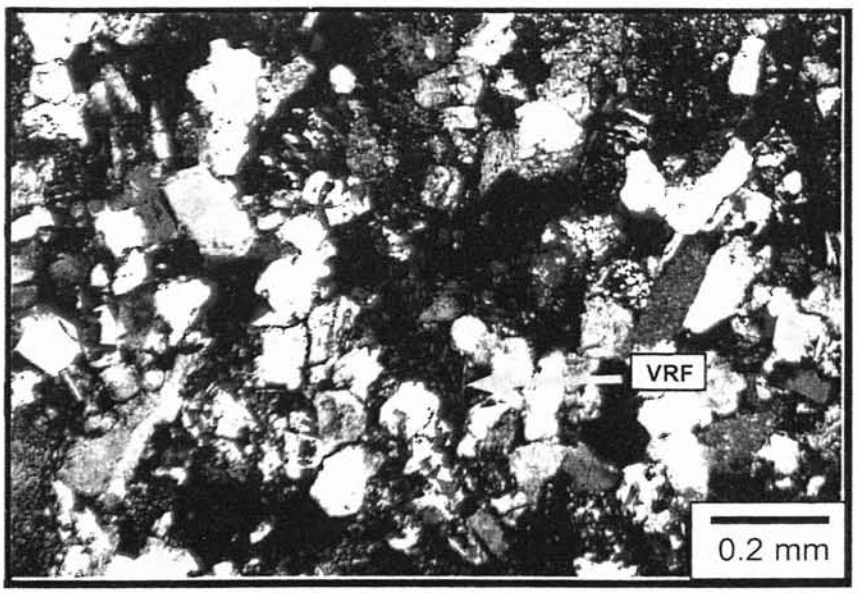

Figure 24. Photomicrograph displays partially dissolved volcanic rock fragment (VRF)
A. Plane polarized light (PPL)
B. Cross polarized light (CPL)

A.

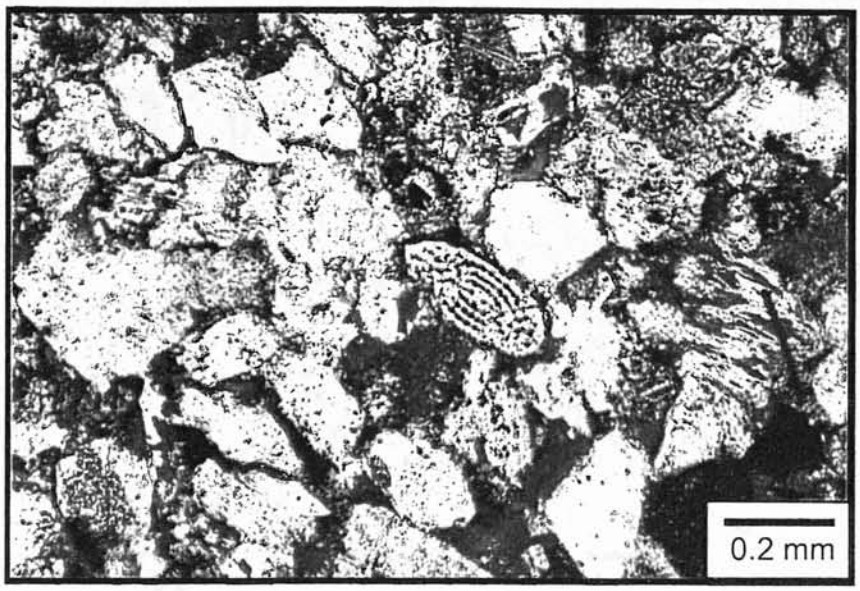

B.

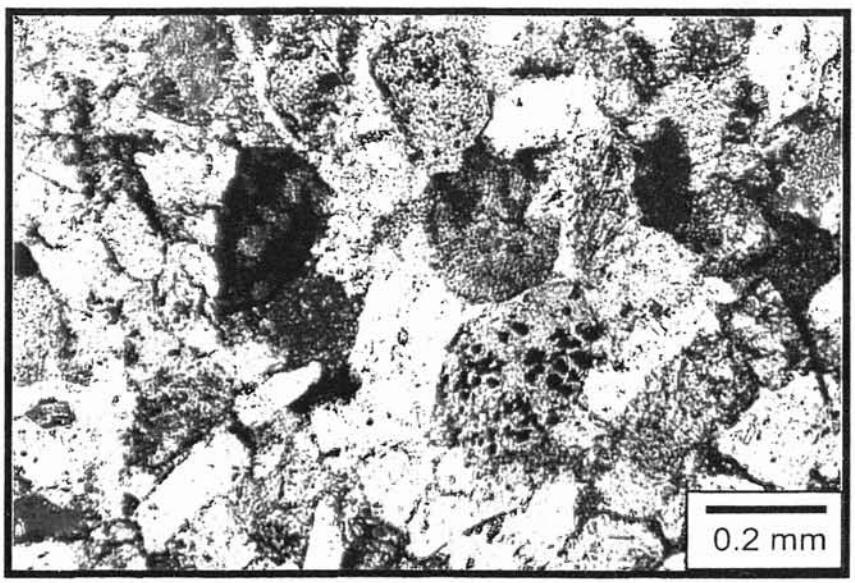

Figure 25. Photomicrograph displays partially dissolved Volcanic rock fragment (VRF)
A. Plane Plorized (PPL)
B. Cross Nichols (XN)

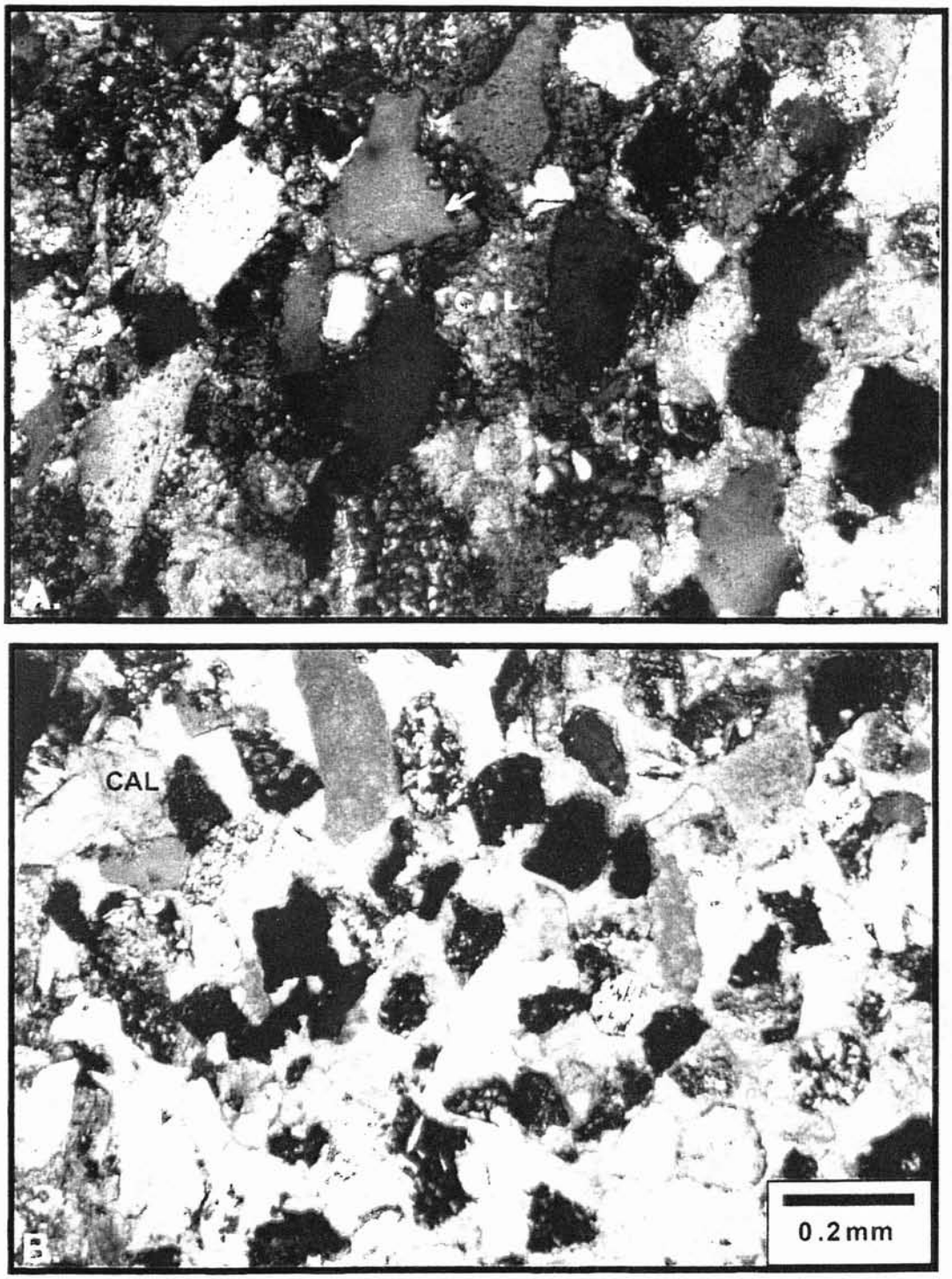

Figure 26. Calcite occluding porosity. A. Cross polarized light (CPL) B. Cross polarized light (CPL)

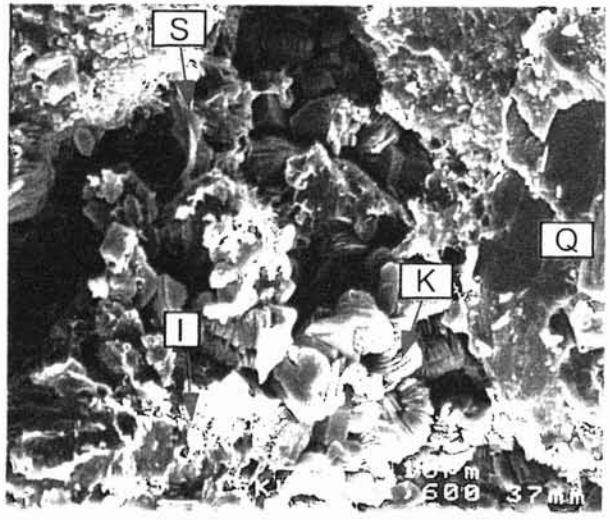

A.

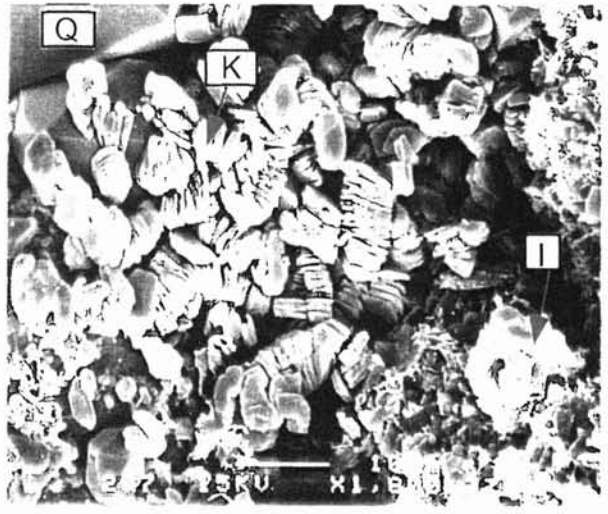

B.

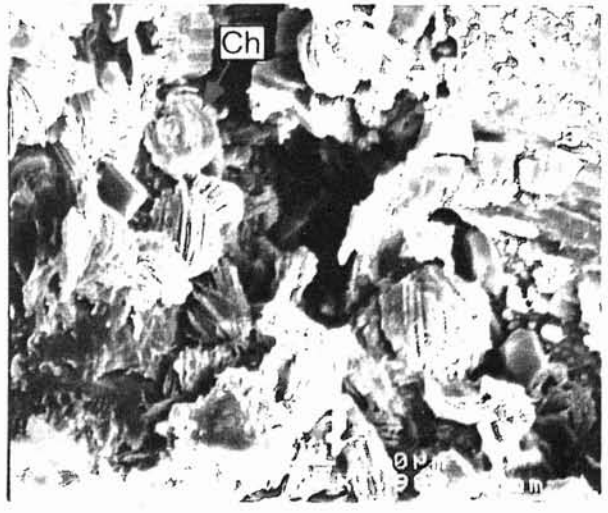

C.

Figure 27. A. Scanning electron photomicrograph (SEM) Pore bridging smectite (S) and illite (I) coating grains. Kaolinite (K) filling pore space. Detrital quartz (Q) grain.
B. Kaolinite (K) filling pore space. C. Chlorite (CH) pore filling.

Scanning electron microspocy (SEM) and x-ray diffraction were used to identify clay minerals. Figure 28 is a x-ray diffractogram with corresponding peaks of all identified clays.

Porosity. Porosity in the highstand systems tract ranges from .2% to 15.2%. Most porosity is secondary intergranular and moldic (Fig. 29). The pore type is dependant upon the zone type. Within reservoir zones, the porosity is approximately 12% and the pore type consists of enlarged and moldic macropores. Conversely, in seal zones the pore type is predominately micropores, and porosity values are reduced to approximately .2-4%. This reduction in porosity is the result of early calcite cementation.

Petrophysical Characteristics

The highstand systems tract contains sandstone units thicker than two feet, therefore conventional logs can be utilized to determine petrophysical charteristics. Log curves used to evaluate sandstones were primarly the spontaneous potential (SP), gamma ray, neutron porosity, density porosity, and resistivity.

Spontaneous Potential. The Spontaneous Potential (SP) in tract I deviates from the shale base line -15 to -30 millivolts (Fig. 30). Thick beds (>2 ft) typically deviate approximately –23 to –30 millivolts whereas thin beds deviate less than -20 millivolts.

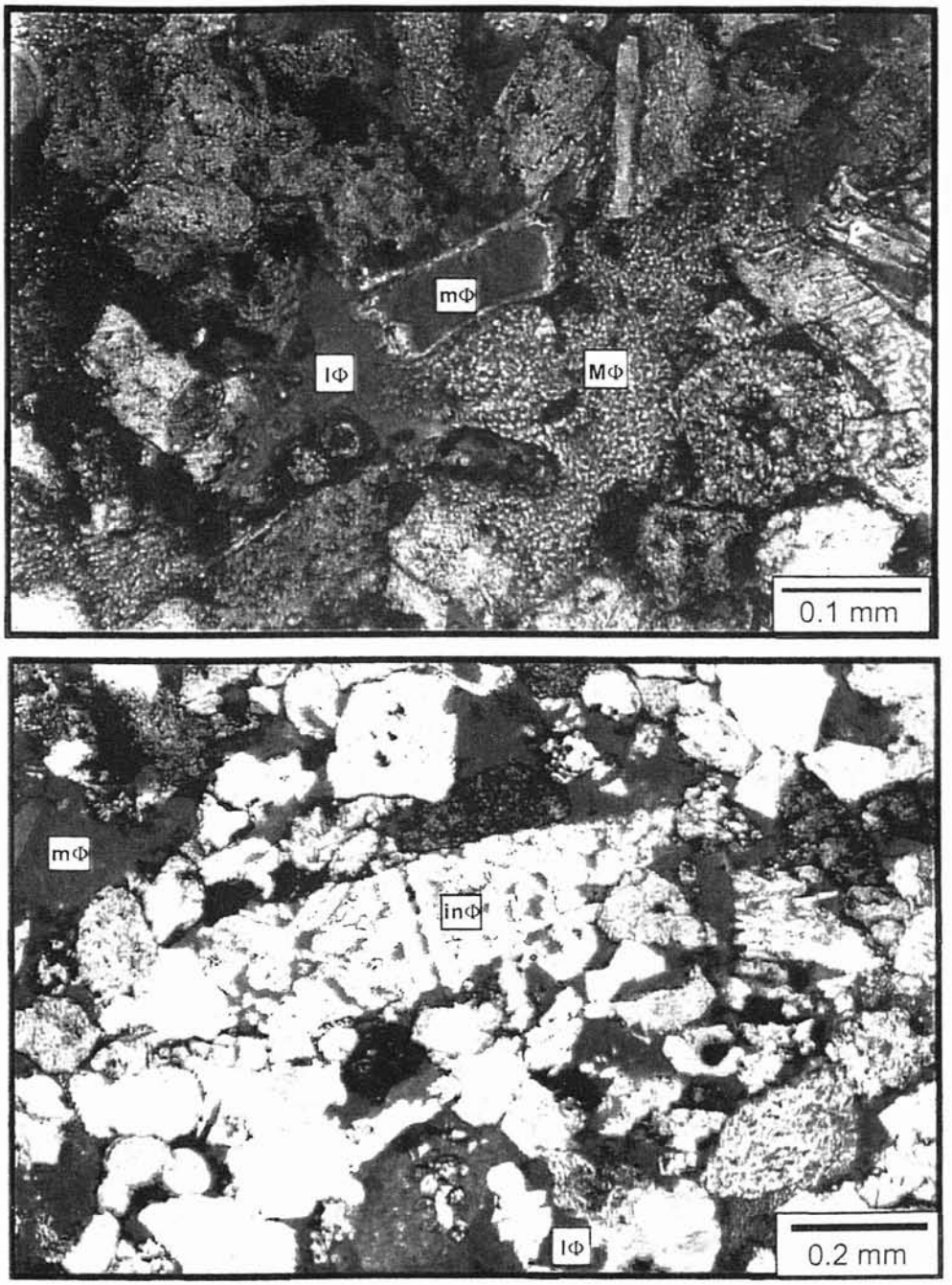

Figure 29. Photomicrograph of secondary intergranular porosity (IΦ), moldic porosity (mΦ), microporosity (MΦ), and intragranular porosity(inΦ). (PPL)

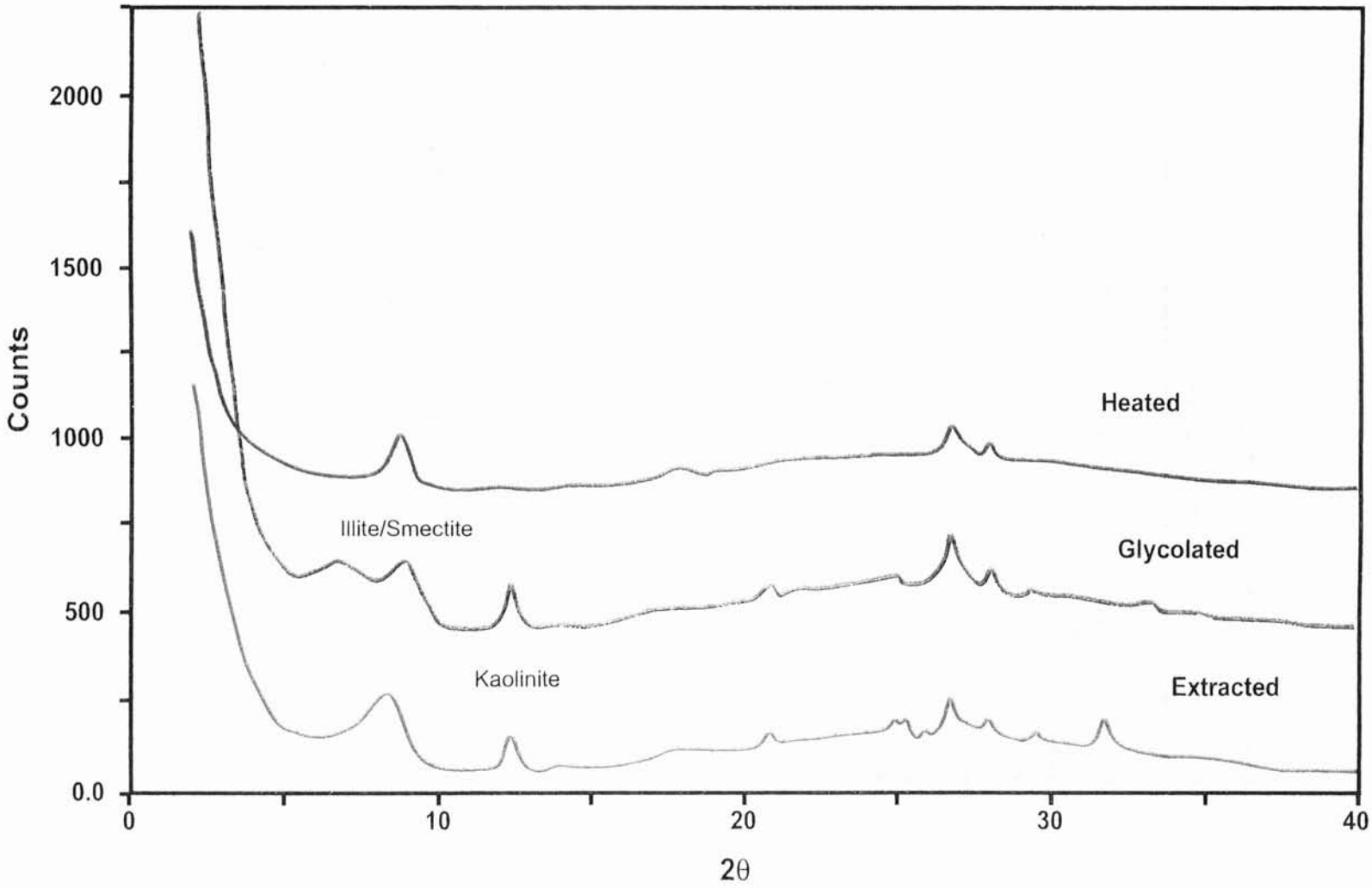

Figure 28. X-ray diffratogram of the E.G. Canales #19 9147 (9000 ft. sandstone). Illite/Smectite mixed layer clay and kaolinite are the most abundant clay types.

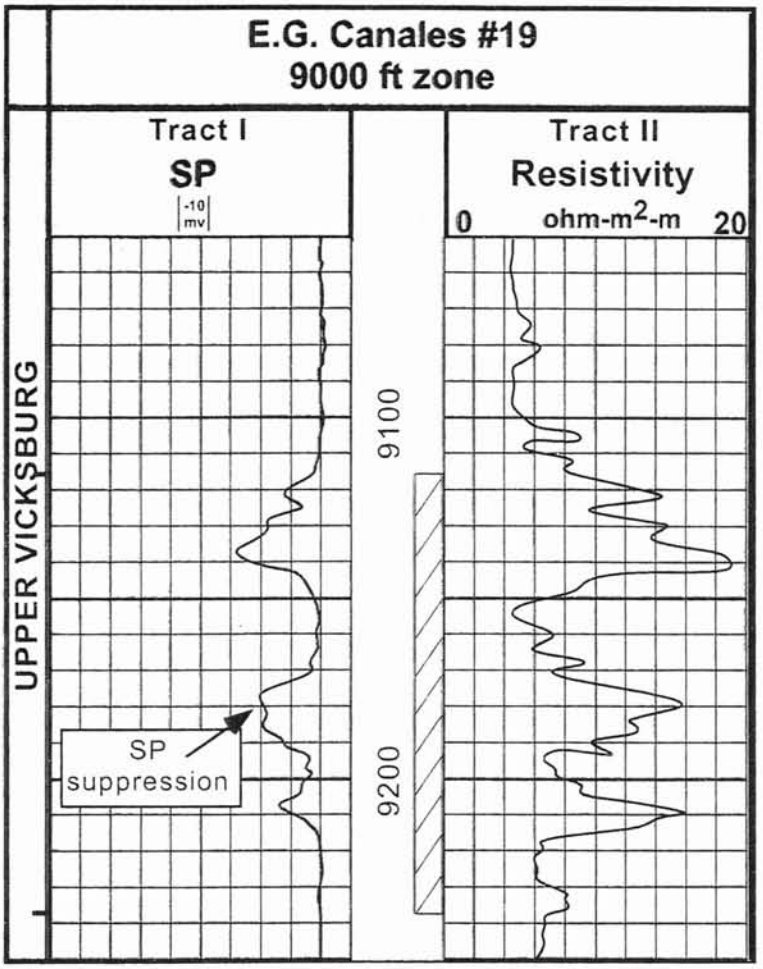

Figure 30. Well log response from the 9000 ft. interval depicting characteristic spontaneous potential (SP) and resistivity measurements.

Gamma ray. Gamma ray measurements range from 30 to 70 API. Typically gamma ray measurements in intervals with high resistivity spikes read approximately 45 API units. On the other hand measurements taken between the spikes are greater than 50 API units.

Porosity Logs. Porosity is determined using neutron and density logs. The neutron porosity curve typically reads higher than the density curve. This is the result of to clay content within this interval. The separation between the two porosity curves within sandy interval is approximately 10%, however within shaly intervals the separation is approximately 22%. This indicates the neutron porosity curve is errornously affected by clay content and results in higher porosity measurements.

Resisitivity Logs. The resistivity log used to evaluate the HST is Rt, or deep resistivity. The resistivity for relatively clean and porous reservoirs is approximately 12 ohm-m^2-m (Fig. 31). SP suppression occurs in intervals that are highly cemented, thus the corresponding resistivities tend to peak at approximately 18 ohm-m^2-m. In this case, SP suppressions are independent of sandstone thickness.

Rock Architecture: Reservoir vs. Seal

Architecture or fabric of reservoir and seal zones was evaluated using petrologic, petrophysical and capillary pressure techniques. Petrologic characteristics such as

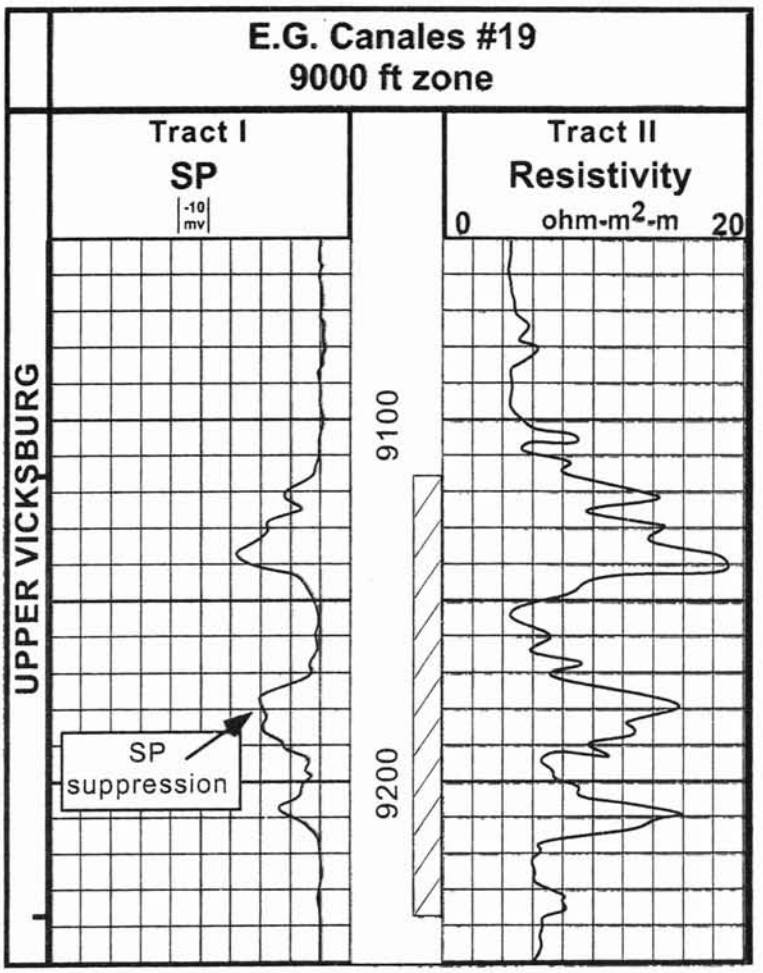

Figure 31. Well log response from the 9000 ft. interval depicting characteristic resistivity measurements.

constituents, grain size, thin section porosity, and cementation dictate the architecture of a rock. Reservoir and seal intervals typically have identical constituents. However, reservoir zones typically have larger grain size and porosity than seal zones. Calcite cementation generally increases in seal zones. Capillary pressure was used to quantify the amount of sealing capacity and type of pore structure within reservoir and seal zones.

Capillary pressure

Capillary pressure measurements were acquired for reservoir and seals in core from the E.G Canales #26 and the A.T. Canales #19. Seals within the HST have relatively low hydrocarbon column heights (HCH) and displacement pressures (Pd). These lower pressures indicate these seals are likely to break more readily. The HCH for the seal zones within the HST is approximately 120 ft and displacement pressure (Pd) ranges from 600-700 psi (Fig. 32). The pore type within seal zones is mainly micropores with approximate radii of .1 to .05 microns. The HST seals are similar to seal zones identified in the lowstand systems tract.

Reservoirs-quality sandstones are more prevalent than seal-quality within the HST cores analyzed. The HCH for reservoirs ranged from .6 to 15 feet, and displacement pressure was approximately 23 psi (Fig. 33). The pore structure is dominated by macropores, which have pore throat radii greater than 1 micron. Reservoirs have relative

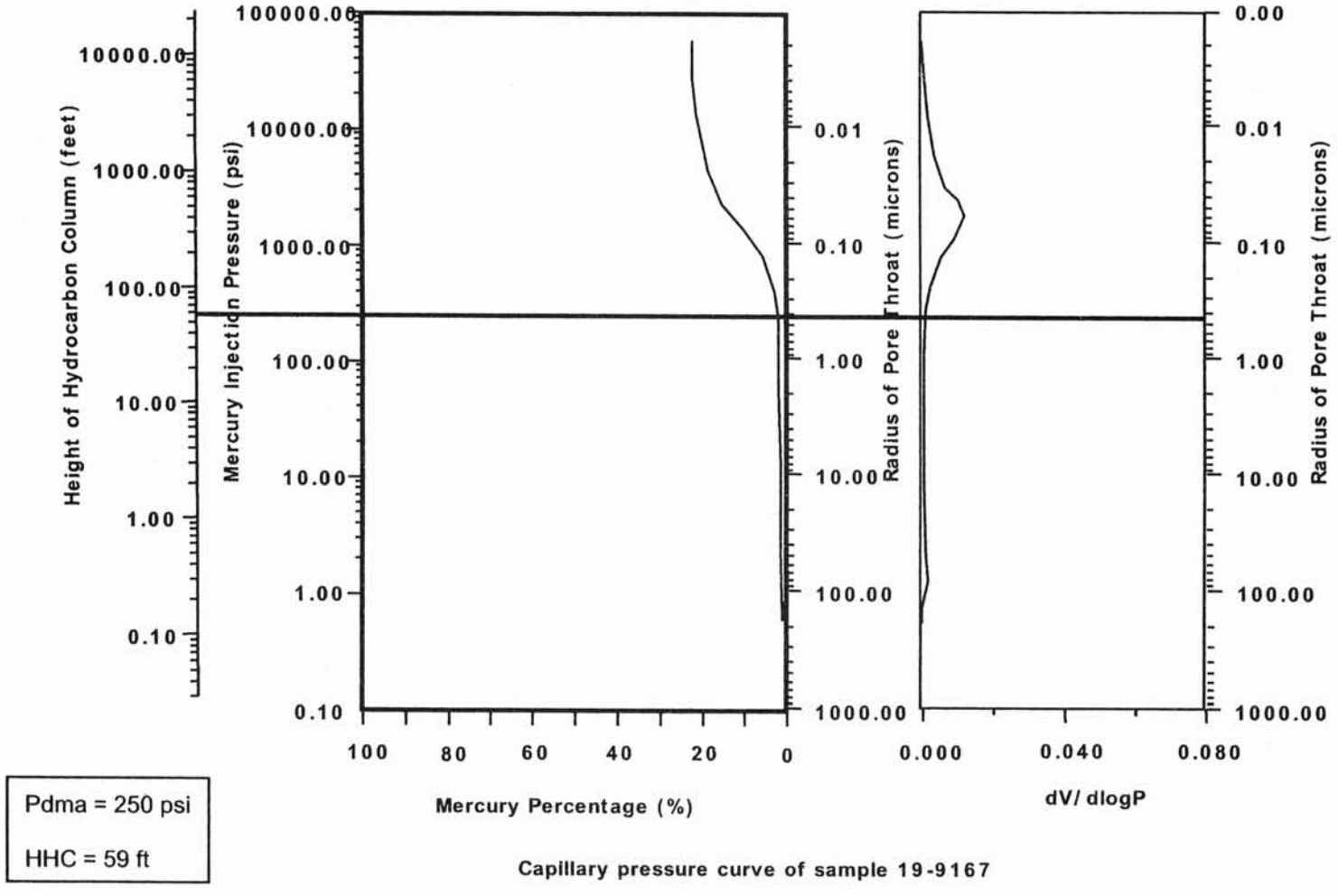

Fig 31. Capillary Pressure Curves indicating seal interval within the HST. HCH is 120ft and Pd typically ranges from 600-700 psi.

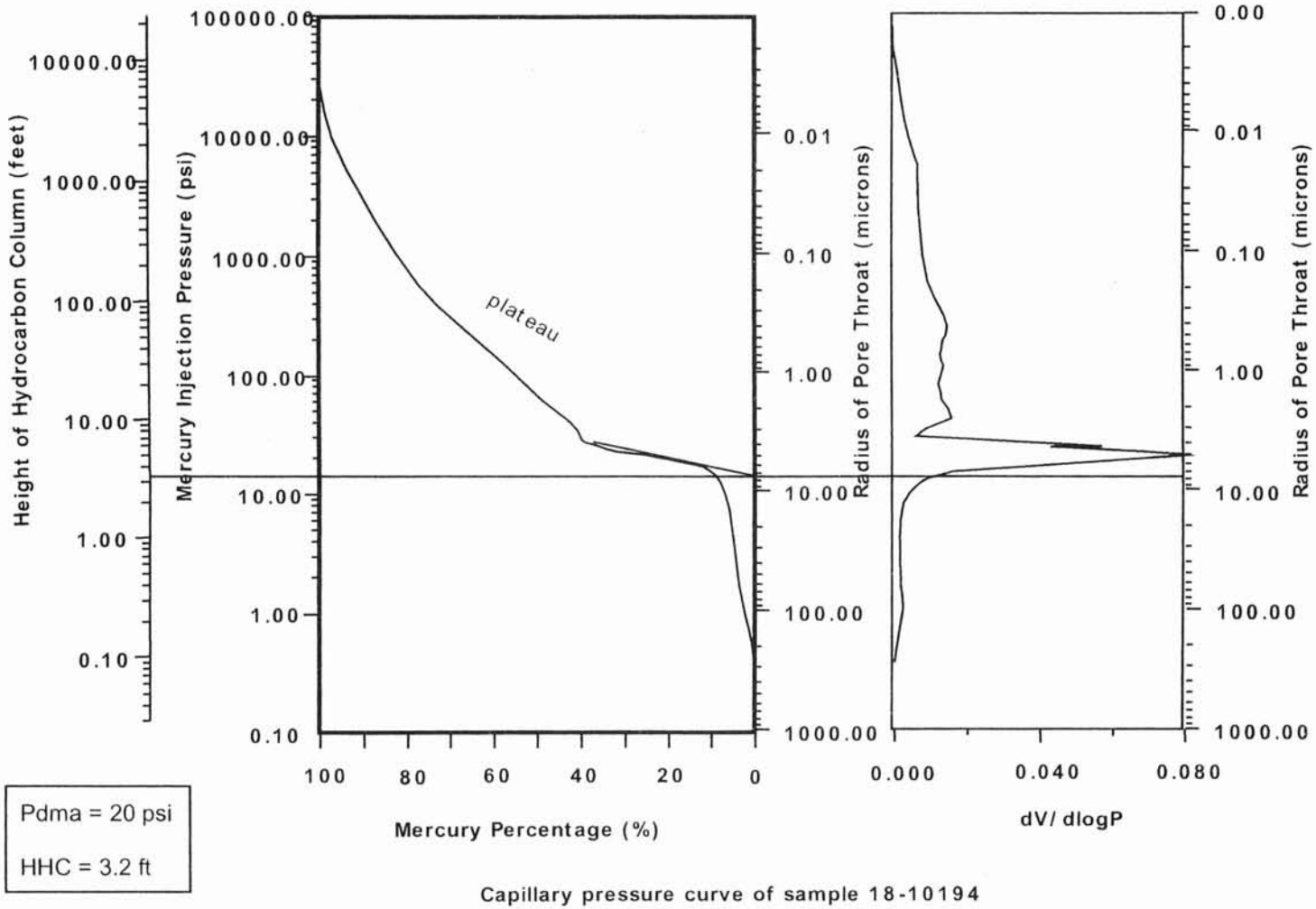

Fig 32. Capillary Pressure of reservoir interval. 19-9144

high porosity and permeability and only small amounts of calcite. Therefore they can not prevent fluid migration.

In conclusion, the cored interval within the HST, contains more reservoirs than seals. Seals are present, however they exhibit relatively low HCH and displacement pressures. These seals lack the integrity to trap and contain large columns of hydrocarbons. as seals in other systems tracts. Therefore, structural traps must be relied upon to trap fluids. In TCB field, the structural trap is the rollover anticline.

Reservoir controls of the Transgressive Systems Tract

Introduction

Transgressive systems tract rocks in TCB field were examined in the A.T. Canales #81 and #85 wells (Fig. 34). The TST is represented by an interval of low resistivity/ low contrast (LR/LC) rock. The sandstone packages within this interval are difficult to detect due to their thinly bedded nature and interbedded shale. The evaluation of these reservoirs using conventional wire-line logging tools is difficult. However, both wells were logged using micro-imaging tools and high-resolution resistivity and porosity logs that greatly enhanced interpretation.

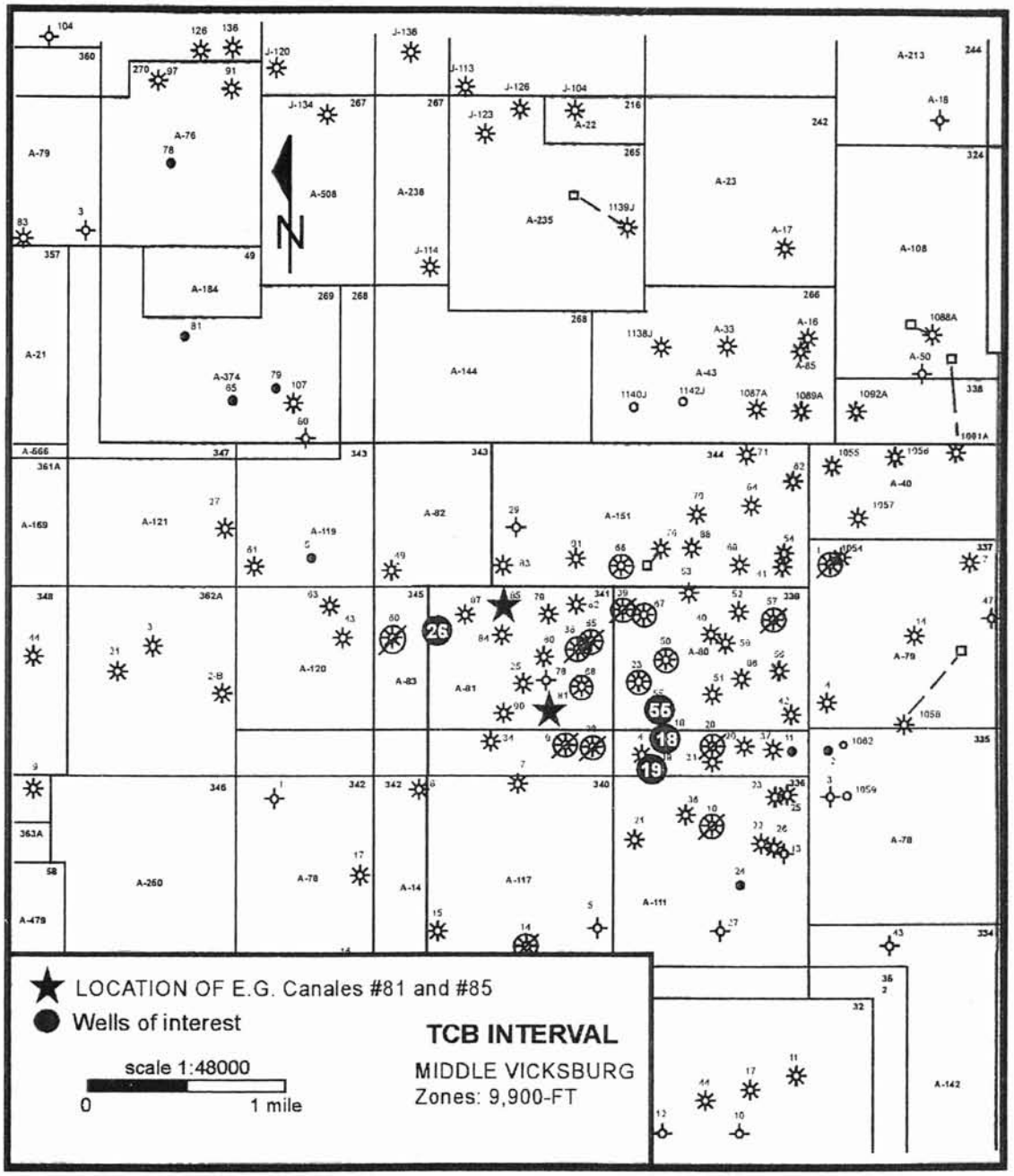

Figure 34. Location map of core studied, the location of the A.T. Canales #81 and #85 in the Middle Vicksburg interval.

Petrology

Classification

The major detrital constituents in the 9900-ft Vicksburg sandstones are quartz, feldspar, chert mineral grains and volcanic and metamorphic rock fragments. The sandstones were classified on the basis of the relative percentages of these grains using the Folk (1974) QRF ternary diagram. The classification ranged from sublitharenite, feldspathic litharenite, subarkose and lithic arkose (Fig. 35). The present average compositions for both cores plotted as feldspathic litharenites. Restoring dissolved feldspar and rock fragments to their original volumes would shift the classification toward the base of the feldspathic litharenite and lithic arkose zones.

Detrital Constituents

The 9900-ft sandstone interval is primarily silty to very-fine grained sandstone and shale. Quartz is the major constituent, while feldspar and sedimentary and volcanic rock fragments are present in lesser amounts (Fig. 36). Minor constituents include chert, metamorphic rock fragments, muscovite, biotite, glauconite, zircon, pyrite, tourmaline and foraminferia.

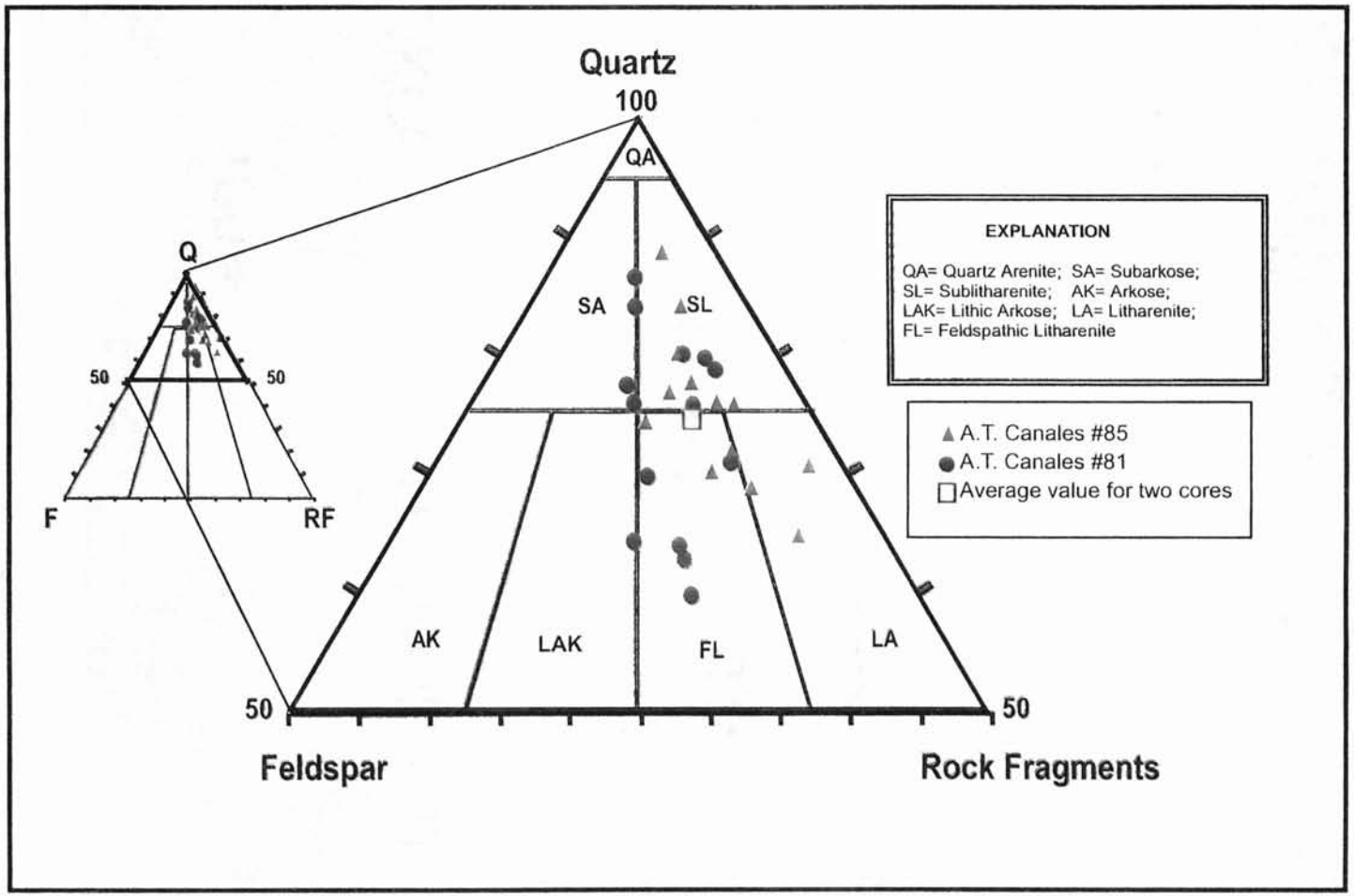

Figure 35. Composition of the 9900-ft sandstone plotted on QRF diagrams (Folk, 1974).

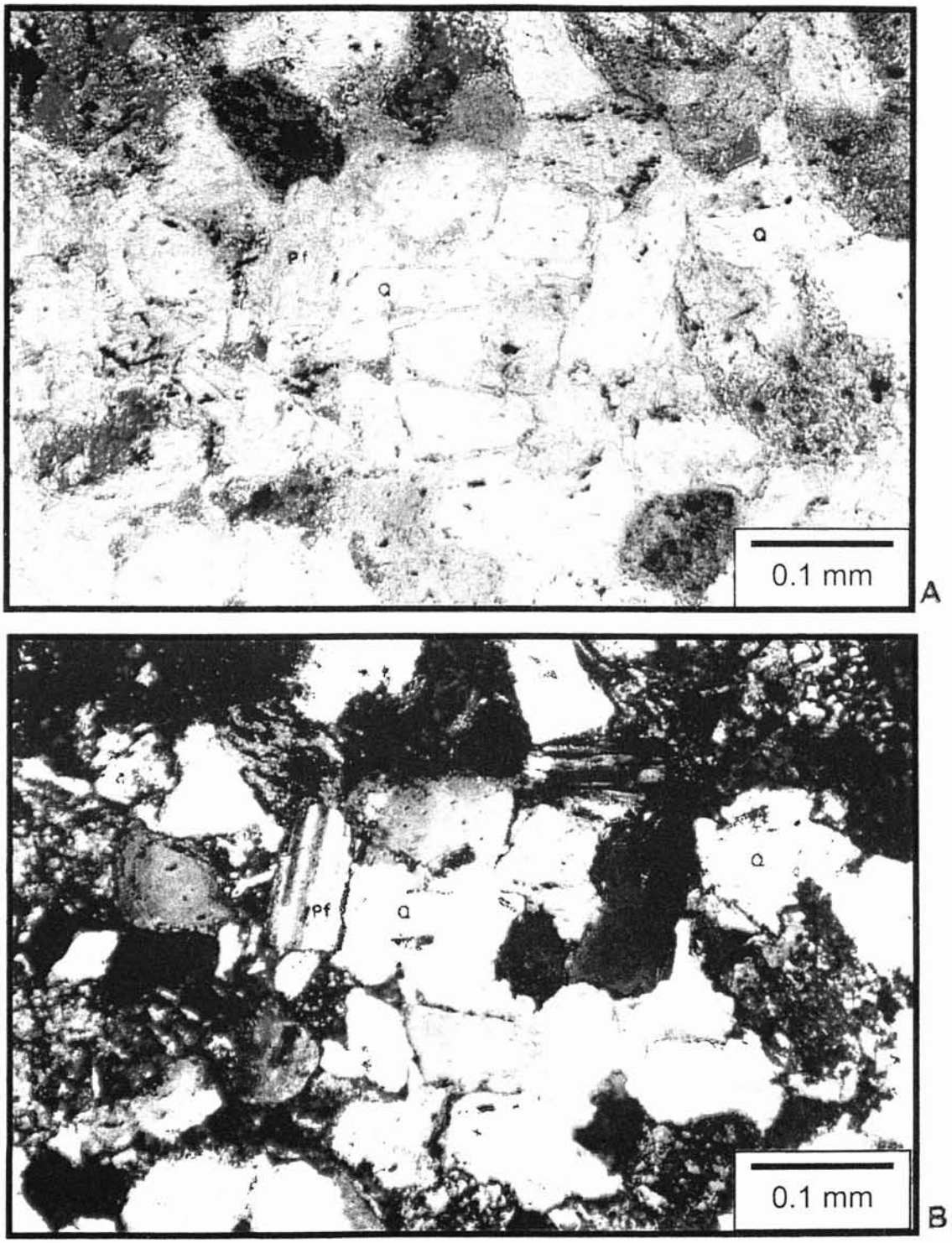

Figure 36. Quartz (Q) and plagioclase feldspar (Pf) are major framework grains in the 9900-ft sandstone. Albite twinning is characteristic of plagioclase.
A. Plane-polarized light (PPL).
B. Cross-polarized light (CPL).

Diagenetic Constituents

Sandstones not cemented early in burial often display signs of compaction. Flexible and soft components were ductily deformed. Argillaceous and volcanic rock fragments flowed between quartz grains forming pseudomatrix. Elongate muscovite and biotite grains were bent or fractured by harder quartz and feldspar grains (Fig. 37). Chemical diagenesis has significantly modified the Vicksburg sandstones during several episodes of cementation and dissolution. Calcite is the dominant cement, but silica cement is significant in certain areas.

Carbonate Cement. Calcite is the major cement and completely occludes porosity in some sandstones. Calcite replaces quartz grains and forms poikilotopic texture where quartz grains "float" in calcite cement (Fig. 38). Zones cemented by calcite are identified as white color bands on FMI logs and high intensity peaks on FIS charts (Fig. 39).

Silica Cement. Silica Cement occurs as syntaxial quartz overgrowth (Fig. 40). The overgrowths are easily recognized when they are separated from the detrital grain by a clay "dust rim". In some cases, the boundaries between the overgrowths and detrital grains are not distinct, but the cement contains fewer inclusions than the detrital grain. Silica cement is more prevalent in cleaner sandstones with lesser amounts of clays. Here advanced stages of overgrowth occurred. Silica-cemented zones appeared as white color bands on the microimaging logs.

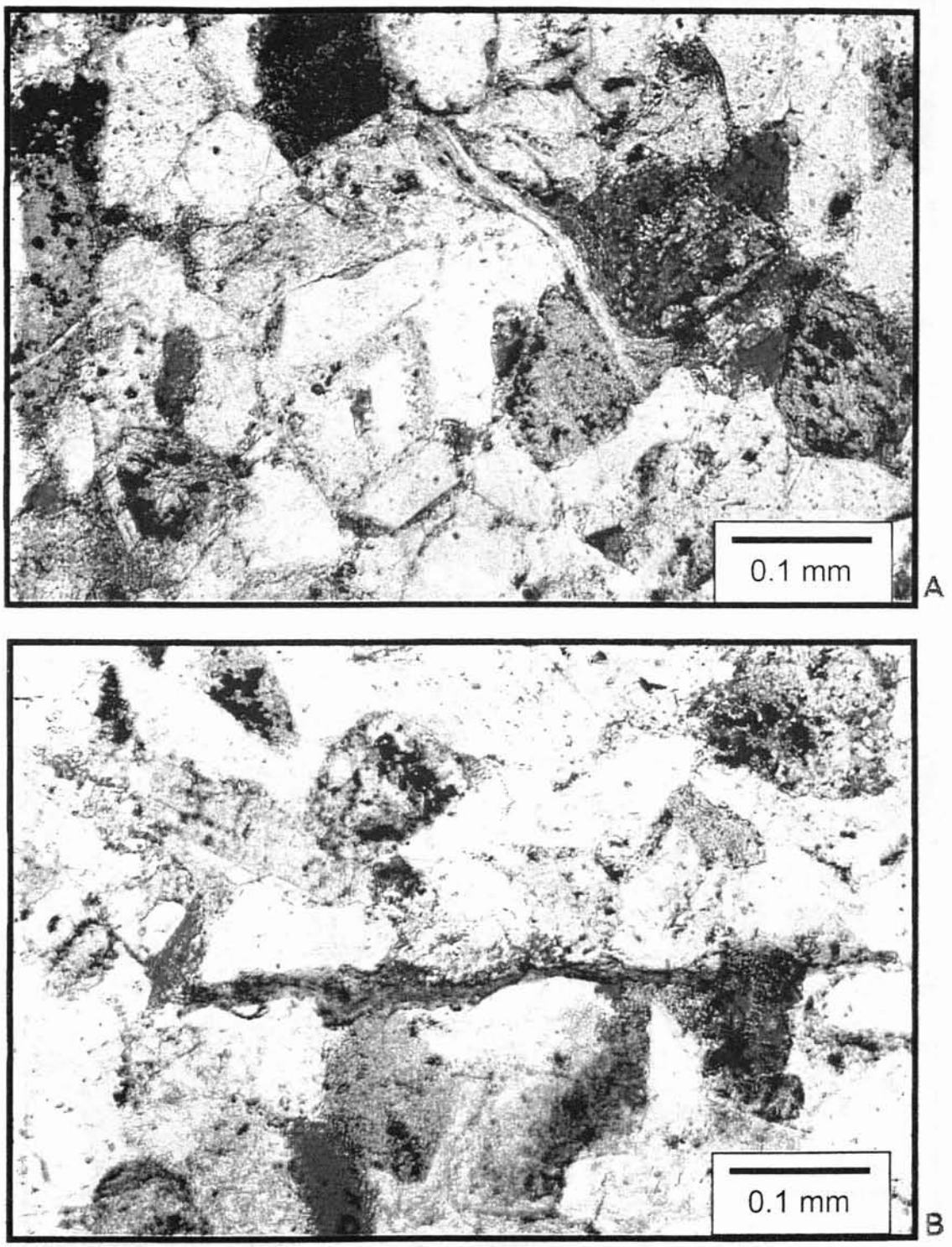

Figure 37. Compaction deformation of muscovite (A) and biotite (B) between harder quartz and feldspar grains.
A. PPL B. PPL

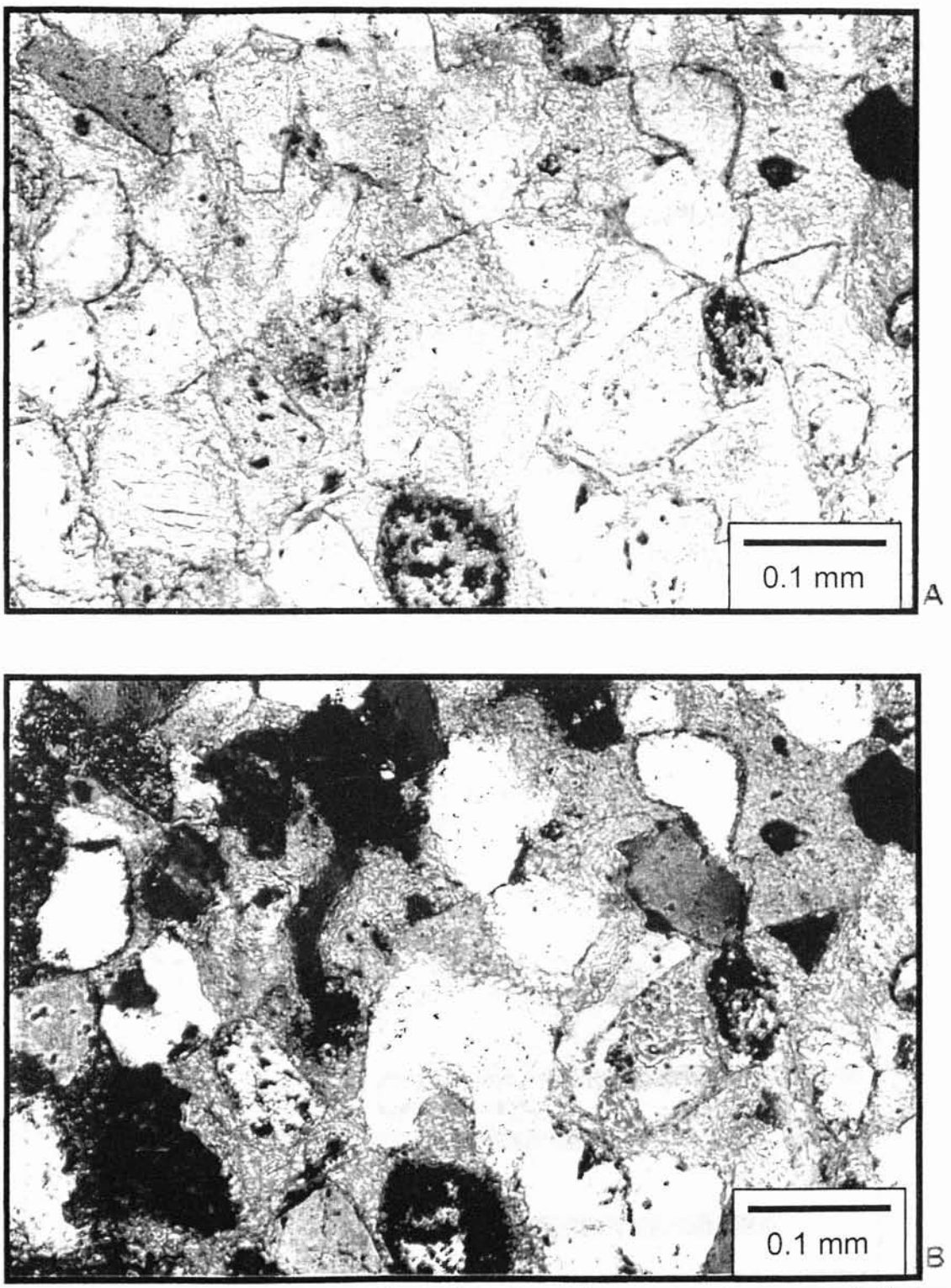

Figure 38. Poikilotopic texture formed by the replacement of quartz and other framework grains by calcite cement.
A. PPL B. CPL

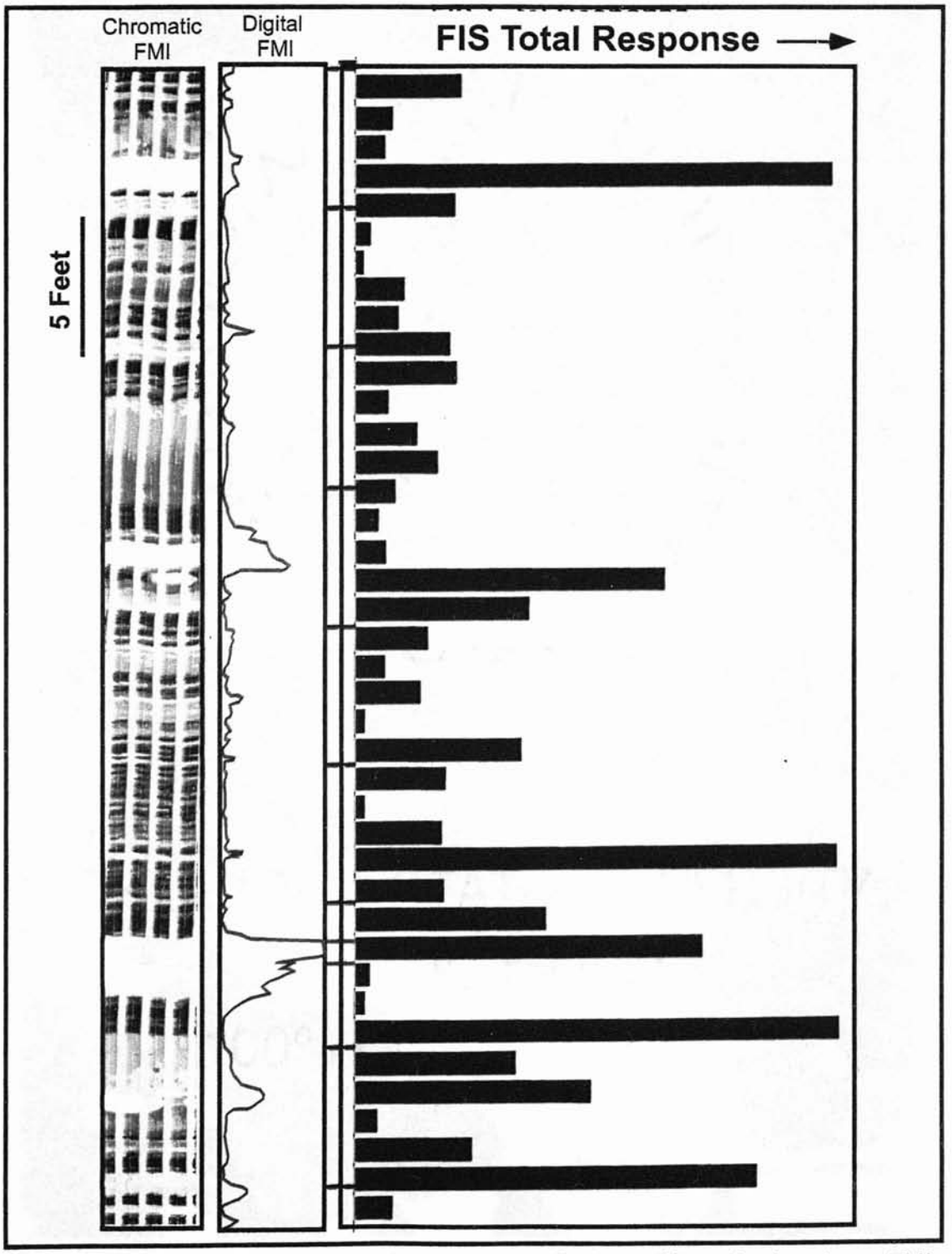

Figure 39. Zones cemented by calcite are identified as white color bands on FMI logs and high intensity peaks on FIS charts.
(Modified after Deyhim 2000)

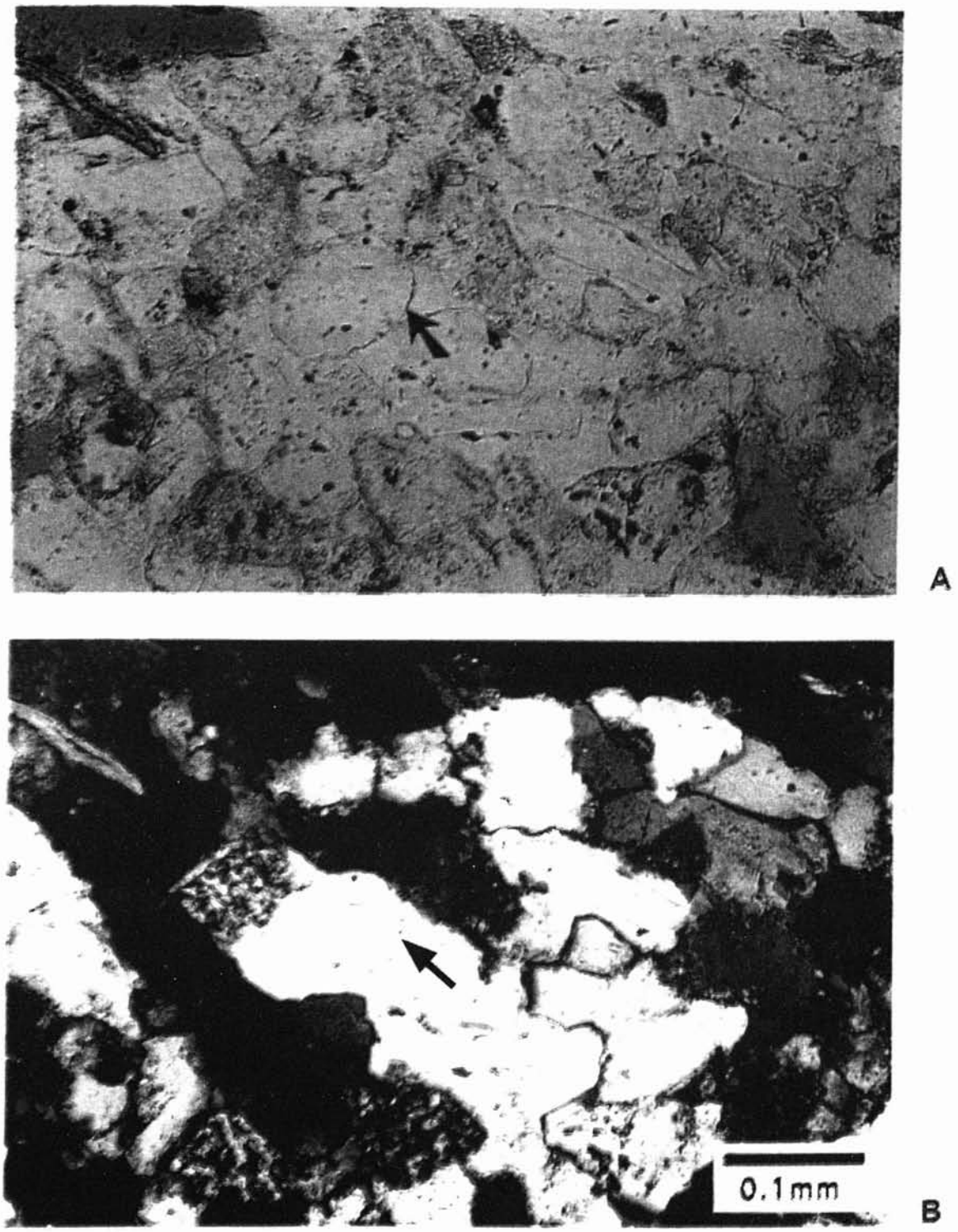

Figure 40. Silica cement in the form of syntaxial quartz overgrowths. Clay dust rims (arrows) separate cement from detrital grains.
A. PPL B. CPL

Clay minerals. The clay minerals within this interval are authigenic illite-smectite mixed layer, illite, kaolinite and chlorite. Mixed layer illite-smectite clay is the most common and is identified by its characteristic peaks on X-ray diffractograms (Fig. 41). SEM photomicrographs revealed that mixed-layer illite-smectite is pore lining and bridging (Fig. 42). Kaolinite is the second most common clay within this interval. It was identified using x-ray diffraction and SEM. Authigenic illite occurs as highly birefringent crystals that line pores. It is found throughout the core, but is not abundant. Chlorite is a minor clay constituent that was identified by X-ray and SEM.

Porosity

Primary and secondary porosity are preserved in the 9900-ft sandstone. Volumetrically, secondary porosity is much more significant than primary. Primary porosity is believed to have provided the conduits for pore-fluid migration that resulted in partial or complete dissolution of metastable constituents such as VRF and feldspar.

Petrophysical Characteristics

Petrophysical properties of the transgressive systems tract (9,900-ft sandstones) were evaluated in the A.T. Canales #81 and A.T. Canales #85. The 9,900-ft sandstones are represented on logs by low-resistivity/ low-contrast signatures. The thinly

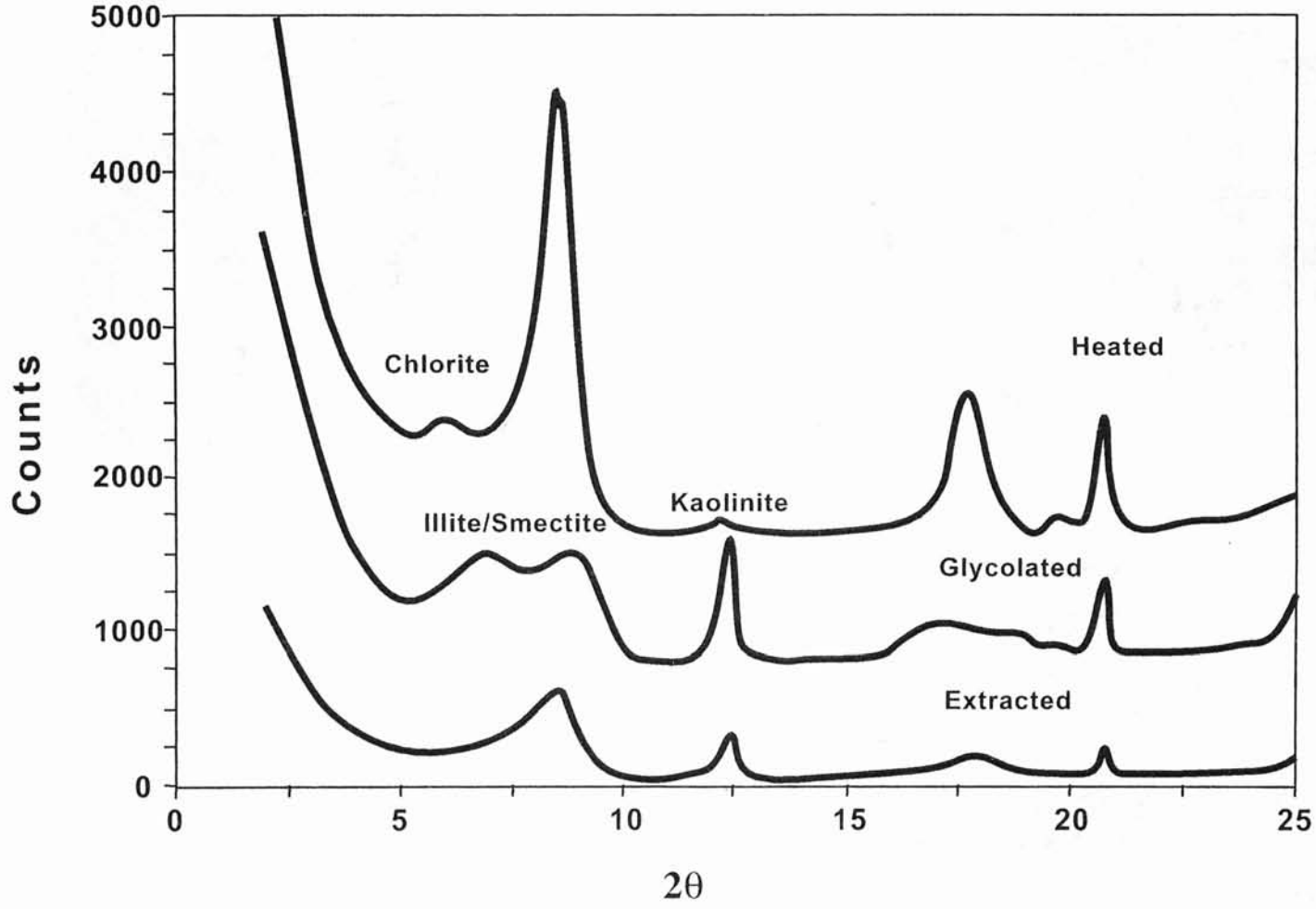

Figure 41. X-ray diffractogram of the A.T. Canales #81 (9,900-ft sandstone) distinguishing the different clay types

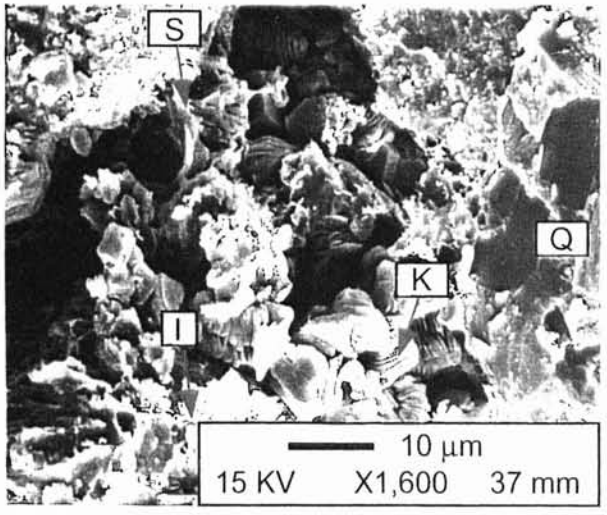

A.

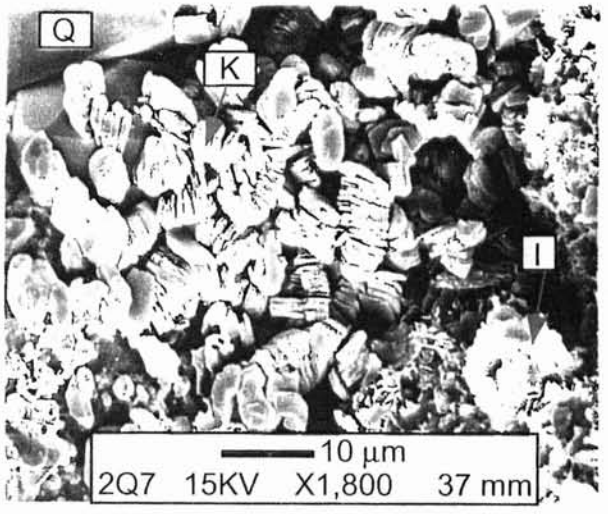

B.

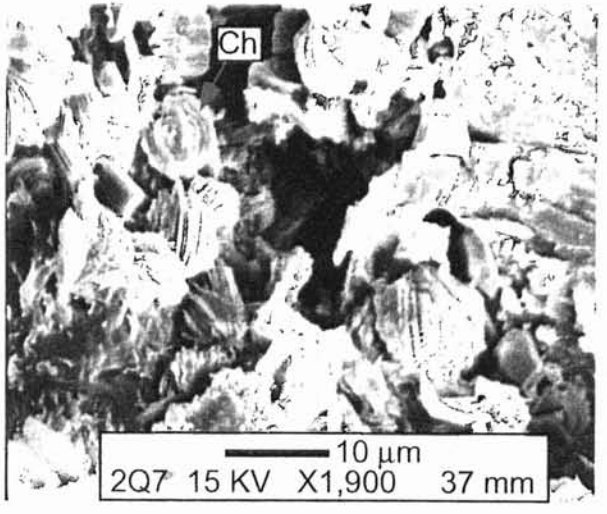

C.

Figure 41. A. Scanning electron photomicrograph (SEM) Pore bridging smectite (S) and illite (I) coating grains. Kaolinite (K) filling pore space. Detrital quartz (Q) grain.
B. Kaolinite (K) filling pore space. C. Chlorite (CH) pore filling.

bedded nature of the TST results in erroneous high water saturations (Sw) calculations when using conventional logs. The vertical resolution of most conventional logs is greater than 1.5 feet and many thin bedded sandstones are not defined by conventional log tools.

Spontaneous Potential (SP). Tract I of the log suite contains two curves: spontaneous potential (SP) and gamma ray. SP deviation is usually one chart division or less from the shale base line (Fig. 43). Slightly thicker sandstone beds with lower resistivity have increased SP deviation of 1.5 to 2 chart divisions or 15 to 20 millivolts. Sandstones with high resisitivity peaks are tightly cemented and have suppressed the SP deflection to one chart division or 10 millivolts.

Gamma ray. Gamma ray logs are valuable lithologic tools. The gamma ray curve deviates from the shale base line 30-40 API units when resistivity measurements are high. The gamma ray deviated less than 35 API units in between the resisitivity spikes.

Porosity Logs. TST rocks contain large amounts of clay. This clay content affects the neutron-density porosity curves. As a result of clay content and the thin-bedded nature, neutron porosity is greater than density porosity, and gas effect (density porosity > neutron porosity) is rarely seen.

In sandy zones, the separation between the neutron porosity and the density porosity is approximately 11.5%. On the other hand, shale zone separation is higher at approximately 15%.

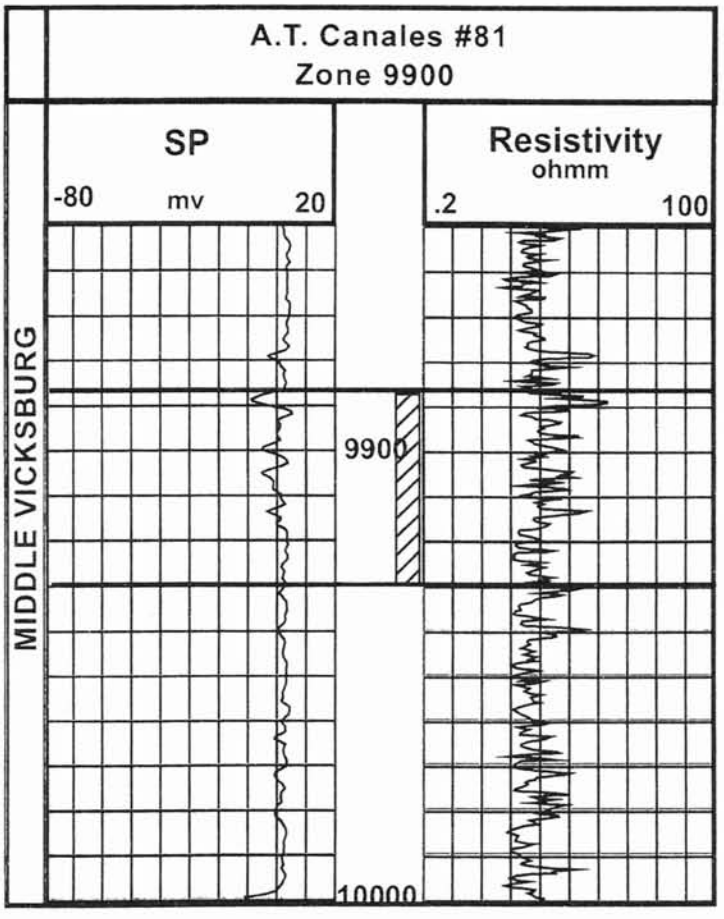

Figure 43. Conventional well log response of the 9900 ft. interval displays low contrast / low resistivity signatures. The SP deviates one chart division or less from the shale base line .

High resolution logs. The 10 and 20 inch array induction resistivity logs signatures provided higher resolution resistivity measurements. The array induction curves detect sandstone intervals that are one foot thick, and are useful when dealing with thinly bedded shaly sandstones.

High resolution gamma ray logs do not resolve sandstone beds thinner than 2-3 feet. However, this tool will identify shales less than 1-ft thick, and is very useful in picking bed boundaries.

High resolution neutron-density porosity logs improve porosity assessment. However, clay minerals affect the neutron tool, which responds to the OH- ion concentrations. As a result, the neutron porosity is usually deceptively higher than the density porosity. Density porosity correlates better to the core plug derived porosity and is more useful in determining porosity within the shaly LR/LC sandstones.

Architecture: reservoir vs. seal

Formation Micro-imaging

Microimaging logs were available across the transgressive systems tract (TST) in the A.T. Canales #81 and #85 wells. Al-Shaieb et. al (2000) and Deyhim (2000) used

microimaging, in conjuction with high resolution resistivity, porosity logs, and core data to distinguish reservoir and seal zones.

Microimaging of the A.T Canales #81 and #85 wellbore established four chromatic zones.

The yellow zone is porous sandstone with minor clay content. The clays within this zone inhibited quartz overgrowth and thus preserved porosity. The porosity types are moldic and enlarged. The yellow zone has the highest porosity and permeability, 21% and 0.16 md respectively (Fig. 44). The abundance of porosity and permeability are readily apparent in thin sections. The yellow zone is considered to be a potential reservoir in the TCB field.

The orange zone is very similar to the yellow zone. However, it contains increased clay content (Fig. 45). The porosity is approximately 18% while permeability decreases to 0.06md.

The brown zone consisted of clay-rich rocks such as shales and shaly siltstones (Fig.46). Porosity in the clay-rich rocks was approximately 18% while permeability was approximately 0.005md.

The white zone represents resistive sandstones with abundant calcite cement (Fig 47). The presence of calcite cement occluded porosity and created a seal. Porosity ranged from 5-12%, while permeability of the white zone ranged from 0.001-0.015 md.

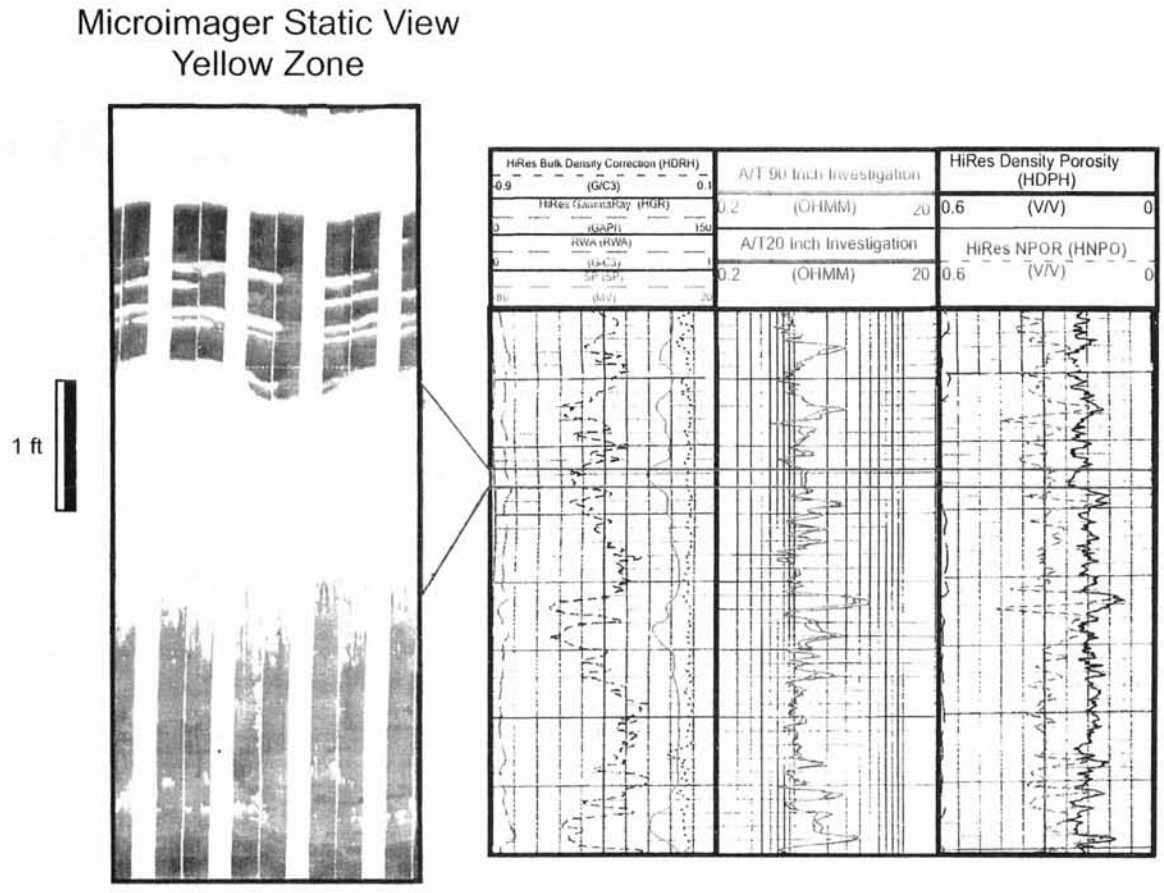

Figure 44. Wireline log characteristics of static view chromatic zone. Porosity and permeability measurements are from conventional core analysis. LR/LC 9900-ft sandstone, TCB field.

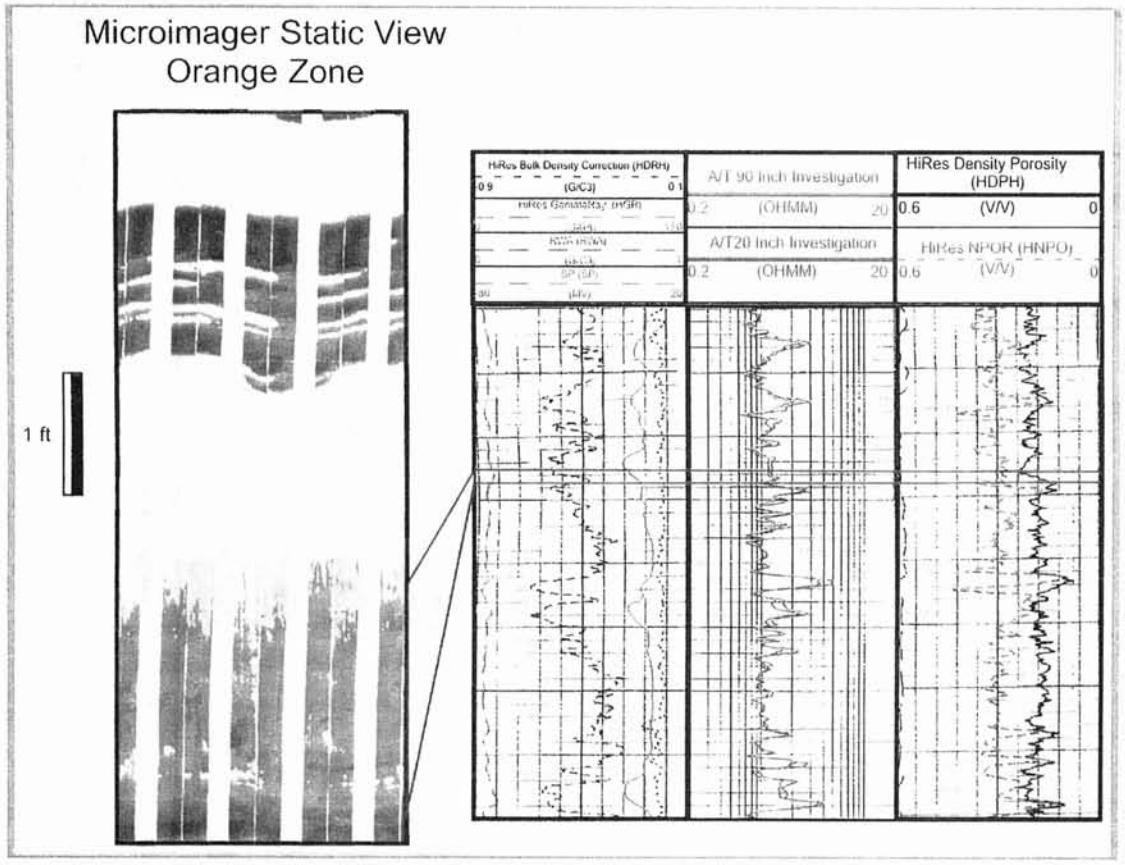

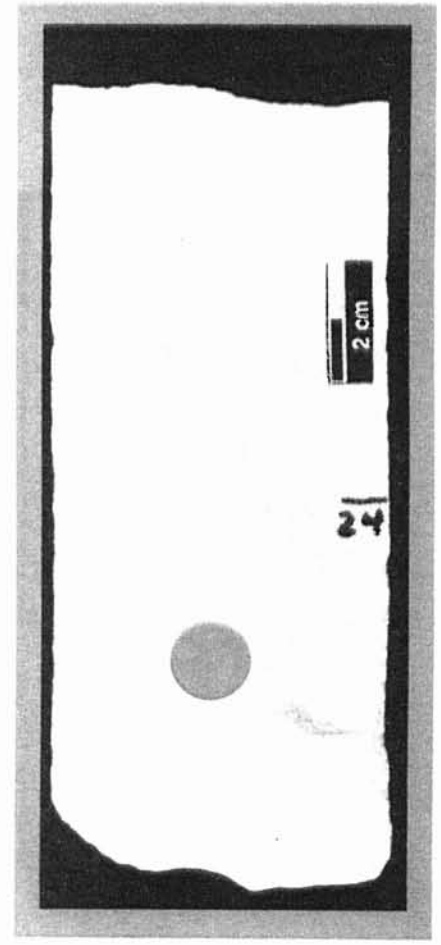

Figure 45. The orange zones is similar to the yellow zone with the addition of increased clay content .

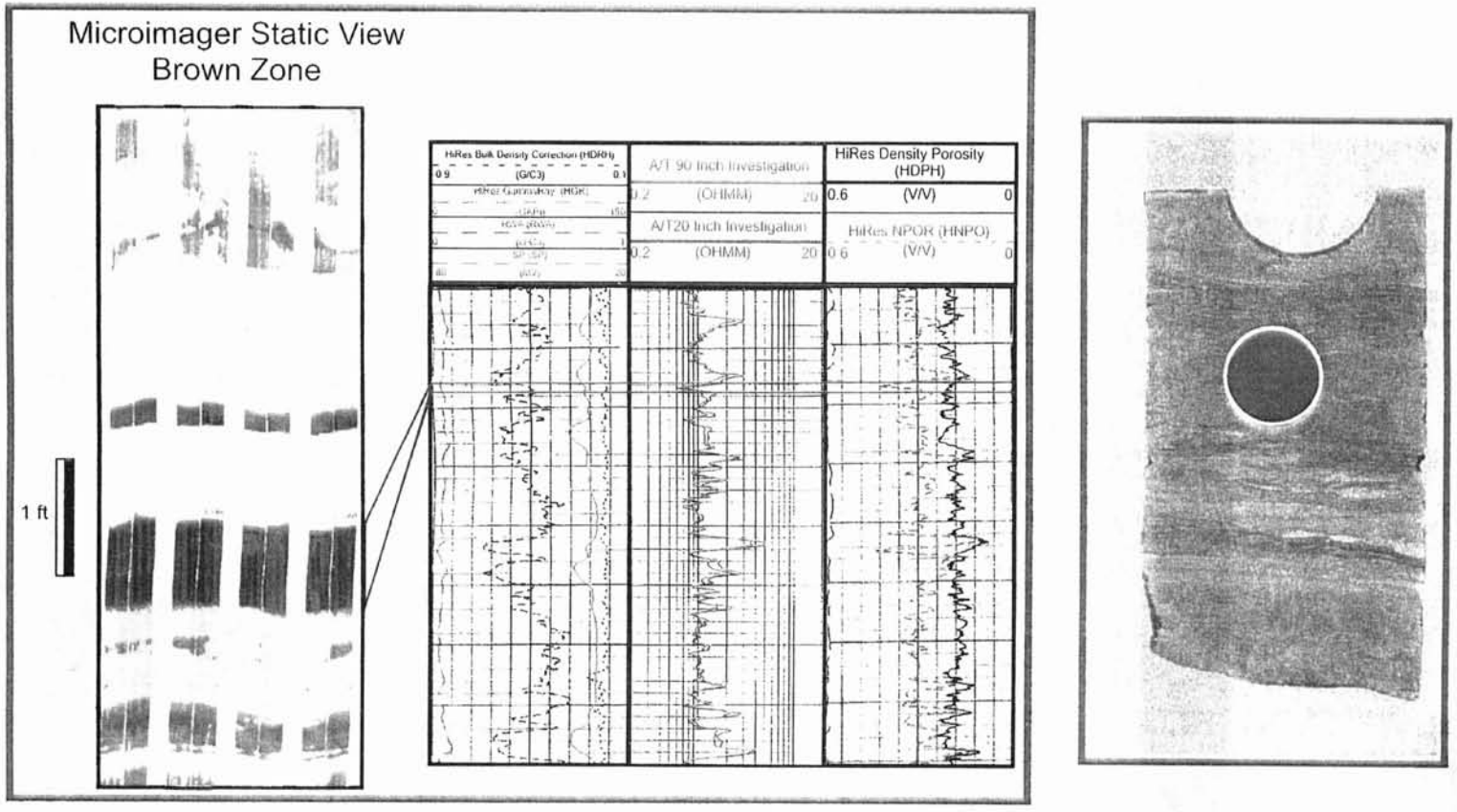

Figure 46. Brown zone consisted of clay-rich rocks such as shales and shaly siltstones.

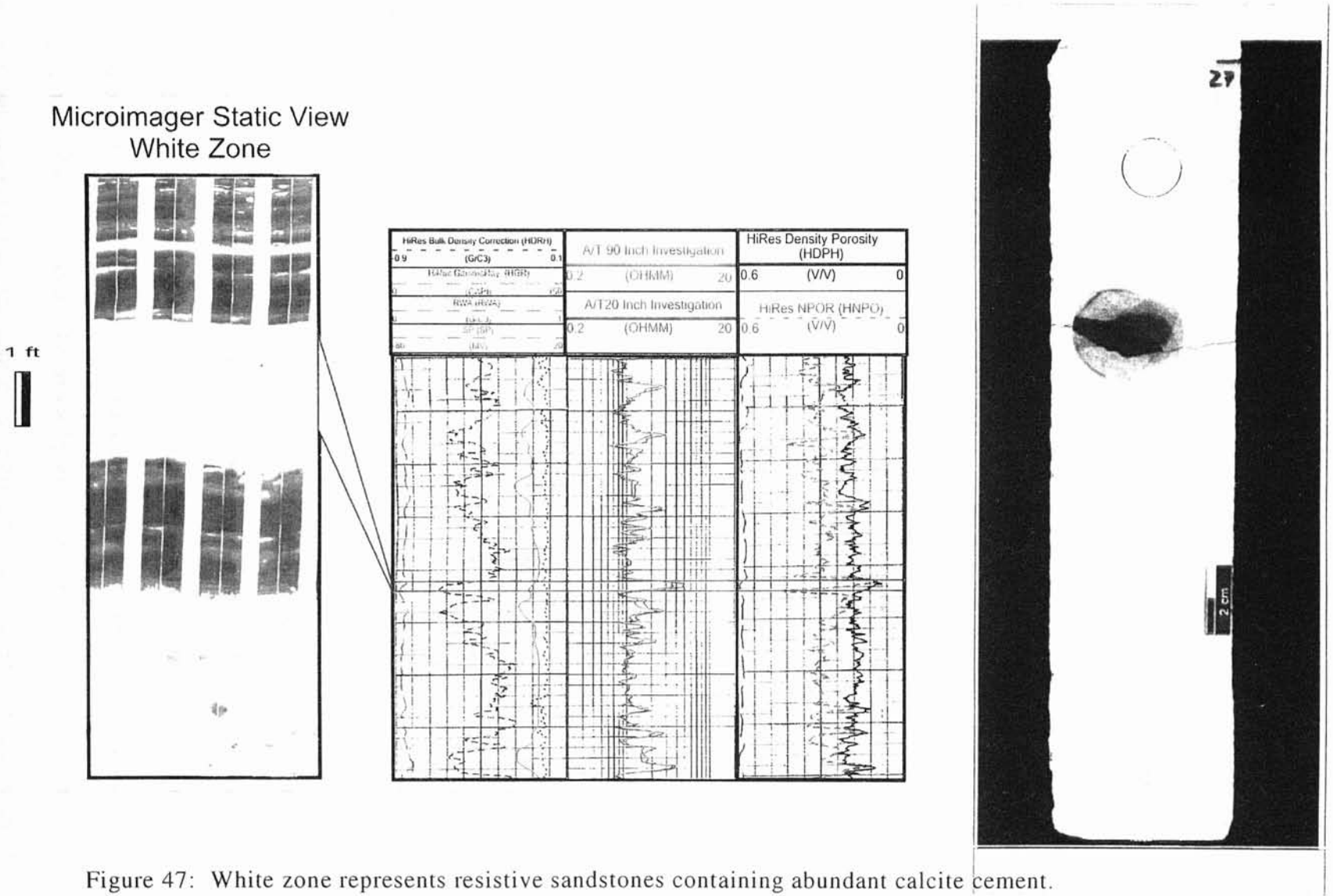

Figure 47: White zone represents resistive sandstones containing abundant calcite cement.

Capillary Pressure

Capillary pressure data were obtained to determine sealing capacity and pore structure for each microimaged chromatic zone.

White zones have the highest displacement pressures (Pd) at approximately 2454 psi. The highest gas column height will hold 547 feet without leaking (Fig. 48). Yellow zones have the lowest displacement pressures (less than 200 psi) and gas column heights that average less than 10 feet (Fig. 49). Orange zones displayed a wide range of displacement pressures and gas column heights. One orange zone sample displayed microporosity, but no apparent moldic porosity, with a displacement pressure of 682 psi and gas column height of 152 ft. However, a second orange zone sample exhibited typical values for displacement of 171 psi and gas column height of 38 feet (Fig. 50).

Pore throat size, sorting, and distribution were derived from capillary pressure curves. The sorting of pore throats reflects the rock ability to accept hydrocarbons. Pore space in well sorted rocks rapidly saturate with hydrocarbons once a threshold buoyancy pressure is reached. Poorly sorted rocks saturate slower and require a pressure increase over a much broader range to obtain the same hydrocarbon saturations (Jennings, 1987). Pore throat sorting for all samples ranges from moderately to poorly sorted. Median pore-throat size ranges from 0.03 to 0.96 microns. Median pore throat size for white zones was less than 0.1 micron. Yellow zones have median pore throat apertures that range from 0.2 to 0.96 microns. Orange zones have a wide range of median pore throat apertures that reflect the amount of dispersed pore-filling clay. Mercury injection curves for most yellow and orange zone samples indicated a bimodal distribution of pore-throat

White Zone

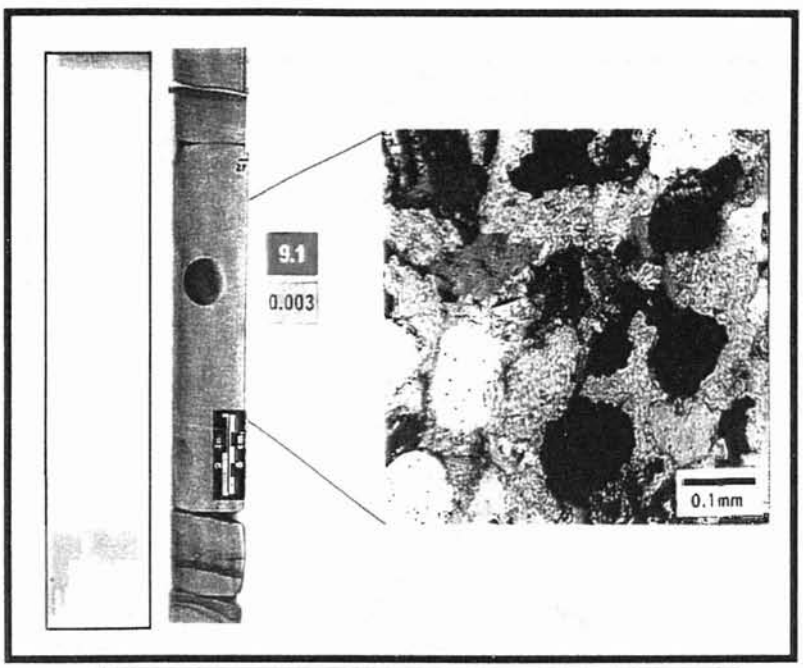

Pdma = 2454 psi

HHC = 547 ft

Median rc = 0.03 μm

Mode rc = 0.01 μm

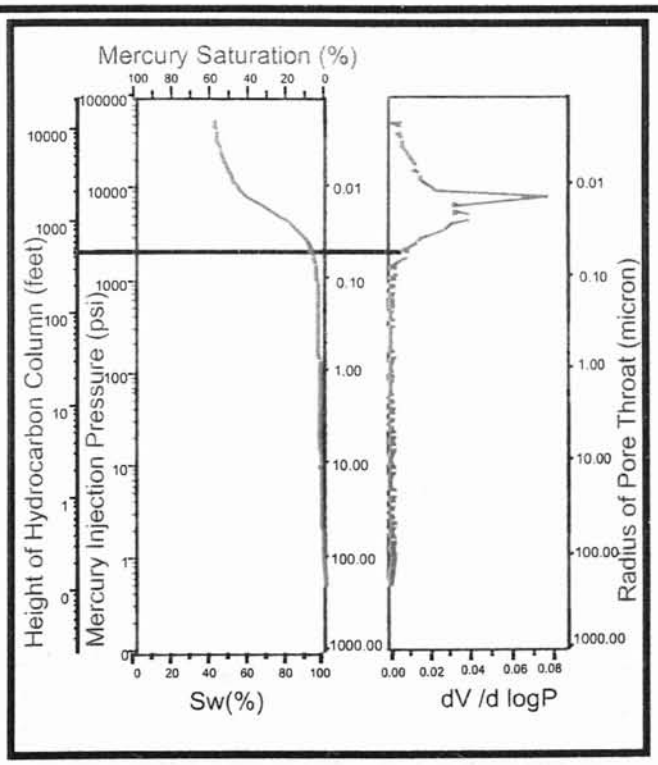

Figure 48. White zone

A. FMI, core photo, and photomicrograph of white zone with low porosity and permeability due to increased cementation.

B. Capillary pressure measurements depict high displacement pressure (Pdma), and highest hydrocarbon column heights (HCH).

Yellow Zone

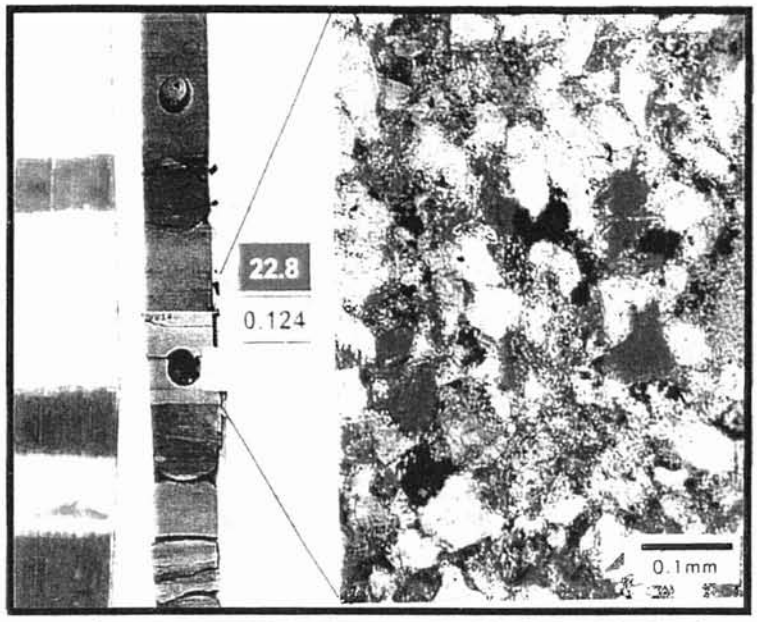

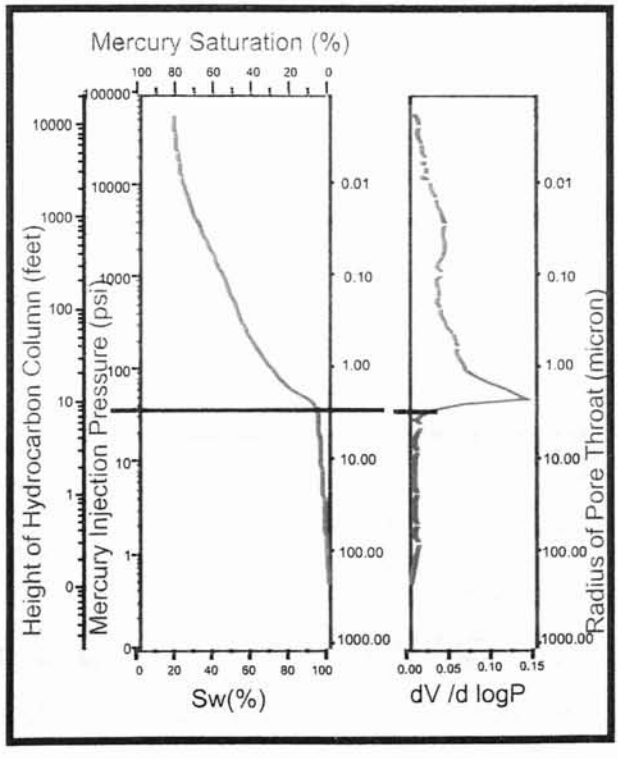

Pdma = 39 psi

HHC = 8.8 ft

Mode rc = 1.99 **u** m

Median rc = 0.58 **u** m

Figure 49. Yellow Zone

A. Photomicrograph of yellow zone with moldic porosity.

B. Capillary pressure data demonstrates low displacement pressures (Pdma), and low gas column (Hpd) height.

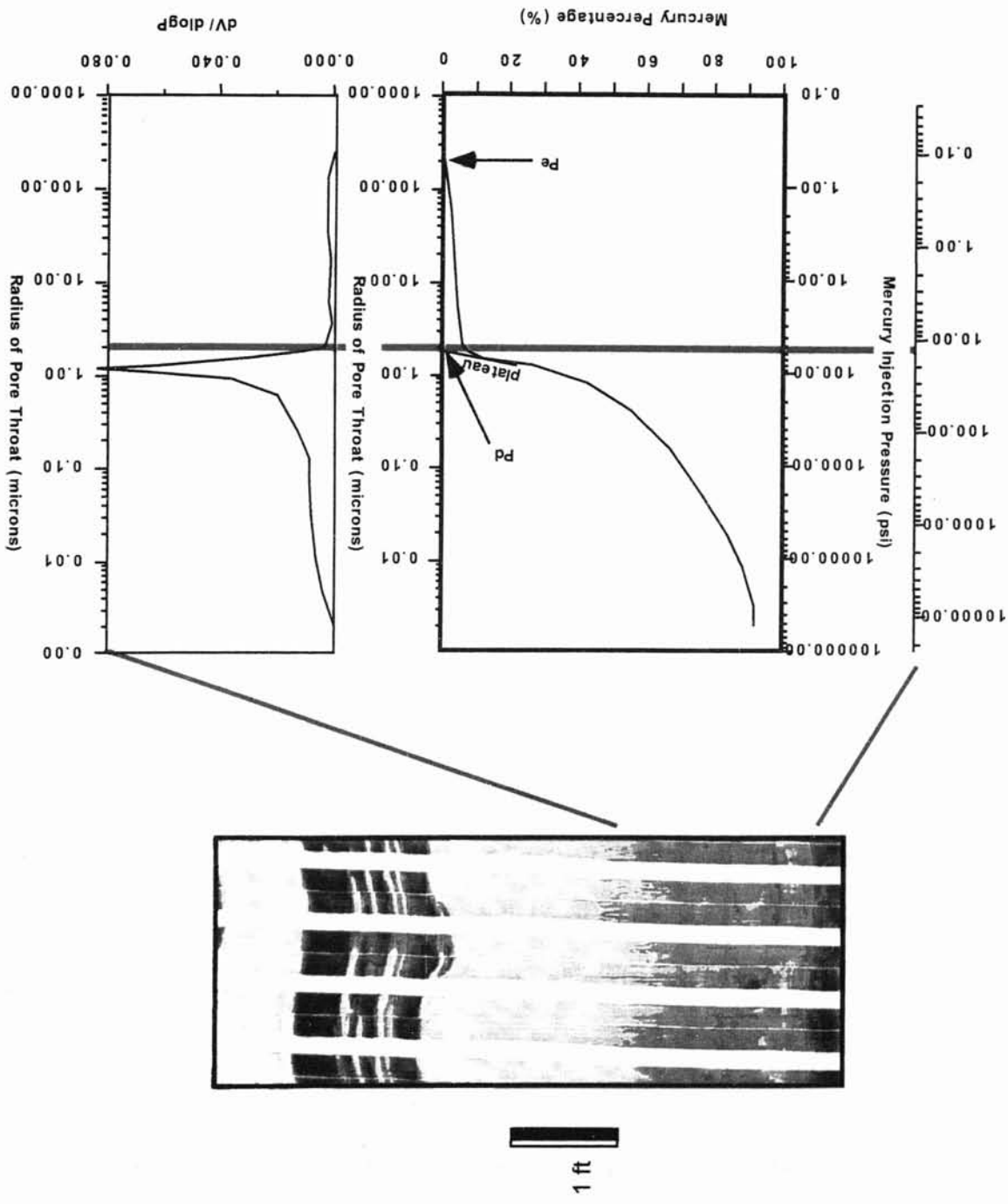

Figure 50. Orange zones display a wide variety of capillary pressure measurements. This is likely due to the amount of clay content within these intervals .

apertures between large moldic pores and clay-grain micropores between authigenic clay particles and within partially dissolved grains (Fig. 51).

Reservoir controls of the Lowstand systems tract

Introduction

The lowstand systems tract (LST) intervals were studied in the E.G. Canales #18 well and included the 10,250-ft, 10,500-ft and10,600-ft sandstone (Fig. 52). According to the QRF diagram by Folk, the sandstones within the LST interval range from litharenite, feldspathic litharenite to sublitharenite (Fig. 53).

Petrology

Detrital Constituents. Quartz is the most abundant and represents approximately 30% of the rock. Quartz grains are often corroded and display straight extinction. Plagioclase grains within this interval represented a slightly lower percentage (4.8). Plagioclase grains displayed typical albite twinning and were often affected by partial to complete dissolution. Volcanic rock fragements (VRF) were present and added to secondary porosity by dissolution. Figure 54 depicts the major detrital constituents within the LST such as quartz, plagioclase and VRF. Other detrital constituents were carbonate rock fragments, glauconite, biotite, foraminifera, metamorphic rock fragments, and sedimentary rock fragments.

A.

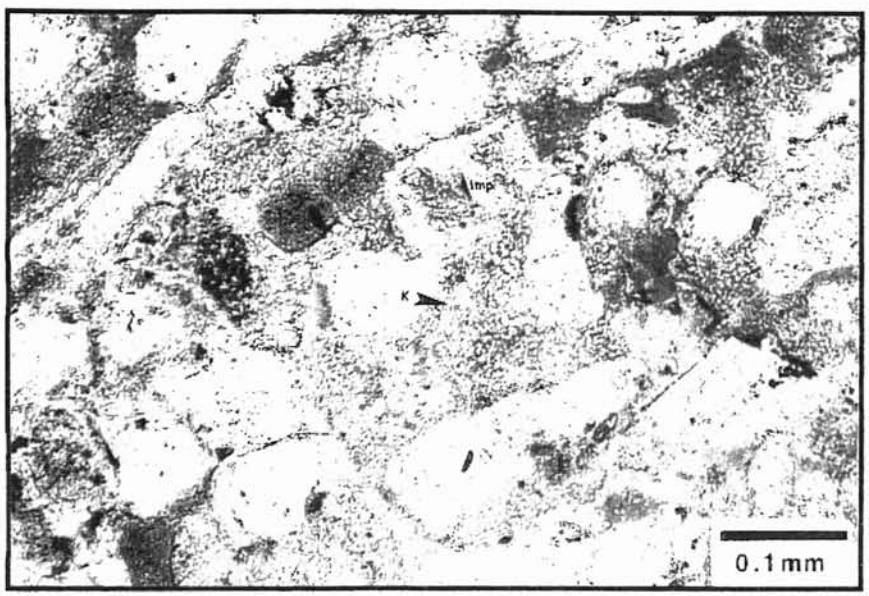

B.

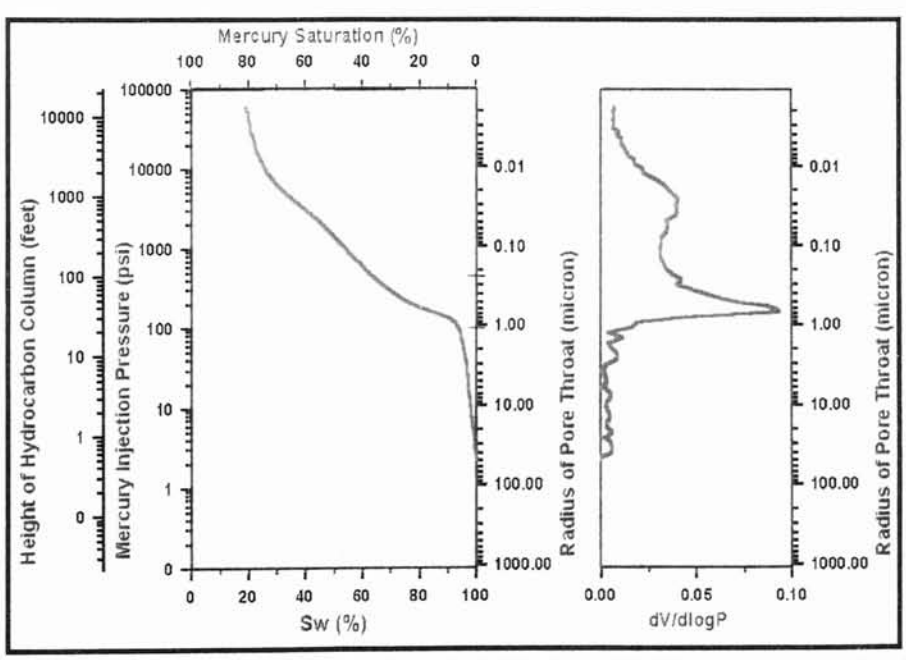

Figure 51. A. Photomicrograph of macro and micro-porosity.

B. Capillary pressure curves showing bimodal pore throat sizes.

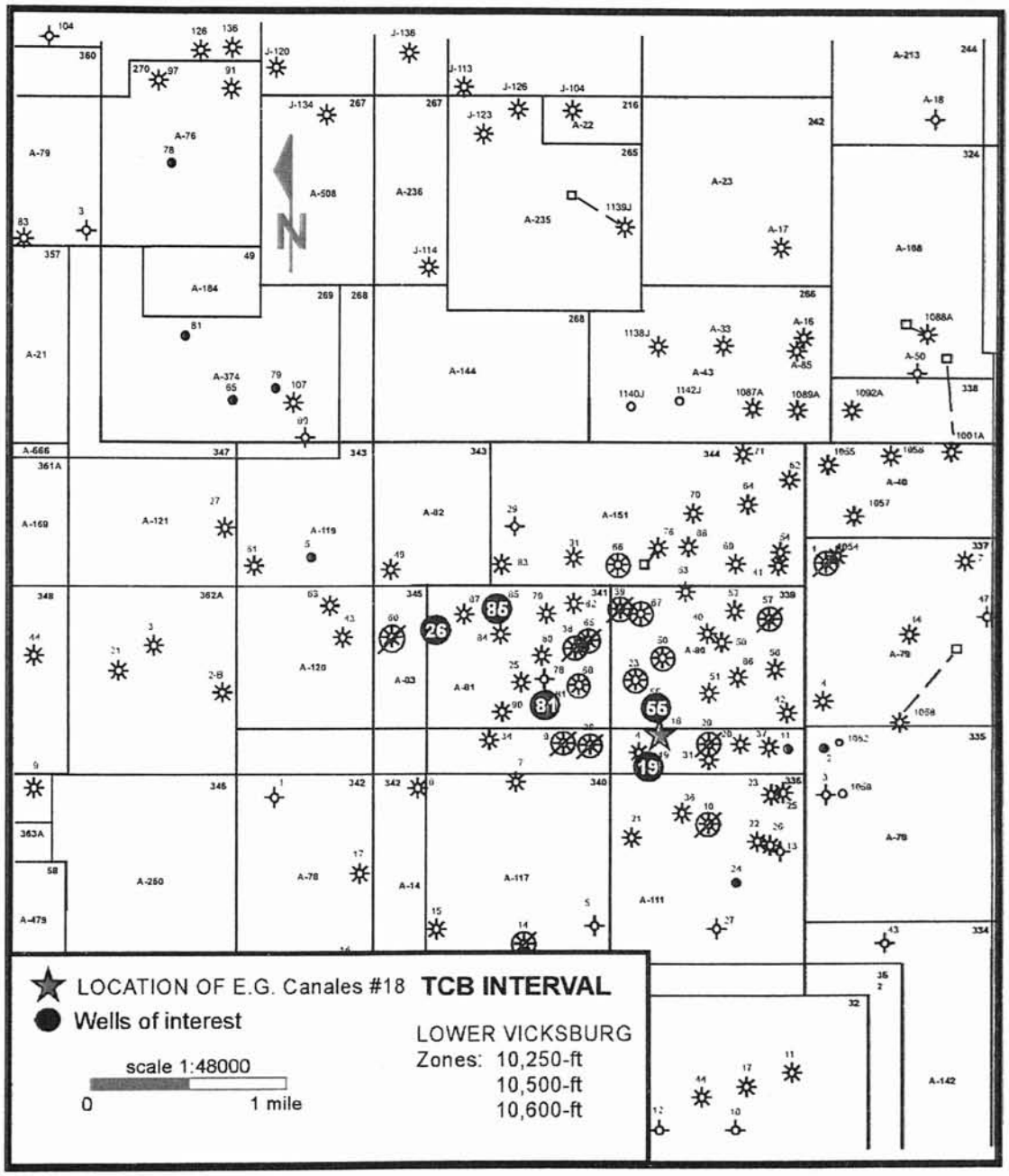

Figure 52. Location map of core studied, the E.G.Canales #18 in the Lower Vicksburg interval.

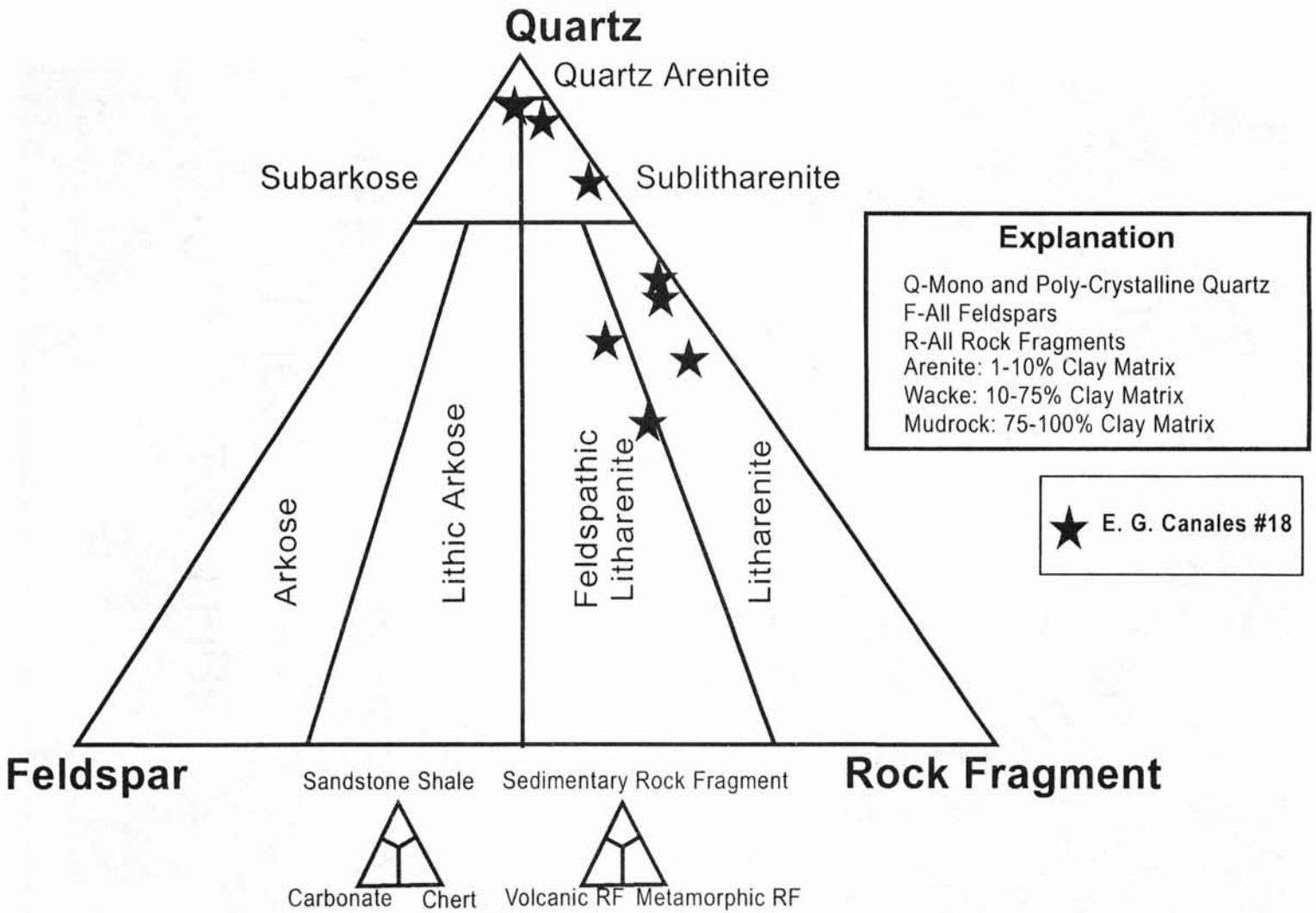

Figure 53. QRF diagram of the LST interval.

A.

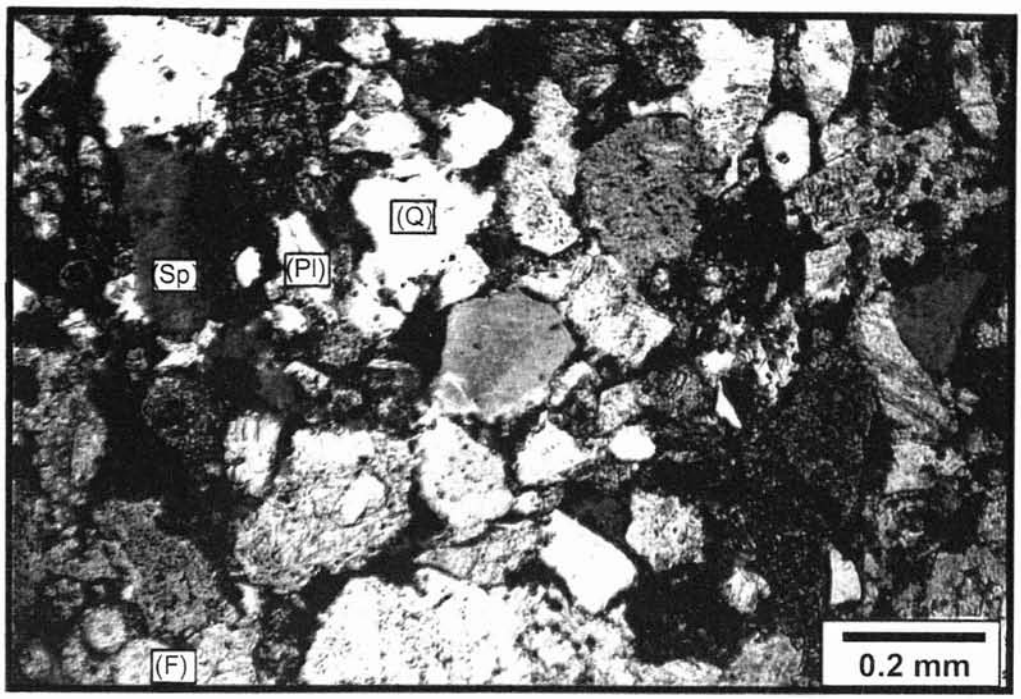

B.

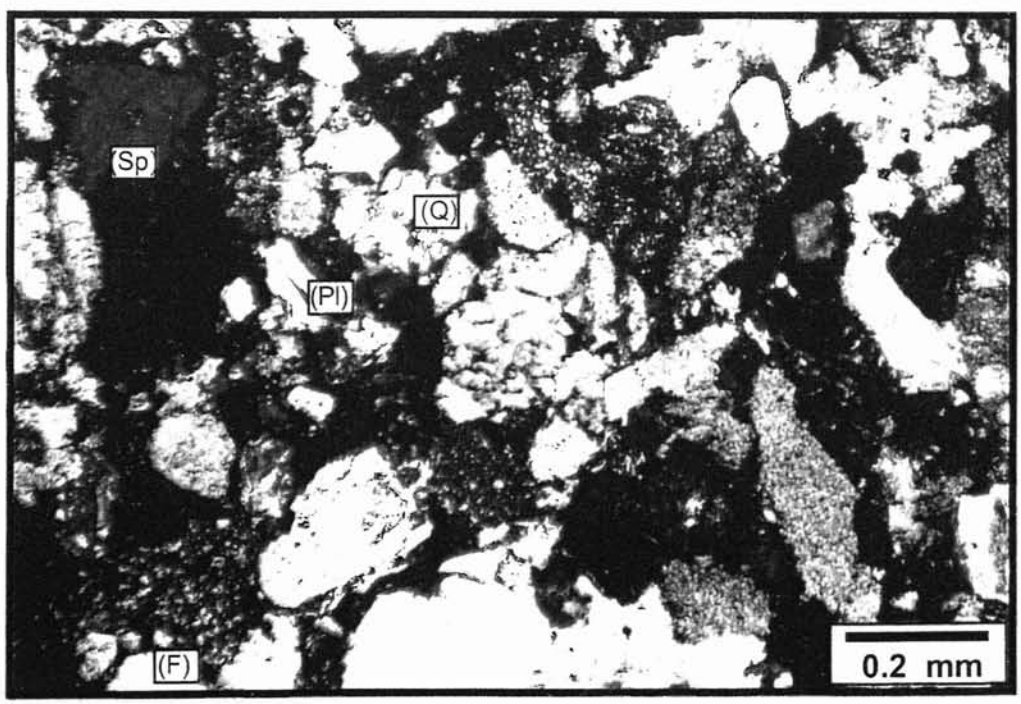

Figure 54. Photomicrograph showing quartz (q), plagioclase (Pl), secondary porosity (Sp) and forams (F). These are the typical constituents within the LST.
A. plain polarized light (PPL) B. Cross-nichols (XN).

Diagenetic Consituents

Cements. The main cement type in the LST in TCB field was calcite. Calcite occluded porosity and corroded grains (Fig. 55). Siderite is less abundant than calcite and fills pore space. Quartz overgrowths were not abundant within the LST. Quartz overgrowths require a relatively clay-free environment. Clays inhibited quartz overgrowths from nucleating and helped preserve porosity in the LST sandstones.

Clay Minerals

LST sandstones contain approximately 2-5% authigenic clay. The types of clays identified within the samples are illite/smectite mixed layer clay, chlorite and kaolinite (Fig. 56). These clays aided in the preservation of porosity and were more abundant when early calcite cementation did not occur.

Porosity

Secondary porosity was the dominant porosity type in LST rocks and resulted from the dissolution of plagioclase, volcanic rock fragments (VRF), and minor amounts of quartz (Fig. 57). The most common type of secondary porosity was intergranular and moldic porosity.

Primary porosity was less common, but was an important conduit for corrosive fluids that generation secondary porosity.

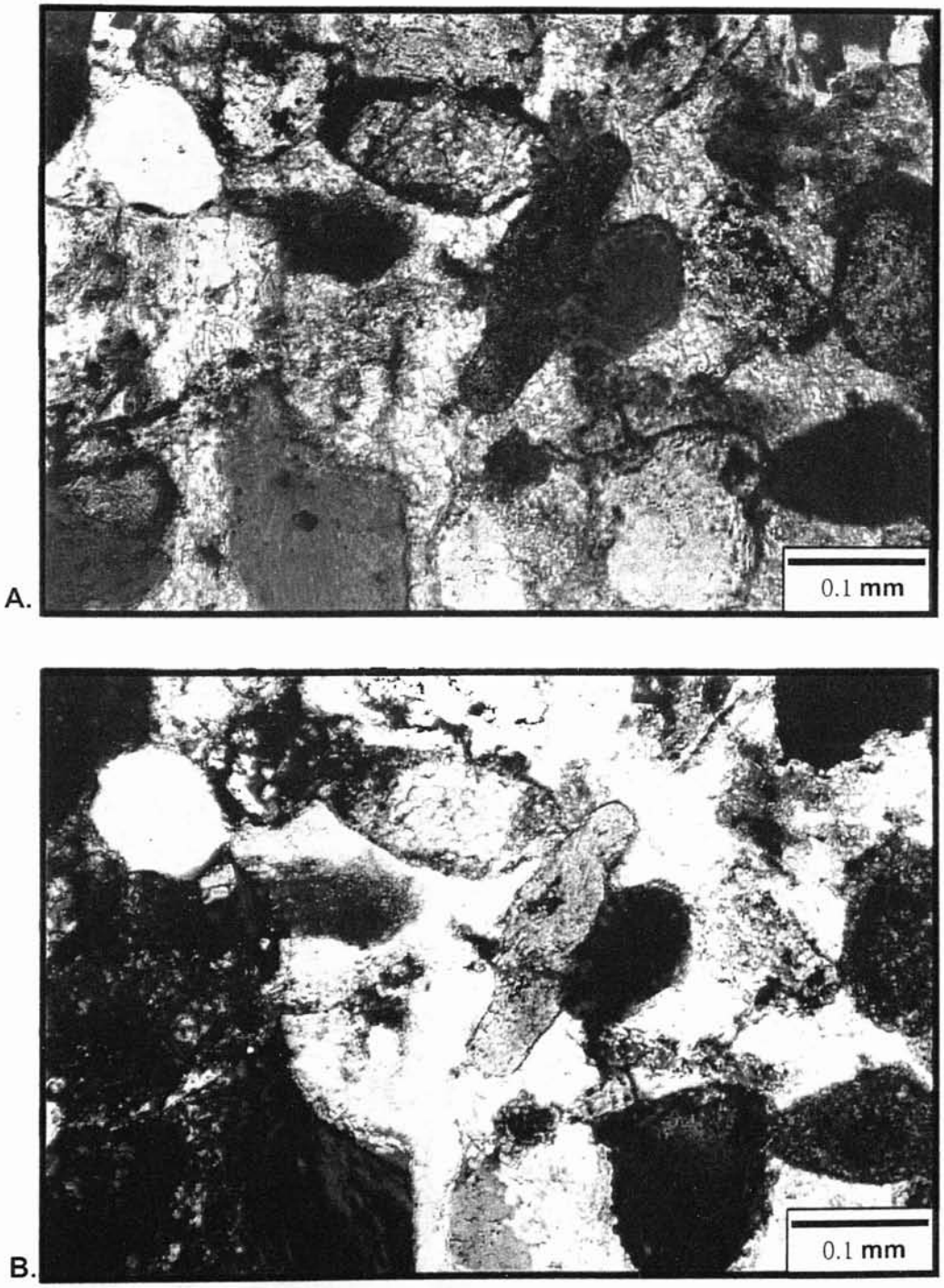

Figure 55. Photomicrograph of calicte occluding porosity and corroding grains.
A. Plane ploarized light (PPL).
B. Cross ploarized light (CPL).

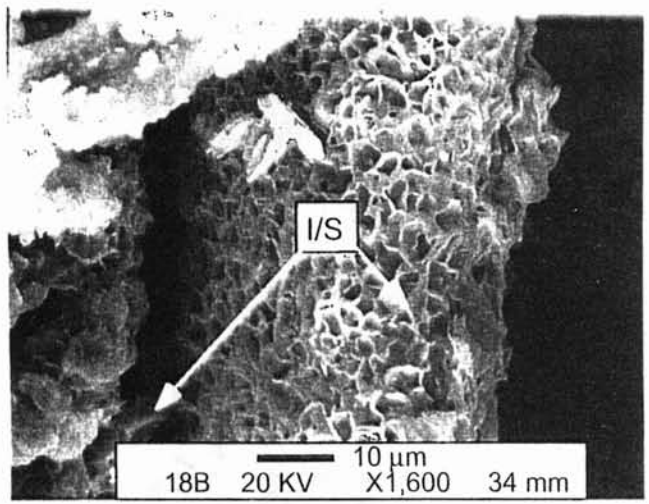

A.

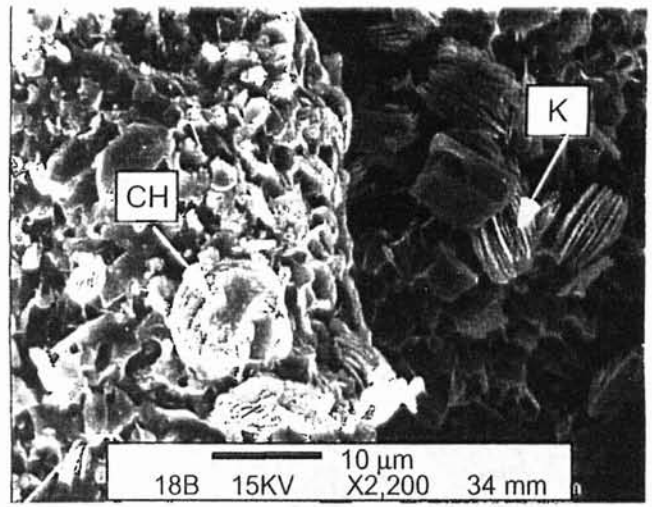

B.

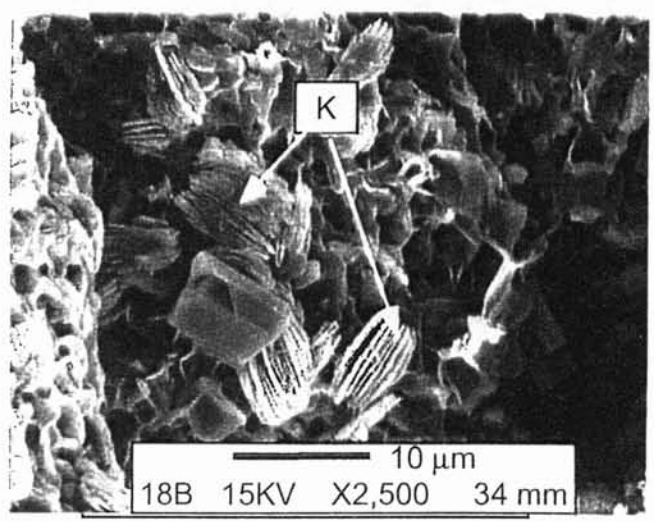

C.

Figure 56. A. Scanning electron photomicrograph (SEM) Pore bridging and grain coating illite/smectite (I/S)
B. Kaolinite (K) filling pore space andChlorite rosettes(CH).
C. Kaolinite (K) filling pore space.

A.

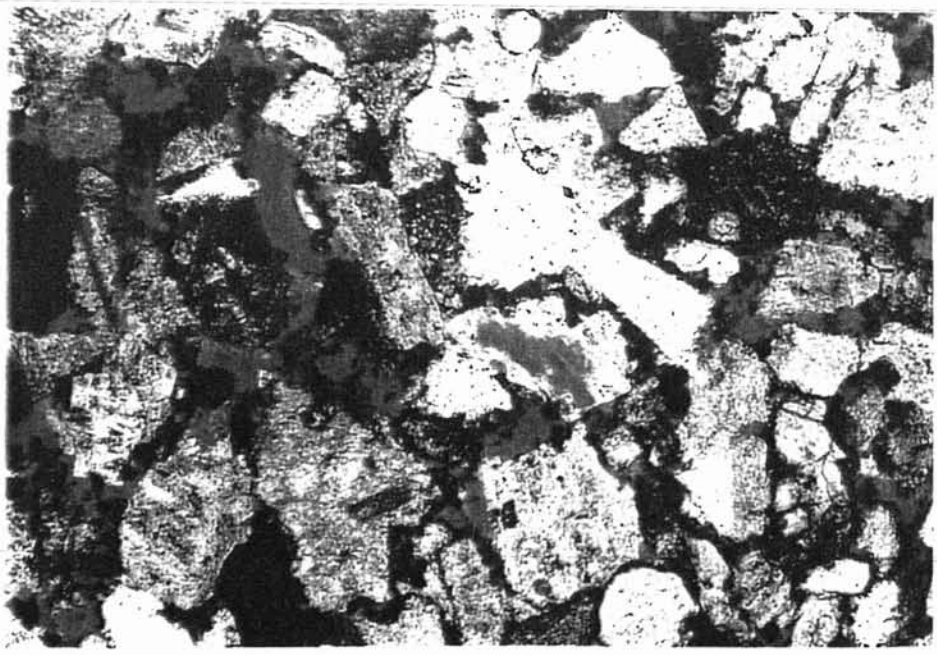

B.

Figure 57. Photomicrographs displaying secondary porosity and dissolution of plagioclase. A. Plain polarized light (PPL) B. Plain polarized light (PPL)

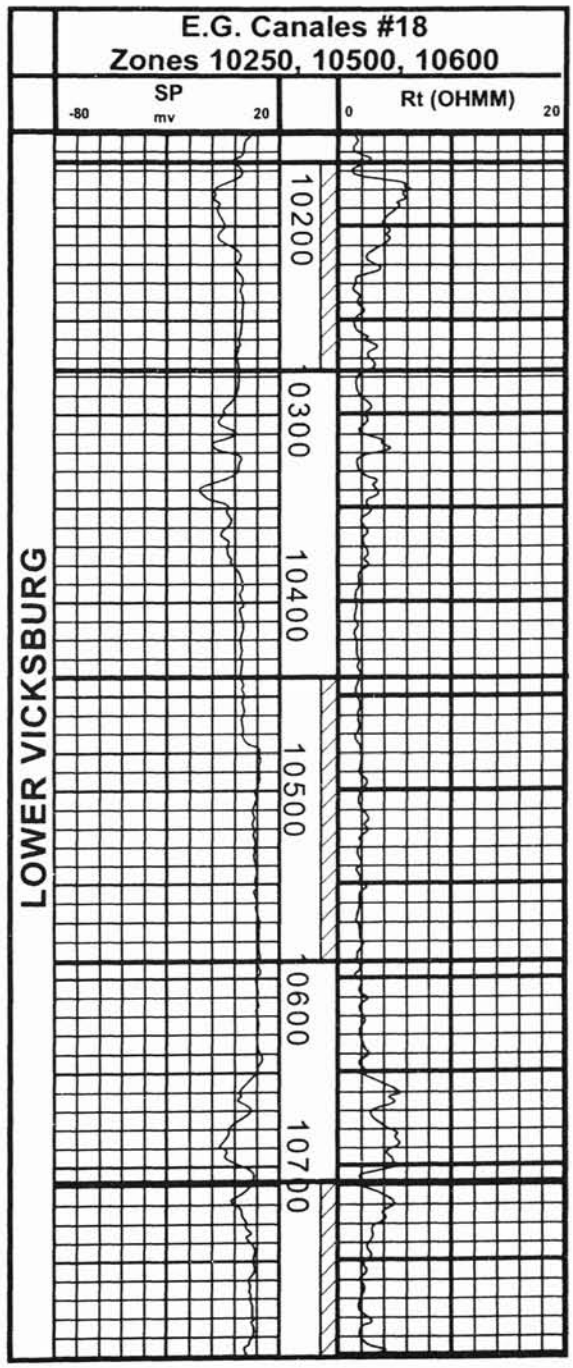

Figure. 58 Tract I SP curve demonstrates deviation of 10-20 mv from the shale base line across LST sandstones

sandstone resistivity ranged from 11-18 ohm-m2-m, depending on the amount of cementation.

Porosity Logs. LST sandstones contained a considerable amount of clay. This clay content increased the neutron porosity measurements. Therefore, shaly zones have approximately 20% separation between the neutron and density porosity curves. In sandy zones the separation was less, at approximately 9%.

Capillary pressure

Two distinct intervals were identified within the LST: seals and reservoirs. Reservoirs have HCH values less than 250 ft, indicating higher porosity and permeability (Fig. 59). The pore types within these intervals were dominantly macropores with radii of approximately 105 microns (Fig. 60). On the other hand, samples with HCH values from 275-1000 ft and pore throat radii from .1-. 01 microns indicate the presence of microporosity and sealing capability (Fig. 61).

Intervals with increased calcite cementation and smaller grain size have high HCH (greater than 250 ft), mostly microporosity, and lower permeability and porosity. Reservoirs within the LST are zones with larger grain size and less calcite cementation. Clays are more abundant in these zones that indicated lack of early cementation and preservation of porosity. Reservoir HCH values were less than 250 ft and macroporosity was the dominant type.

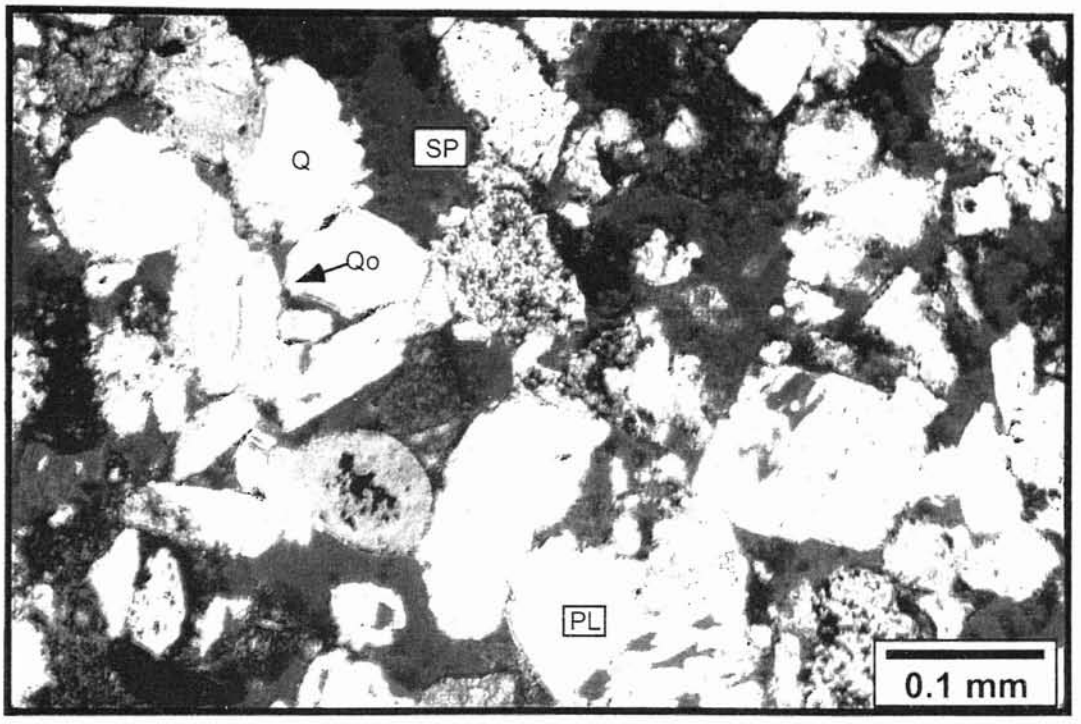

Figure 59. A. Photomicrograph of monocrystalline quartz (Q) and plagioclase (Pl). Secondary porosity (Sp) is commonndue to dissolution of grains such as plagioclase. This porosity is classified as macroporosity and can be identified with capillary pressure measurements.

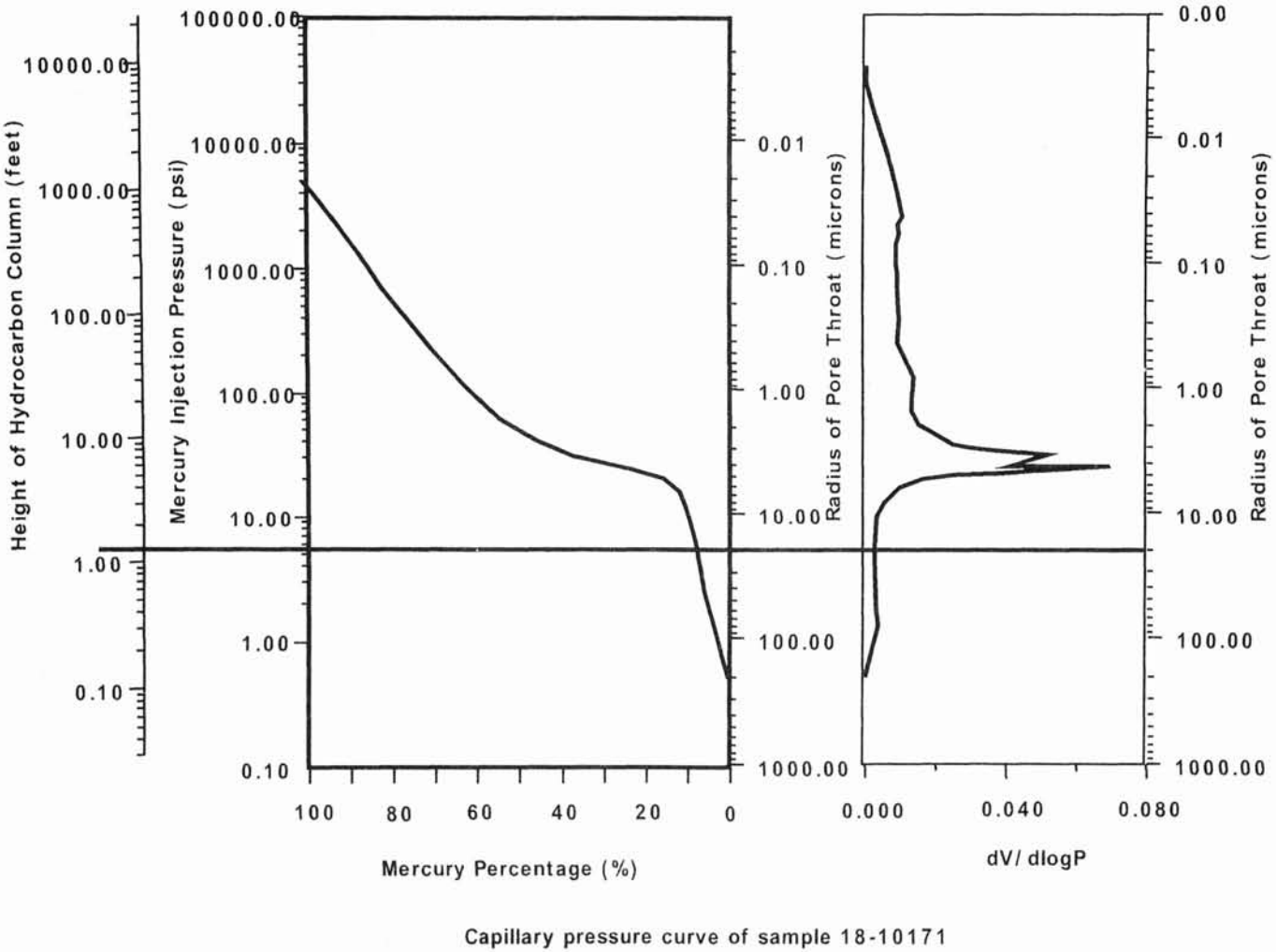

Figure 60: Capillary pressure curves demonstrate reservoir quality sandstone with higher porosity and permeability.

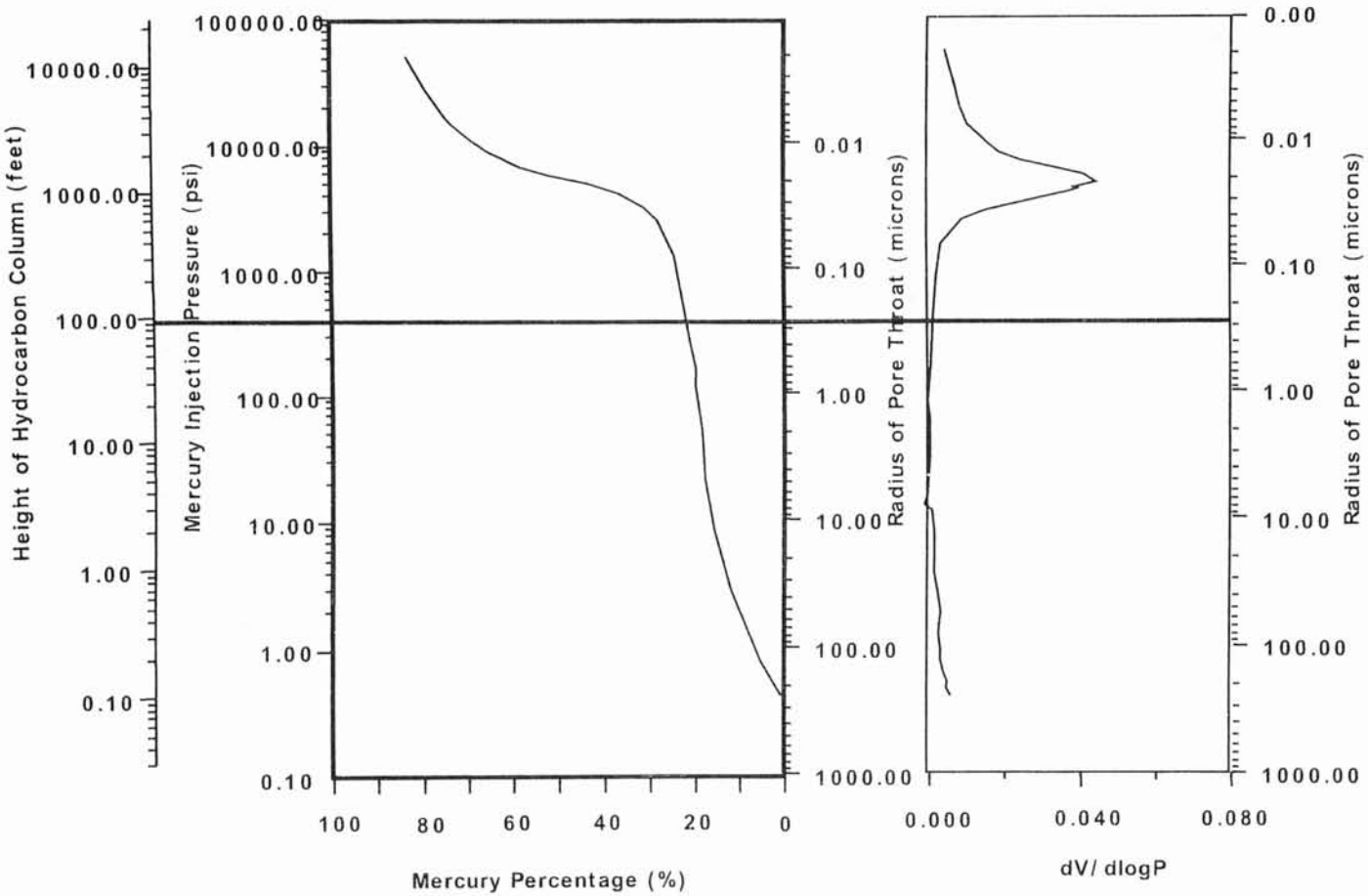

Figure 61. Capillary pressure curve demonstrates higher HCH values and microporosity which is indicative of a sealing interval.

Chapter IV

Comparative Analysis of the Vicksburg Reservoirs

Introduction

Vicksburg reservoirs were analyzed comparatively for some features that affect trapping mechanisms and production potential. Features examined were 1) bed thickness 2) grain size 3) porosity and permeability and 4) sealing capacity.

Bed Thickness

The Vicksburg is a formation, which is a lithologically distinctive unit of scale large enough to be mappable at the surface and in the subsurface. Formations may be divided into smaller stratigraphic units called members. Members may then be divided into smaller distinctive units called beds. Beds, which are the smallest formal lithostratigraphic unit, are defined as tabular or lenticular layers of sedimentary rock that have lithologic, textural, or structural unity that clearly distinguishes beds from other layers. (Boggs, 1995) In this case, the bed thickness was determined of sandstones within each core of interest.

Bed thickness is important to identify the type of evaluation tools needed to resolve boundaries and determine fluid types. Beds greater than 2 feet thick can be evaluated

using conventional logging techniques. Bed thicknesses less than 2 feet thick must be evaluated using high-resolution logs and mircoimaging tools.

Bed thickness was determined by integrating conventional wire-line logs, high-resolution logs, and core. Sandstone beds were defined as uniform lithologic units (sandstone) with spontaneous potential (SP) deflection of –10 to -20 mv and/or gamma ray value approximately 40-50 API units less than a shale average.

Highstand systems tract (HST). The HST reservoirs (9,000- ft sandstones) contained beds that are thicker than the TST but slightly thinner than the LST interval. These beds range from <1 ft to 24 feet and average 3.9 feet. The beds greater than 2 feet represent approximately 53% of the rock within the HST reservoirs.

Trangressive systems tract (TST). TST reservoirs (9,900-ft sandstone) contained the thinnest beds within the Vicksburg wells studied. Most sandstone intervals were not readily evident on conventional logs. However, using microimaging tools and high-resolution logs the thin sandstone beds can be identified. Most of the sandstone beds in the TST were thinner than 1 foot.

Lowstand systems tract (LST). LST reservoirs (10,250-ft, 10,500-ft, 10,600-ft sandstones) contained the thickest beds, which ranged from 6 inches to 25 feet and average 6.6 feet. Beds greater than 2 feet represent 67% of the rock within the LST reservoirs, while 33% of beds were less than two feet.

Grain Size

Grain sizes were determined primarily by thin-section analysis. Therefore, this study focused on the evaluation of the grain size through the point count technique. Fifty-two thin sections were prepared across the Vicksburg interval, and a total of 520 point counts were conducted. These results are summarized in chart 1.

	Bed Thickness (Ft)	Grain Size (mm)
Highstand systems tract (HST)	3.9	0.11
Trangressive systems tract (TST)	<1.0	0.05-0.14
Lowstand systems tract (LST)	6.6	0.251

	Porosity seal zone (%)	Porosity reservoir zone (%)	Permeability seal zone (md)	Permeability reservoir zone (md)	Porosity feet (20 Ft interval)
Highstand systems tract (HST)	7-15	19-21	0.001-0.05	>10	14
Trangressive systems tract (TST)	5-12	15-23	0.0010-0.015	0.01-3	6
Lowstand systems tract (LST)	7-15	19.5-23	0.01-0.2	>0.6	19

Chart 1.

Highstand systems tract (HST). The average grain size from all sandstones in the highstand systems tract was approximately 0.11 millimeters. According to the Wentworth scale (Folk, 1968), the HST is classified as a very fine-grained sandstone.

Transgressive systems tract (TST). The grain sizes in the transgressive systems tract sandstones ranged from .05 to .14 millimeters. According to the Wentworth scale (Folk, 1968), the TST is classified as a coarse siltstone to very fine sandstones. The smaller grain size within the TST increases its sealing capacity.

Lowstand systems tract (LST). The average grain size in the LST sandstones was approximately .2506 millimeters. This is the largest grain size in the Vicksburg cores and thin sections studied. This increased grain size ultimately resulted in higher porosity and permeability.

Porosity and Permeability

Secondary porosity is the main type of porosity identified within the Vicksburg sandstones. Secondary porosity developed as result of destructive diagenesis such as dissolution of rock fragments, grains, matrix and/or cement by formation fluids. The most commonly dissolved constituents were plagioclase grains and volcanic rock fragments. Porosity was determined using core plug analysis, and thin section point counts. Core plug porosity values were higher than thin section values as a result of microporosity, which can not be accurately identified by the point count method.

Permeability was determined solely by core plug analysis. Permeability is the property of a rock to transmit fluid. It is the measure of the fluids ability to move through the rock and is measured in millidarcies (md).

Porosity and permeability varied within and between the systems tracts. General trends were evident and illustrated differences between them.

Lowstand systems tract. The porosity and permeability study in the E.G. Canales #18 focused on three sandstone intervals: 10,250-ft, 10,500-ft, and 10,600-ft sandstones. All intervals displayed the same general trend of three distinct populations: (Fig. 62). Core plug porosity ranged from 7 to 23% for the three sandstones.

1. Seal zones: porosity ranges from 7-15% and permeability .01-.2 md. These zones contained abundant calcite cement that occluded most porosity and limits permeability
2. Intermediate zones: porosity ranges from 15-19.5% and permeability .18-.4 md. These zones displayed some calcite cement and have increased clay content.
3. Reservoir zones: porosity ranges from 19.5-23% and permeability greater than .6 md. These zones have moderate to slight calcite cementation and increased moldic and intergranular porosity, thus resulting in higher permeability measurements.

The LST reservoir quality was evaluated by determining porosity feet. A porosity foot is the number of feet greater than 15% percent porosity over a set interval (20ft). This evaluation was completed utilizing core analysis and neutron/density porosity logs for the 10,250-ft and 10,600-ft sandstones. The 10,500-ft sandstone interval was shale in the cored wells and not used in this evaluation. Porosity feet calculated from the core and logs of the 10,250-ft sandstone, is approximately 19 feet. In the 10,600-ft sandstone interval, variation between the core and log analysis was evident.

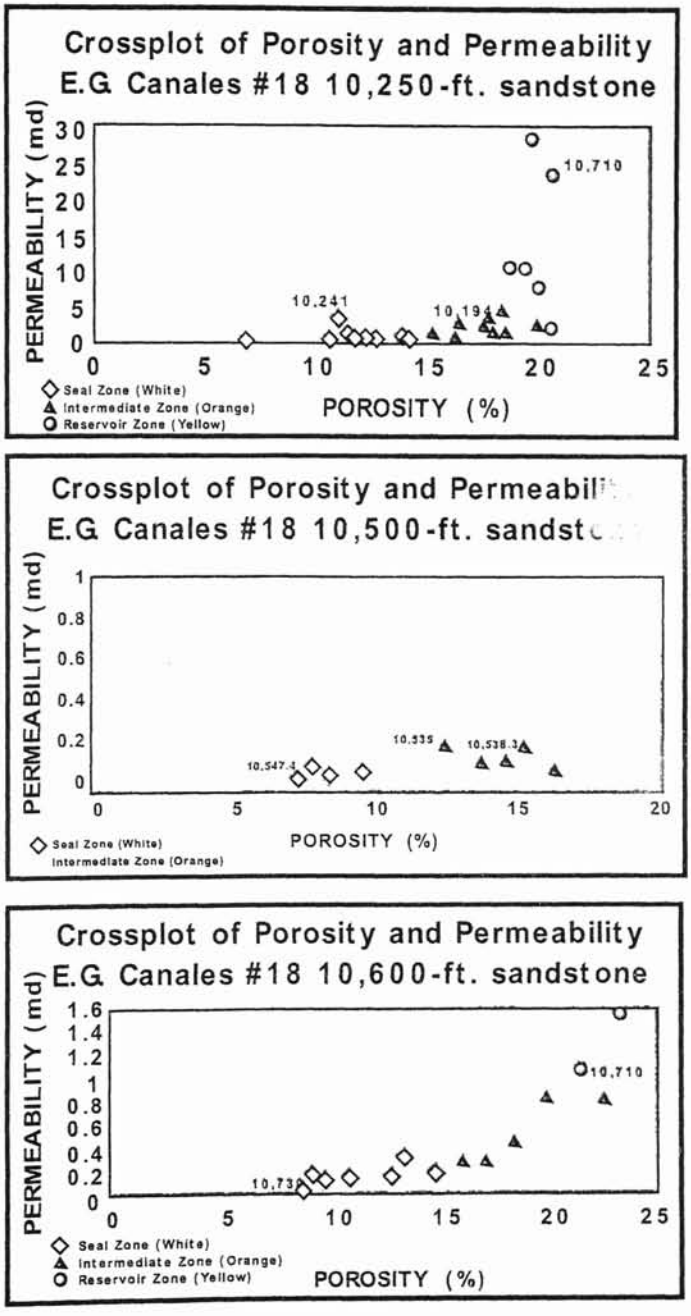

Figure 62. Porosity/Permeability crossplot demonstrates a general trend of three distinct populations

One interval showed close correlation between the core and log measurements (Porosity feet log: 12, core: 13). On the other hand, another interval of the 10,500-ft sandstone indicated a difference in log/core analysis (Porosity feet log: 17, core 5). This is likely the result of bias introduced during core sampling, and porosity averaging by logging.

Transgressive systems tract. The A.T. Canales #81 and #85 (9900-ft sand) displayed the same general trend as the LST and TST (Fig. 63). However, within this interval microimaging was utilized due to the thin-bedded nature. Microimaging data were correlated to core and thin sections to match constituents with the resistivities of the chromatic zones. Three porosity and permeability zones were identified in the TST. Based on correlations, the white zones were highly cemented with calcium carbonate and are considered as a seal zone. The yellow chromatic zone has high porosity and permeability and considered to be reservoir zones. The orange chromatic zone has increased clay contents, along with some calcite cementation. The orange zones are considered to be the intermediate zones. The brown chromatic zones are typically shale intervals.

1. Seal zone (White zone): porosity ranging from 5-12% and permeability approximately .0010-.015md.
2. Intermediate (Orange zone): porosity ranging from 14-17.5% and permeability .001-.005 md
3. Reservoir zone (Yellow zone): porosity ranging from 15-23% and permeability .01md – 3 md.

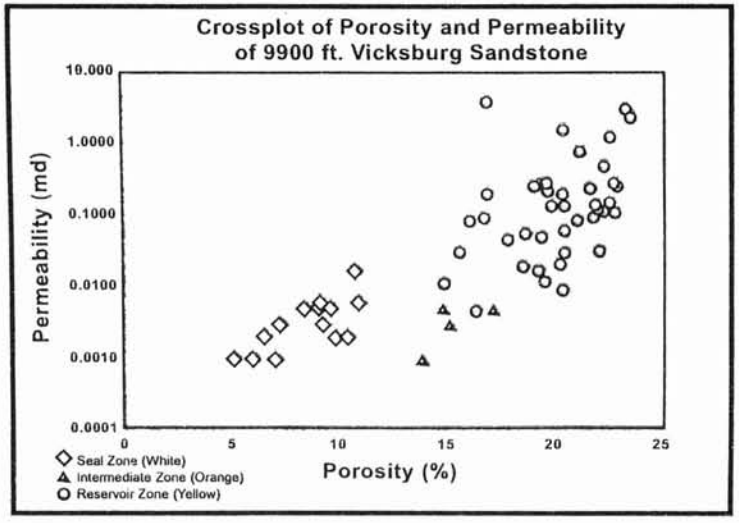

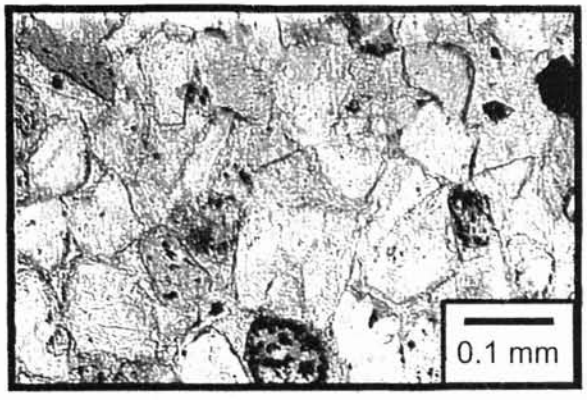

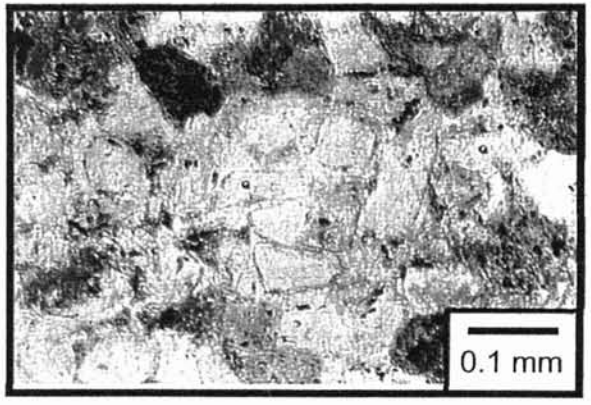

Figure 63 Porosity/Permeability crossplot demonstrating the same general treand as the LST and HST intervals

The porosity feet for the TST sandstones was evaluated using log and core analyses. The log analysis indicated porosity feet value of 6 and core analysis value of 15.

Highstand systems tract (HST). The HST has the highest porosity and permeability of all the systems tracts. Three porosity and permeability zones were also recognized in highstand systems tracts (Fig. 64).

1. Seal zone (white): porosity was approximately 7-15% and permeability was 0.001 to .05 md.
2. Intermediate zone (orange): porosity ranges from 15-19% and permeability was .1 to 4 md.
3. Reservoir zone (yellow): porosity is 19- 21% and permeability was greater than 10 md.

Porosity/feet within the HST was evaluated using log analysis only. The porosity/feet was determined to be approximately 14 ft.

Seal Capacity

Seal capacity is the maximum hydrocarbon column the seal can hold before it leaks. Seal capacity is determined by: Hmax = Pds-Pdr/ 0.433 (pw-phc)

- Hmax is the maximum height of the hydrocarbon column held in feet
- Pds is the brine displacement pressure of the seal rock (grams per cubic centimeter)

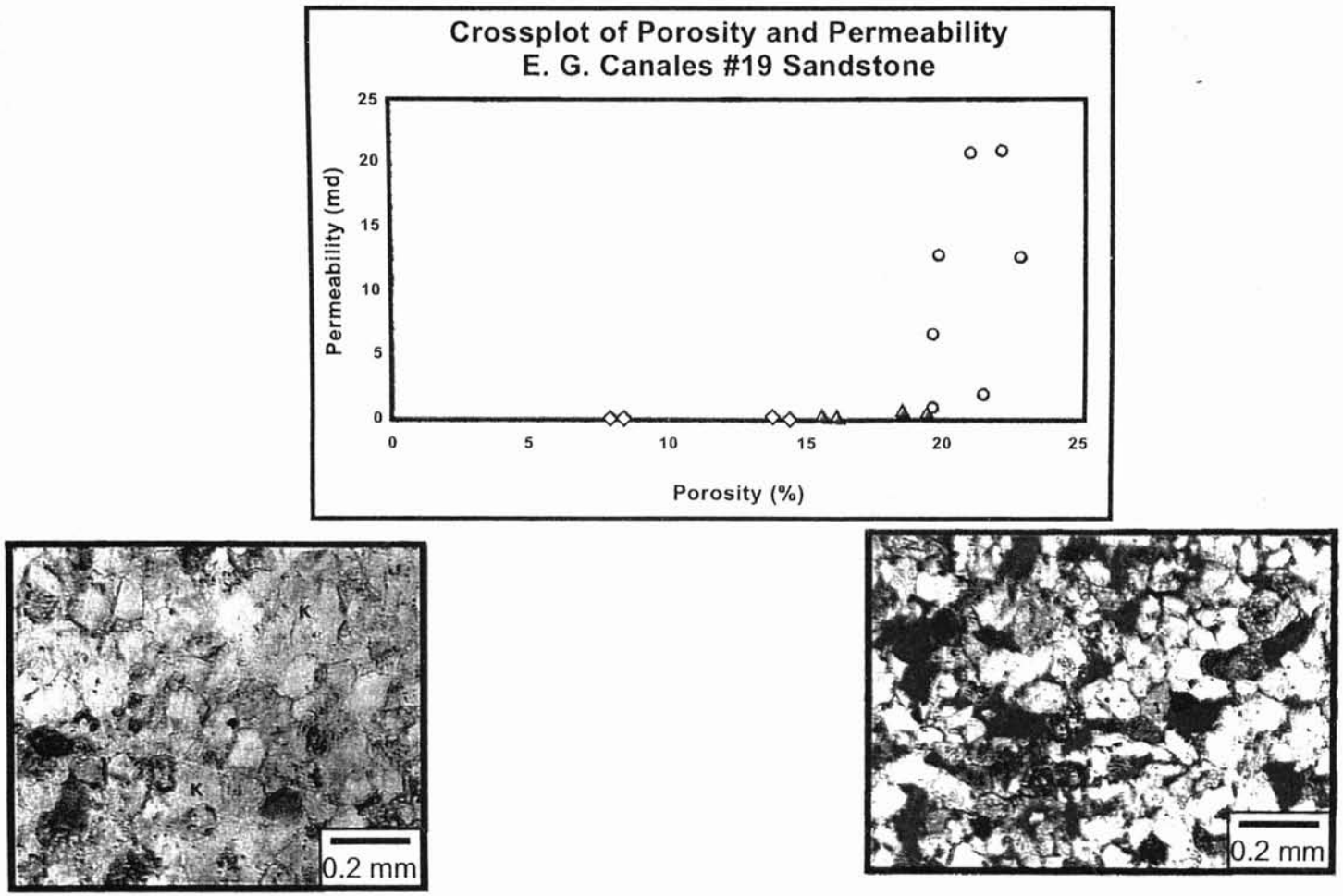

Figure 64. Porosity/Permeability crossplot demonstrate the three intervals (yellow, oreange, and brown.).

- Pdr is the brine displacement pressure of the reservoir rock (grams per cubic centimeter)

In terms of seal capacity, which was determined by capillary pressure measurements the highest displacements pressures within all systems tracts is in calcite-cemented zones (white zones). The Hmax or HCH of seals in the highstand systems tract was approximately 75 feet. While, HCH of seals in the trangressive systems tract ranges from 100 to 300 feet. However, the HCH of seals in the lowstand systems tract ranged from 200- 1000 feet (Appendix A). The lowstand systems tract represented the most effective seal based on the amount of hydrocarbon column the seal can hold without leaking. However the TST has more seals per 30 feet interval. The TST seals are likely to be more competent.

Summary

Constituents, porosity and permeability are similar throughout all systems tracts. However, the most striking differences were bed thickness, porosity feet and number of seals per interval. The bed thickness was greatest within the HST and LST. The transgressive systems tract was thinly bedded, which created difficulty when evaluating with conventional methods. Porosity/feet was based on the average porosity over a 10-30 feet interval. The HST and LST represented the greatest porosity feet at approximately 20%. While the TST, was less due to the interbedded sandstone and shale characteristics. The number of seals per interval was also remarkably different. The HST and LST contained fewer seals than the TST.

These differences impacted the trapping of oil and gas and well productivity. In general the highly compartmentalized TST was productive over a larger area and wider range of structural positions. The more homogeneous LST and HST reservoirs were productive where rollover provides anticlinal closure to trap oil and gas.

Chapter V

Conclusions

Vicksburg sandstones in TCB field provided an opportunity to examine the influence of sequence stratigraphy and rock architecture on reservoir quality. The three sandstone types: HST, TST and LST have reservoir qualities that relate to their depositional fabric and diagenetic histories. Seals and reservoirs can be determined by capillary pressure measurements. High hydrocarbon-column heights (HCH) are indicative of seals. Conversely, reservoirs have low HCHs. Depositional setting and sequence-stratigraphic framework of Vicksburg sandstones influences their trapping style and productivity.

Highstand systems tract

HST reservoirs are less compartmentalized than the other systems tracts and are on average thick enough (3.9 ft) to be evaluated by conventional logs. These reservoirs are productive only where sandstones are folded over the crest of the rollover anticline. The HST is considered to be a conventional reservoir that is characterized by thicker and cleaner sandstone intervals with few shale interbeds.

On the average, the sandstones are very fine-grained. Porosity and permeability range from 7 to 23% and 0.01 to greater than 0.6 md respectively. Seal zones generally have 7-15% porosity and 0.01 to 0.2md permeability. Reservoir porosities range between 19.5-

23%. Permeability is generally greater than 0.6 md. Porosity/feet is approximately 14 to 20. The HST sealing capacity is approximately 75 feet of hydrocarbons.

Transgressive systems tract

TST reservoirs are highly compartmentalized by internal seals and produced over a wide range of structural positions on rollover anticlines. TST reservoirs are typically less than one foot thick. Therefore, conventional logs are not useful in evaluating these intervals. Specialized tools such as microimaging and high-resolution logs are imperative to determine correct porosity and water saturation measurements. TST reservoirs are productive over much larger areas than LST and HST.

The average grain size in a TST reservoir is coarse silt to very fine grain sand. Porosity ranges from 5-23% and permeability from 0.0010-0.015md. Seal (white) zone porosity is approximately 7%, while permeability is 0.0010 md. Reservoir (yellow) zone porosity is approximately 20%, while permeability increases to approximately 0.015md. Sealing capacity of the TST interval is approximately 100-300 ft of hydrocarbon column.

Lowstand systems tract

LST reservoirs have sandstone beds that are approximately 6.6 feet thick. This characteristic allows evaluation by conventional methods. The average grain size is 0.251 millimeters, which is considered to be very fine-grained sandstone. Porosity and

permeability vary from 7-23% and 0.01-0.2 md, respectively. Porosity is approximately 21% and permeability is greater than 0.6 md in reservoirs. Conversely, in seal zones, the porosity and permeability is greatly reduced to approximately 10% and 0.01-0.2 md respectively. In terms of sealing capacity, the LST can support 200-1000 feet of hydrocarbon column. Trapping in LST reservoirs is closely related to anticlinal closure associate with rollover anticlines.

REFERENCES

Al-Shaieb, Z., J. Puckette, A. A. Abdalla, V. Tigert, and P. J. Ortoleva, The banded character of pressure seals: Basin Compartments and Seals AAPG Memoir, v. 61, 1994, p. 351-367.

Al-Shaieb, Zuhair, Jim Puckette, Jay Patchett, Phebe Deyhim, Han Li, Amy Close, and Ryan Birkenfeld, Oklahoma State University Search and Discovery Article #20004 (2000).

Al-Shaieb, Zuhair, Jim Puckette, Jay Patchett, Phebe Deyhim, Han Li, Amy Close, and Ryan Birkenfeld, Oklahoma State University, Gas Research Institute, GRI Contract No. 5097-260-3777

Al-Shaieb, Z., J. Puckette, P. Blubaugh, P. Deyhim and H. Li, "Identification of reservoir and seal facies in the Vicksburg Formation, TCB field, Kleberg County, Texas", Topical Report to Gas Research Institute, Document No. GRI- 98/0240, 2000.

Al-Shaieb, Z., J. Puckette, P. Blubaugh, P. Deyhim and H. Li, Characterization of the low-contrast 9900-ft sandstone, Vicksburg Formation, TCB field, Kleberg County, Texas: Topical Report to Gas Research Institute, Document No. GRI-98/0240, 1998.

Asquith, G., 1982, Basic well log analysis for geologists, AAPG Methods in Exploration Series Number 3.

Birkenfeld, Ryan., Sequence Stratigraphy as a control of Depositional Facies in the Oligocene Vicksburg Sandstone, TCB Field, Kleberg County, Texas. May 2001.

Boggs, Sam Jr., 1985, Principles of Sedimentology and Stratigraphy Second Edition.

Coleman, J. M. C., Depositional systems and tectonic/eustatic history of the Oligocene Vicksburg episode of the Northern Gulf Coast: The University of Texas at Austin, Ph.D. dissertation, 1990.

Combes, J. M., The Vicksburg Formation of Texas: Depositional systems Distribution, Sequence Stratigraphy, and Petroleum Geology: AAPG Bull, v. 77, no. 11, 1993, p. 1942-1970.

Deyhim, Phebe M., Compartmentalization and Overpressuring of the Oligocene Vicksburg Sandstone, TCB Field, Kleberg County, Texas. December, 2000

Hall, D., Applying Fluid Inclusions to Petroleum Exploration and Production: Fluid Inclusion Technologies, Inc., 1999.

Halliburton, "Electrical Micro Imaging Service—Discover what you are missing", 1997.

Han, J. H., 1981, Genetic stratigraphy and associated growth structures of the Vicksburg Formation, South Texas: Ph.D. dissertation, University of Texas, Austin, Texas.

Han, Li., Characterization and Petrophysical Analysis of "Low-Contrast" thin Bedded Vicksburg Reservoirs, TCB Field, Kleberg County, Texas. July 2000.

Hansen, S. M., T. Feet, Identification and evaluation of turbidite and other deepwater sands using open hole logs and borehole images, Fine-grained Turbidite Systems: AAPG Memoir v.72/SEPM Special Publication No. 68, 1999, p. 319-338.

International Oil Scouts Association, International Oil and Gas Development Yearbook, Review of 1995 Production, v. 66, 1997, 1071p.

Jennings, J. B., Capillary Pressure Techniques: Application to Exploration and Development: AAPG Bulletin v. 71, 1987, p. 1196-1209.

Loucks, R.G., D. L. Richmann and K. D. Milliken " Factors controlling Reservoir Quality in Tertiary Sandstones and Their Significance to Geopressured Geothermal Production", 1981, Bureau of Economic Geology—University of Texas at Austin.

Nanz, R. H. Jr., "Genesis of Oligocene sandstone reservoirs, Seelingson Field, Jim Wells and Kelberg Counties, Texas", AAPG Bulletin, v. 38, 1954, p. 96-117.

Petroleum Information/Dwights, Natural Gas Well Production Histories, 1999.

Schlumberger, "FMI"—Fullbore Formation MicroImager", Pamphlet SMP-5145/M-090253. Houston: Schlumberger Wireline & Testing, 1992.

Schlumberger, 1972, Log interpretation, Volume 1-Principles: Schlumberger Ltd., New York, p.113.

Shelton, J. W., "Models of sand and sandstone deposits: a methodology for determining sand genesis and trend", Oklahoma Geol. Survey Bulletin, v. 118, 1973, p. 30-32.

Sneider, R.M., and J. T. Kulha, Low-resistivity, low contrast productive sands, workshop, 1995.

Taylor, D. A., and Z. Al-Shaieb, Oligocene Vicksburg sandstones of the Tijerina-Canales-Blucher field: a south Texas jambalaya: Gulf Coast Association of Geological Societies Transactions, Vol. 36, 1986, p. 315-339.

Vavra, C.L., Kaldi, J.G., and Sneider, R.M, 1992, Geological applications of capillary pressure: AAPG Bulletin, v. 76, p.840-850.

Williamson, J. D., Gulf Coast Cenozoic history: G.C.A.G.S. Transactions, v. 9, 1959, p. 15-29.

VITA

Amy Rebecca Close

Candidate for the Degree of

Master of Science

Thesis: INTEGRATED APPROACH TO THE EXPLORATION OF THE OLIGOCENE VICKSBURG RESERVOIRS, TCB FIELD, KLEBERG COUNTY, TEXAS

Major Field: Geology

Biographical:

Personal Data: Born in West Jefferson, North Carolina, On February 11, 1977, the daughter of George and Gena Cox.

Education: Graduated from Alleghany High School, Sparta, North Carolina in May 1995; received Bachelor of Science degree in Geology from Oklahoma State University in May 1999. Completed the requirements for the Master of Science degree with a major in Geology at Oklahoma State University in May 2002.

Experience: Research and Teaching Assistant for Petrology and Well Log Analysis, Oklahoma State University.

Professional Memberships: American Association of Petroleum Geologists, Oklahoma State Geological Society.